N° ordre : 2015-16
N° Série : B-269

THESE / AGROCAMPUS OUEST

Sous le label de l'Université Européenne de Bretagne

pour obtenir le diplôme de :

DOCTEUR DE L'INSTITUT SUPERIEUR DES SCIENCES AGRONOMIQUES, AGRO-ALIMENTAIRES, HORTICOLES ET DU PAYSAGE

Spécialité : Food Science

Ecole Doctorale : VAS (Vie-Agro-Santé)

présentée par :

Arlan CALDAS PEREIRA SILVEIRA

THERMODYNAMIC AND HYDRODYNAMIC CHARACTERIZATION OF THE VACUUM EVAPORATION PROCESS DURING CONCENTRATION OF DAIRY PRODUCTS IN A FALLING FILM EVAPORATOR

soutenue le 12 octobre de 2015 devant la commission d'Examen

Composition du jury :

Martine Esteban-Decloux, Professor, AgroParisTech, France	Reviewer
Joël Scher, Professor, Université de Lorraine, France	Reviewer
Guillaume Delaplace, Research director, CNRS/INRA, France	Member
Bernard Cuq, Professor, SupAgro, Montpellier, France	Member
Antônio Fernandes de Carvalho, Professor, UFV, Brazil	PhD Supervisor
Romain Jeantet, Professor, Agrocampus Ouest, France	PhD Co-Supervisor
Bernard Rémond, R&D Manager, GEA Process Engineering, France	Guest

REMERCIMENTS

A l'issue de mon doctorat, je suis convaincu que la thèse est loin d'être un travail solitaire. En effet, je n'aurais jamais pu réaliser ce travail doctoral sans le soutien d'un grand nombre de personnes dont la générosité, la bonne humeur et l'intérêt manifestés à l'égard de ma recherche m'ont permis de progresser dans cette phase délicate de « l'apprenti-chercheur ».

J’exprime toute ma reconnaissance à Jöelle Léonil et à Sylvie Lortal pour m’avoir accueilli au sein du STLO et permis de mener bien ce projet dans d’excellentes conditions humaines et professionnelles.

Je voudrais remercier mon jury de thèse, Dr. Martine Decloux, Dr. Joël Scher, Dr. Guillaume Delaplace, Dr. Bernard Cuq, Dr. Antônio Fernandes de Carvalho, Dr. Romain Jeantet, et Dr. Bernard Rémond. Votre présence le jour de ma soutenance ainsi que le temps dédié à l’appréciation de mon manuscrit de thèse ont été un grand honneur pour moi.

Je remercie mon encadrant et chef, Pierre Schuck, que je considère plutôt comme un ami. Pour moi Pierre est un exemple de professionnalisme et de gentillesse. Il était gratifiant de travailler en sachant qu'en cas de doute ou de problème, Pierre me conseillerait avec le sourire. Merci Pierre pour ta patience, tes conseils, tes enseignements, pour ton exemple d’engagement sérieux, et pour ta façon positive de voir les problèmes. Merci beaucoup papa Schuck.

S'il y a une personne qui m'a toujours soutenu, cru en moi et aidé avec tout ce dont j'avais besoin, c'est sans doute le Professor Antônio Fernandes de Carvalho. Merci pour l’encouragement, la confiance et le soutien qui n’ont jamais cessé dès lors que nous avons commencé à travailler ensemble.

Merci à Romain Jeantet de m'avoir encadré et d’avoir joué le rôle de relecteur final de mes travaux scientifiques. Romain tu es un exemple pour moi d’un excellent ingénieur et scientifique. Un grand merci à toi pour toute la rigueur scientifique que tu m’as apprise.

Je suis heureux d'avoir eu la chance de travailler et d'être officieusement encadré par Gaëlle Tanguy. Merci pour ta relecture enrichissante de toutes mes publications, pour la relecture scrupuleuse de mon manuscrit de thèse et tes suggestions toujours avisées. Tu m'as permis Gaëlle de clarifier mes pensées parfois embrouillées. Tes remarques très pertinentes ont fait avancer ma réflexion d'un point de vue scientifique.

Je tiens à remercier deux messieurs sans qui les résultats de mes travaux scientifiques ne seraient jamais arrivés à la moitié d'où ils en sont aujourd'hui. Merci Serge Méjean et Laurent Fromont, j'ai appris beaucoup, beaucoup avec vous. Vous m'avez aidé non seulement avec la partie technique de mon sujet de doctorat, mais aussi appris à ne jamais laisser tomber, à persévérer, à toujours trouver une solution aux problèmes insolubles. Merci Laurent d'avoir partagé tes connaissances de 15 ans de marine et d'avoir toujours été disponible pour me dépanner quand j'avais besoin. Merci Serge pour le partage de tes connaissances sans fin dans le domaine de la concentration et du séchage. Merci d'être toujours prêt à m'aider et souriant.

Merci à tous les gens qui travaillent sur la plateforme Lait. Merci de m'avoir supporté pendant ces années de travail à vos côtés. Merci pour la superbe ambiance et pour toute l'aide et la compréhension dont vous avez fait preuve avec moi. Merci à vous Nadine, Gilles et Bénédicte. Merci Benoit (Benolé) pour l'amitié et les moments drôles partagés pendant ces années.

Merci Rachel Boutrou, d'avoir aidé tous les jeunes chercheurs du STLO avec ton merveilleux travail. Merci d'avoir élargi le champ de ma vision scientifique. Merci de t'être préoccupée et de m'avoir aidé avec la vulgarisation scientifique.

Pendant mes quatre ans au sein du STLO j'ai aussi eu la chance de partager le bureau avec des personnes que je respecte et admire profondément. Merci à Gwenollé Gernigion pour la compagnie, les discussions scientifiques, l'aide pour les premières démarches scientifiques au sein du STLO et pour l'apprentissage de la culture bretonne. Merci à Peng Zhu pour ton amitié

et pour être un exemple de professionnalisme pour moi. Je dois maintenant remercier ma maman française, qui mérite un paragraphe entier.

Merci à toi Anne Dolivet, pour toute la compagnie, les partages, les discussions, les renseignements, les bonnes idées, les sourires, le soutien et pleins d'autres choses que tu m'as offertes pendant nos trois ans de partage de bureau. Tu es quelqu'un de très important pour moi, et l'amitié que j'ai pour toi et pour toute la famille Dolivet durera toute la vie. Merci de m'avoir pris comme ton fils adoptif ici en France. Tu fais partie de ma vie.

Merci à Paulette Amet, Jéssica Musseaut, et Michel Ravailler pour le chaleureux « Bonjour » et le sourire quotidien. Merci Paulette d'avoir organisé les pauses de 16h et de t'être toujours préoccupée des nouveaux arrivants.

Merci à ma chère amie Lélia Lacou, tu es une amie que je garderai toujours.

Merci à ma sœur Chinoise, Lina.

Merci a mon chouchou, Gérardine (Gérard). Merci pour ta bonne humeur Gérard. J'espère que tu viendras me visiter au Brésil.

Merci à mes amis bichonas, Naaman Nogueira, Federico Casanova et Xavier Thomas. Vous trois mes potes sont des cadeaux que j'ai eu la chance d'avoir. J'en profite également pour remercier la famille Thomas, qui a été à plusieurs reprises comme ma famille française.

Merci à l'équipe Carinhosos. Je tiens à vous vraiment très très fort. Marilia, Samira et Gui, les soirées, voyages et le temps passé avec vous sont inoubliables et épiques. Merci Samira pour les câlins, le respect et les conseils. Merci Marilia d'être toujours sympa et réceptive, tu donnes envie de rester à tes côtés, avec toute ton énergie très captivante. Merci à Gui d'être présent dans ma vie depuis si longtemps et d'être mon compagnon de trajet scientifique.

Heureusement que mes parents et mes frères sont là pour me changer les idées. Ils ont tous cru en moi et ouf ! Maintenant j'y suis ! Alors merci à mon papa Hélcio Caldas Silveira et à ma

maman Maristela Pereira Silveira, malgré toutes les difficultés rencontrées vous m'avez laissé rêver grand et avez fait tout le possible et même l'impossible pour que je réussisse. Merci à mes frères Arcanjo Caldas Pereira Silveira et Artur Caldas Pereira Silveira et à ma petite sœur Ana Carolina Varoto Pereira.

Je remercie toutes les personnes avec qui j'ai partagé mes études et notamment ces années de thèse : Marta Rezende, Bruno Nunes, Daniel, Jeferson Geis, José, Raquel, Gustavo, Bia Oliveira, Natalia, Lize Desmaricaux, Estelle, Michele Pinto, Renam Moreira, Flavia figueira, Wendiao Shao, Bruno Gamba, Rosangela Faria, Andreza, Léticia Carmargos, Odeir Filho, João Carneiro, Marciano, Laura Sanchez, Marina, Natalia, Luiza Las, Mariana, Elise Schong, Song, Linda, Matheus, Guillaume, André, Clarisse Lebel, Carlos, Aude, Maude, Gaëtan, Perrine, Andreas, Andreza, Xavier, Adèle, Juliana, Rachid, Rigoberto, Rozenn, Livia etc., et pleins d'autres bons amis qui ne font malheureusement plus partie de ma vie mais qui ont participé à faire de moi ce que je suis aujourd'hui.

J'en oublie certainement encore et je m'en excuse.

Encore un grand merci à tous pour m'avoir conduit à ce jour mémorable.

« Une personne est en mesure de réaliser quoi que ce soit si son enthousiasme n'a pas de limites »
Charles Schwab

THESIS OUTPUTS

Publications

Silveira, A.C.P., Carvalho, A.F., Perrone, Í.T., Fromont, L., Méjean, S., Tanguy, G., Jeantet, R., Schuck, P., 2013. Pilot-scale investigation of effectiveness of evaporation of skim milk compared to water. *Dairy Sci. Technol*. 93, 537–549. doi:10.1007/s13594-013-0138-1

Silveira, A.C.P., Tanguy, G., Perrone, Í.T., Jeantet, R., Ducept, F., de Carvalho, A.F., Schuck, P., 2015. Flow regime assessment in falling film evaporators using residence time distribution functions. *J. Food Eng.* 160, 65–76. doi:10.1016/j.jfoodeng.2015.03.016

Silveira, A.C.P., Tanguy, G., Perrone, Í.T., Jeantet, R., Laurent, F., Floch-Fouéré, C., de Carvalho, A.F., Schuck, P., 2015. Application of residence time distribution functions at different dairy products to indicate fouling during concentration in a falling film evaporator. To submitted in October 2015 at *Journal of Dairy Science*.

Oral presentations

Inauguration de la plateforme lait - STLO, Rennes (France), 2013. Caractérisation du procédé d'évaporation sous vide: démarche et intérêts.

2° Simpósio de Leites Concentrados e Desidratados, Juiz de Fora (Brazil), 2014. Concentração por evaporação à vácuo. Balanço de massa, de energia e tempo de retenção: importância da instrumentação.

Journée technique séchage, Surgères (France), 2014. Caractérisation du procédé de concentration par évaporation sous vide. Bilan énergétique, massique et temps de séjour.

EMChIE-2015, the 7th European Meeting on Chemical Industry and Environment, Terragona (Spain). Flow regime assessment in falling film evaporators using residence time distribution (presented by Gaëlle Tanguy).

ICEF12, 12th International Congress on Engineering and Food, Québec (Canada). Residence time distribution functions applied to skim milk concentration in falling film evaporators.

Poster

5th International Symposium on Spray Dried Dairy Products, St Malo (France), 2012. *Characterization of a vacuum evaporator pilot plant in relation to mass and energy balance.*

TABLE OF CONTENTS

LIST OF ABREVIATIONS AND NOMENCLATURE

Abreviations

1R: first run

2R: second run

3R: third run

α –lg: α-lactoglobumin

β-lg: β-lactoglobulin

CC: consumption costs

CCP: Colloidal calcium phosphate

FFE: Falling film evaporator

IC: Investments costs

LAW: Lactic acid whey

P_c: Condenseur pressure

P_{ev}: Evaporation pressure

R: Roughness

RTD: Residence time distribution

SC: Staff costs

SM: Skim milk

SW: Sweet whey

T1: evaporation tube 1

T2: evaporation tube 2

T3: evaporation tube 3

TC: Total costs

WM: Whole milk

Nomenclatures

A: heating surface (m^2)

A: fraction of feed flow rate going into the reactor set A (-)

Cp: Specific heat ($kJ \cdot kg^{-1} \cdot °C^{-1}$)

C: concentration ($g \cdot kg^{-1}$)

D: tube diameter (m)

D_{ax}: axial diffusion coefficient (-)

e_m: wall thickness (m)

$E_i(t)$: residence time distribution of section i (s)

EE: energy efficiency (% - $w \cdot w^{-1}$)

g: gravity acceleration ($m \cdot s^{-2}$)

H: enthalpy ($kJ \cdot kg^{-1}$)

h: heat transfer coefficient ($kW \cdot m^{-2} \cdot °C^{-1}$)

ΔH_v: latent heat of vaporization ($kJ \cdot kg^{-1}$)

L: length (m)

$\dot{m}$: mass flow rate ($kg \cdot h^{-1}$)

N: number of tanks in series (-)

N_u: Nusselt number

P: Pressure (MPa)

Pe: Peclet number (-)

$\dot{Q}$: heating power (kW)

$\dot{q}_p$: heat loss ($kJ \cdot h^{-1}$)

$R_{fouling}$: termal resistence of the fouling layer ($kW \cdot m^{-2} \cdot °C^{-1}$)

R_{ef}: film Reynolds number (-)

SEC: specific energy consumption ($kJ\ kg^{-1}$)

t: time (s)

t_{min}: minimum residence time (s)

TS: total solids (% - w/w)

U: overall heat transfer coefficient ($kW \cdot m^{-2} \cdot °C^{-1}$)

v_{max}: maximum flow velocity ($m \cdot s^{-1}$)

x(t): tracer injection ($g \cdot kg^{-1}$)

$y_{Ti}(t)$: tracer concentration at the bottom of T_i ($g \cdot kg^{-1}$)

Greek symbols

η: viscosity ($Pa \cdot s^{-1}$)

θ: temperature (°C)

λ_m: thermal conductivity of the wall ($kW \cdot m^{-1} \cdot °C^{-1}$)

v: velocity ($m \cdot s^{-1}$)

ρ: density ($kg \cdot m^{-3}$)

σ: surface tension ($N \cdot m^{-1}$)

Γ: mass flow rate per unit circumference ($kg \cdot s^{-1} \cdot m^{-1}$)

τ: mean residence time (s)

T: shear stress (Pa)

Φ: heat flux ($kW \cdot m^{-2}$)

$\dot{\gamma}$: velocity gradient (s^{-1})

Subscript

abs: absolute

cc: product concentrate

cd: product condensate

cw_{in}: inlet cooling water

cw_{out}: outlet cooling water

ev: evaporation

p_{in}: inlet product

p: product

v_{-1}: steam

v_1: steam condensate

GENERAL INTRODUCTION

Overall cow's milk production and consumption grew by approximately 15% from 2005 to 2014. With the uneven distribution of milk production at the global level, the expected growth in the world population and the rise in standards of living (in particular in developing countries), the dairy market will be confronted with even more massive changes in the next decade. The world market for dairy powders is expanding considerably. The investment in new vacuum evaporators and spray driers is therefore being reported throughout the world to secure outlets. The vacuum evaporation process is mainly used in the dairy industry prior to drying. Moreover the quality of the concentrates influences the final powder quality.

This context clearly drives researches in order to improve the efficiency and control of the vacuum evaporation process. However, few research groups are interested in this topic. The dairy industry has acquired empirical expertise in the vacuum evaporation process, and the research centers in dairy powder are interested, until then, in drying technology (spray dryer). Study of vacuum concentration of dairy products is therefore a challenging for research in food processing engineering.

The goal of this PhD project was to characterize experimentally a falling film evaporator during the concentration of dairy products, by means of thermodynamic and hydrodynamic approaches, in order to study the interactions between the products properties and the operating parameters. A prototype pilot-scale, single-stage falling film evaporator was therefore used to tackle these issues. This equipment was designed to describe the same process as the industrial scale from a hydrodynamic point of view.

This work was therefore divided into three research parts: one on the instrumentation and characterization of a pilot-scale falling film evaporator, another part on the hydrodynamic profile of the vacuum evaporation process, and a third part on the application of the approaches previously developed to other dairy products.

To state the scientific and economic context of the project, a chapter about the trade development of dairy powders and vacuum evaporation research trends (Chapter 1), and a literature review on vacuum evaporation process during concentration of dairy products (Chapter 2) are presented. These chapters are followed by the description of the experimental strategy of the PhD project (Chapter 3). The second part of the thesis presented materials and methods, results and discussion regarding the process of vacuum evaporation of different dairy products. This includes the description of the pilot-scale single stage falling film evaporator used in this study (Chapter 4), the thermodynamic and hydrodynamic characterization of this equipment (Chapter 5, and 6, respectively) and the application of these approaches to other dairy products (Chapter 7). Finally, the main contributions and potential research opportunities are drawn together in the conclusion and in the outlook sections.

PART 1

ECONOMIC AND SCIENTIFIC CONTEXTS

Chapter 1

TRADE DEVELOPMENT OF DRIED DAIRY PRODUCTS AND RESEARCH TRENDS

This chapter introduces the economic background of dairy products, from milk production to powder manufacture. In addition, it provides key statistics concerning dairy powder markets and certain socioeconomic criteria needed to understand the current context. This information is used to draw conclusions regarding the future trends of dairy powders. These include the evolution of the dairy product trade and the socio-economic context. Faced with all these challenges, dairy industries are developing and innovating in order to increase the added value of milk products and to be competitive in the future.

The main aims of this chapter are to:
- provide key statistics on the dairy market (Brazilian, French and global)
- situate dairy powders in the current socio-economic context
- provide highlights of research trends in vacuum evaporation processes

Capítulo 1

DESENVOLVIMENTO DO MERCADO DE PRODUTOS LÁCTEOS DESIDRATADOS E TENDÊNCIAS DE PESQUISAS

Este capítulo apresenta o contexto econômico dos produtos lácteos, desde a produção do leite à fabricação dos pós. Além disso, ele fornece estatísticas importantes relativas ao mercado de lácteos desidratados e certos critérios socioeconômicos necessários para compreender o atual contexto. Estas informações são usadas para prever futuras tendências da evolução do mercado de produtos lácteos e do contexto sócio-econômico deste. Diante de todos esses desafios, a indústria de laticínios está se inovando e desenvolvendo a fim de aumentar o valor agregado de seus produtos visando se tornar mais competitiva no futuro.

Os principais objetivos deste capítulo são:

- fornecer importantes estatísticas sobre o mercado dos produtos lácteos (brasileiro, francês e global)
- situar os produtos lácteos desidratados no atual contexto sócio-econômico
- destacar as tendências de pesquisa dos processos de evaporação a vácuo

Table of contents

1.1. Key dairy market statistics

1.1.1. Milk Production

The worldwide production of milk is forecast to grow by as much as 2% in 2015, a rate similar to previous years, and should reach 805 million tons. Asia is expected to account for most of the increase, but production is projected to rise in all regions (FAO, 2015). The main milk producers are Europe, India, The United States of America, China and Brazil, which have had high production rates over the last 5 years (Fig. 1.1).

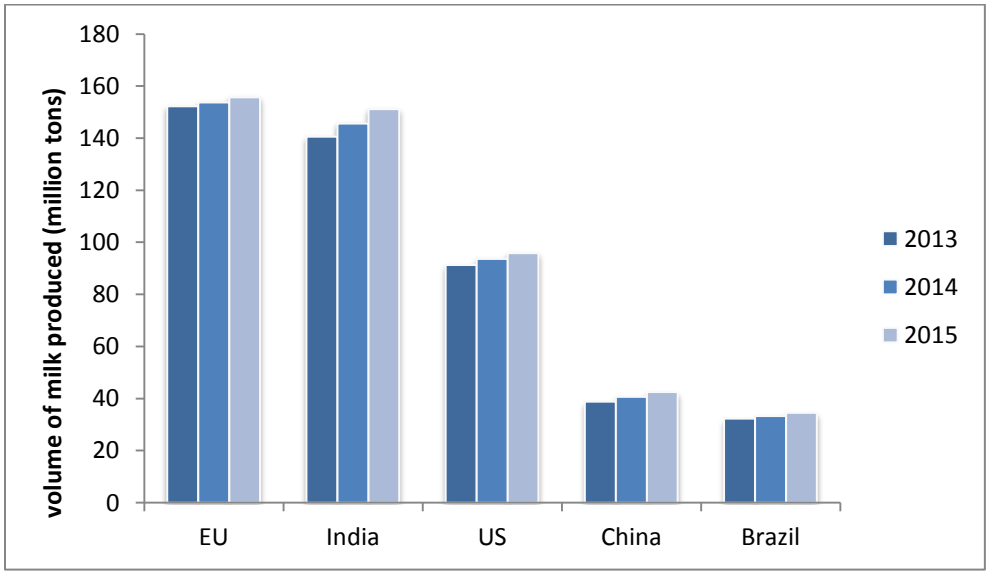

Figure 1.1. Main milk producers (USDA NASS, 2015).

Note: 2015: forecast.

The worldwide production of milk should continue to grow in coming years, reaching a level of 880 million tons in 2020 (Fig. 1.2) (OECD-FAO, 2015).

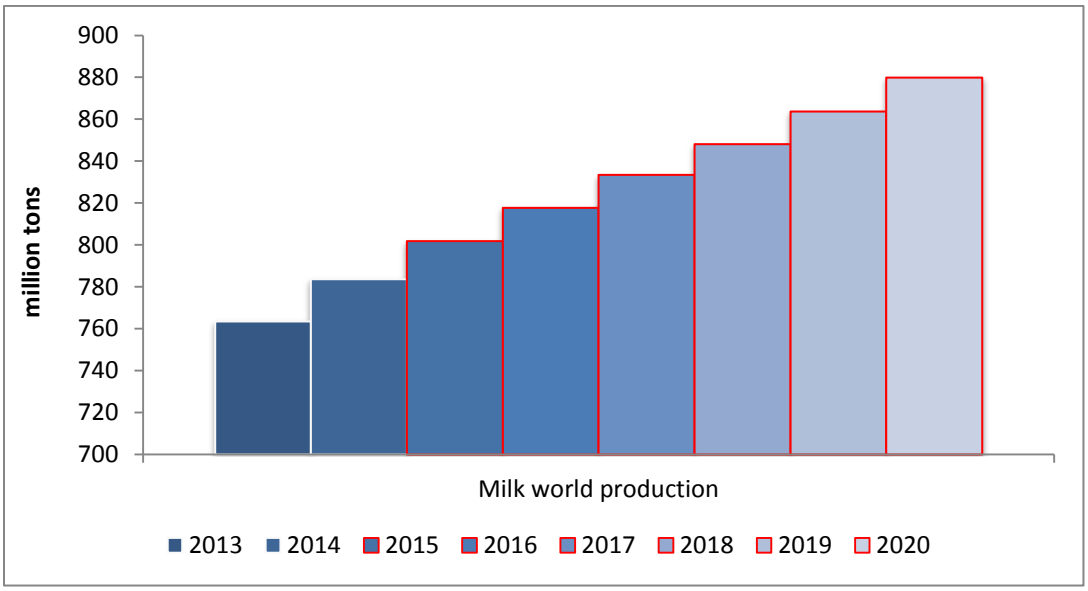

Figure 1.2. Evolution of worldwide production of milk from 2013 to 2020. (2015 to 2020: forecast) (OECD/FAO, 2015).

France is the second highest producer of milk in Europe and the seventh in the world, with 25.3 million tons of milk per year. In France, about 40% of the milk produced is processed and exported (CNIEL, 2015), product manufacture representing a turnover of 27.2 billion euros and generating about 250,000 jobs (CNIEL, 2015). Dairy products to the value of 6.9 billion euros were exported in 2013, with a trade surplus of 3.6 billion euros, an increase of 71% in 10 years.

Brazil is among the five largest producers of milk in the world and has achieved a significant role in the global dairy market. Brazil came from production of 7.3 million tons of milk in the 70s to 35 million tons in 2014 (IBGE, 2015). This year the country is expected to reach the third place as worldwide producer of milk, surpassing Chinese production (FAO, 2015).

1.1.2. World market for dairy powders

The popularity and increasing range of dairy products and the westernization of diets continue to be key factors driving the worldwide dairy market. Among dairy products, the global milk powder market is expanding considerably (Fig. 1.3), e.g. in France around 19% of processed milk volume is transformed into different dairy powders (CNIEL, 2015). This is due to an increasing demand for milk products from countries with milk shortages, in particular emerging countries.

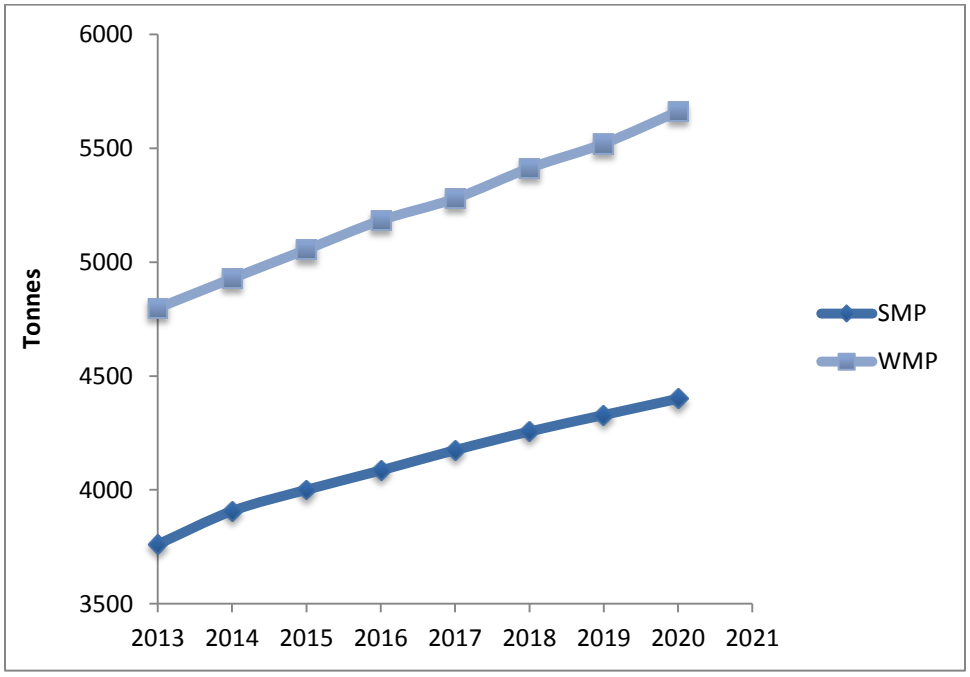

Figure 1.3. Forecasts for worldwide skim milk and whole milk powder production. 2013 and 2014 (estimate), 2015 to 2020 (forecasts) (OECD-FAO, 2015).

Legend: SMP = skim milk powder; WMP = whole milk powder

With a large domestic market and high levels of milk production, Brazil has a different dairy market behavior to that in France. Traditionally, Brazil has always been a major importer of

dairy products, with a negative balance of nearly 0.3 million tons in the 90s. From 2004 to 2008, it was an exporter of dairy products (Fig. 1.4). However, with a growing consumption of dairy products, large world supply and depreciation of the dollar, since 2008 Brazil has again become an importer of dairy products.

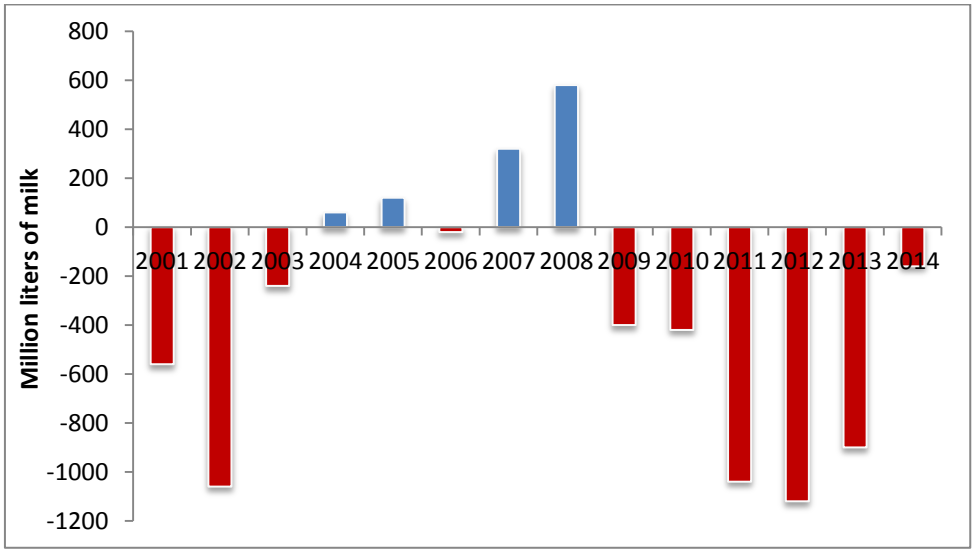

Figure 1.4. Trade balance of Brazilian dairy products from 2001 to 2014 (in milk equivalent) (EMBRAPA, 2010; Milkpoint, 2014).

Due to the country's economic issues and lower GDP growth rate, the consumption of dairy products in Brazil was slowing in 2014. However, in 2014 Brazil increased its turnover of dairy exports by 254.3% compared to 2013 (MDCI, 2014) (Table 1.1). The Brazilian export of dairy products had a favorable scenario in this year.

Table 1.1. Dairy export by Brazil, 2010 to 2014 (MDCI, 2014).

Year	Value (US$ FOB)	Net weight (kg)
2010	131,645,920	53,569,283
2011	97,309,124	37,551,518
2012	92,257,425	38,370,224
2013	93,832,529	38,383,693
2014	332,430,800	83,667,142

With changes in agricultural policy (such as the implementation of a quota system and the dissolution of the price support system), the dairy industry has improved the use of surplus milk production and by-products resulting from cheese and butter production (whey, buttermilk). The development of filtration technology (microfiltration, ultrafiltration, nanofiltration and reverse osmosis) has allowed the production of valuable milk protein fractions (Schuck et al., 2013). Used either as nutritional or functional ingredients, most of these proteins are marketed in dehydrated form. In the last ten years, the nature of dairy powders has changed to more specific intermediate dried products, and powders have been developed as techno-functional ingredients according to their expected functional properties such as gelation, foaming and emulsification. Many new uses of these constituents have appeared with the manufacture of formula products, substitutes and adapted raw material. Dairy powders are therefore used in the development of a wide range of products.

1.1.3. French and Brazilian dried dairy product markets

About 56% of dairy powders produced in France are exported, mainly to the European Union, Asia and the Middle East. The French production of milk powders accounts for approximately 10% of the total world production (IDF, 2013) (Table 1.2).

Table 1.2. French production of dried dairy products (CNIEL, 2015).

Million Euros	2000	2012	2013	2014
Dried Milk	808,767	1,331,673	1,441,526	1,681,190
Skim milk powder	191,095	511,162	475,474	717,389
Whole Milk powder	490,021	235,107	279,457	313,530
Infant Formulae	113,947	539,753	638,743	600,517
Whey powders	212,816	408,028	471,732	447,200
Lactose	10,069	33,040	31,503	26,923
Dairy powders for animal feed	145,323	111,670	106,169	105,670

Dairy dried products are highly significant in the Brazilian dairy market. The domestic demand for dairy products (mainly milk powders) is expanding, as well as global demand. Dairy powders corresponded to 69.6% of Brazilian dairy imports in 2013, 49.4% being skim and whole milk powders, 19.6% whey powder and 0.6% infant formulae (MDCI, 2014).

1.1.4. Developments and investments involving concentrated and dried dairy products

Investment in new spray driers and vacuum evaporators are being reported throughout the world to secure outlets. Indeed, investments of more than 2.5 billion euros are currently predicted for dried dairy products, involving 46 companies, 53 projects and 28 countries (CNIEL, 2012). Over the last two years, 400 million euros of investment were announced or implemented on French territory to produce milk or whey powders (CNIEL, 2015). Fig. 1.5 shows investments of more than 100 million US$ announced and/or finalized in Europe and in America.

A

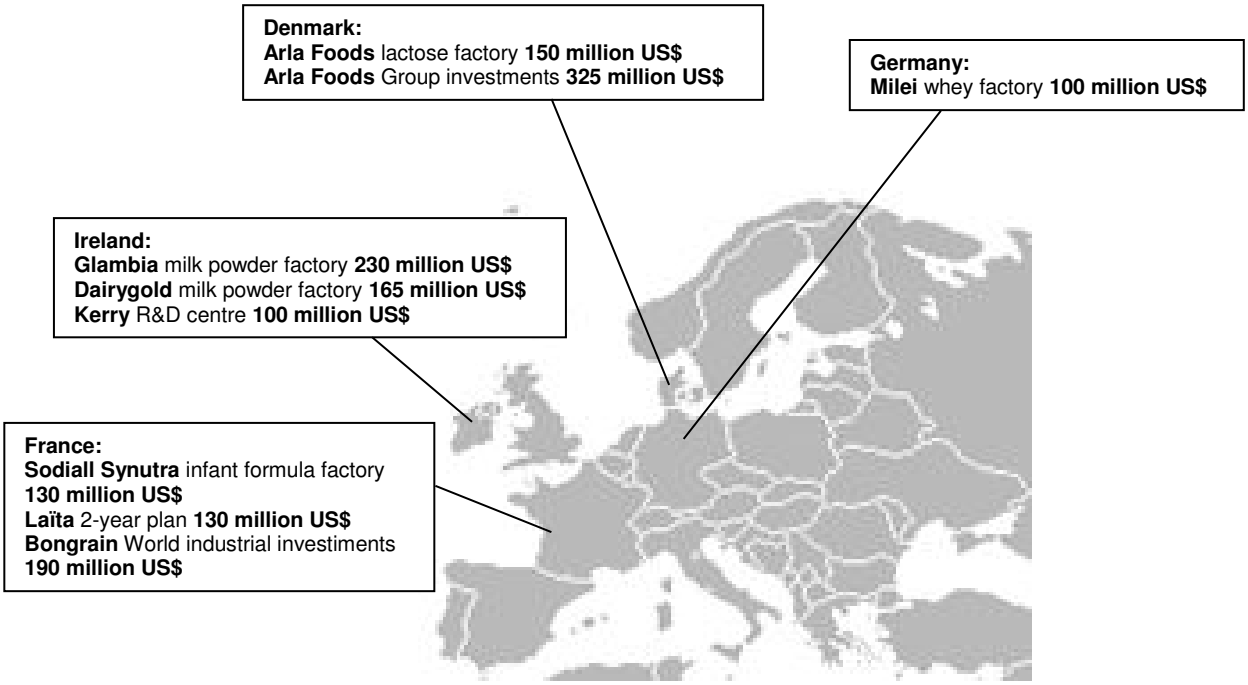
Denmark:
Arla Foods lactose factory 150 million US$
Arla Foods Group investments 325 million US$
Germany:
Milei whey factory 100 million US$
Ireland:
Glambia milk powder factory 230 million US$
Dairygold milk powder factory 165 million US$
Kerry R&D centre 100 million US$
France:
Sodiall Synutra infant formula factory
130 million US$
Laïta 2-year plan 130 million US$
Bongrain World industrial investiments
190 million US$

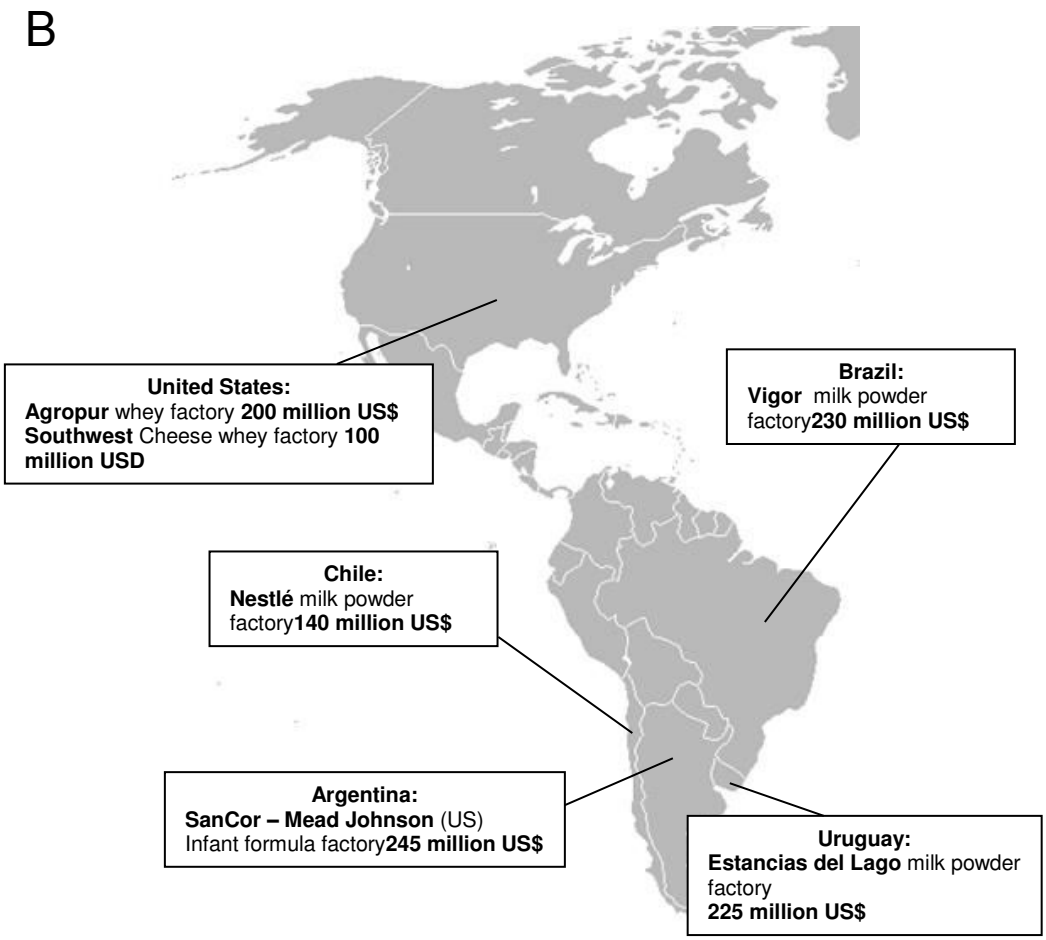

Figure 1.5. Investments of more than 100 million US$ announced and/or finalized in Europe (A) and America (B) (CNIEL, 2015; IDF, 2013).

A combination of newly developing markets for dairy products, particularly in South-East Asia, and the emergence of new entrant countries with rapidly expanding milk production are changing the dynamics of the world dairy industry. With a projected increase in world milk production, it is to be expected that dairy powders will continue to play an important role in facilitating trade of milk solids on an international scale. Vacuum evaporation and spray drying along with existing and novel techniques will continue to be important contributors to ingredient innovation. Increasing intellectual property protection covering novel dried ingredients and processes will be adopted by companies both for defense purposes, and also to exploit commercial opportunities on international markets (Kelly, 2006).

1.2. Worldwide research involving “falling film vacuum evaporators”

Evaporation is the most often used technique in the food industry for concentrating solutions or crystallizing solids from solutions. Of all the existing technology for evaporation of a solution in dairy industries, the falling film evaporator is currently the most frequently used, mainly due to its ability to treat heat-sensitive products.

Considering the economic importance of vacuum evaporation in the production of concentrated / dehydrated dairy products, research aiming to improve the efficiency of the process is necessary. However, few research groups are interested in this topic (Fig. 1.6). The dairy industry has acquired empirical expertise in the vacuum evaporation process, and the research centers in dairy powder are interested, until then, in drying technology (spray dryer). Study of vacuum concentration in dairy products is therefore a challenging and a fertile area for research in food processing engineering.

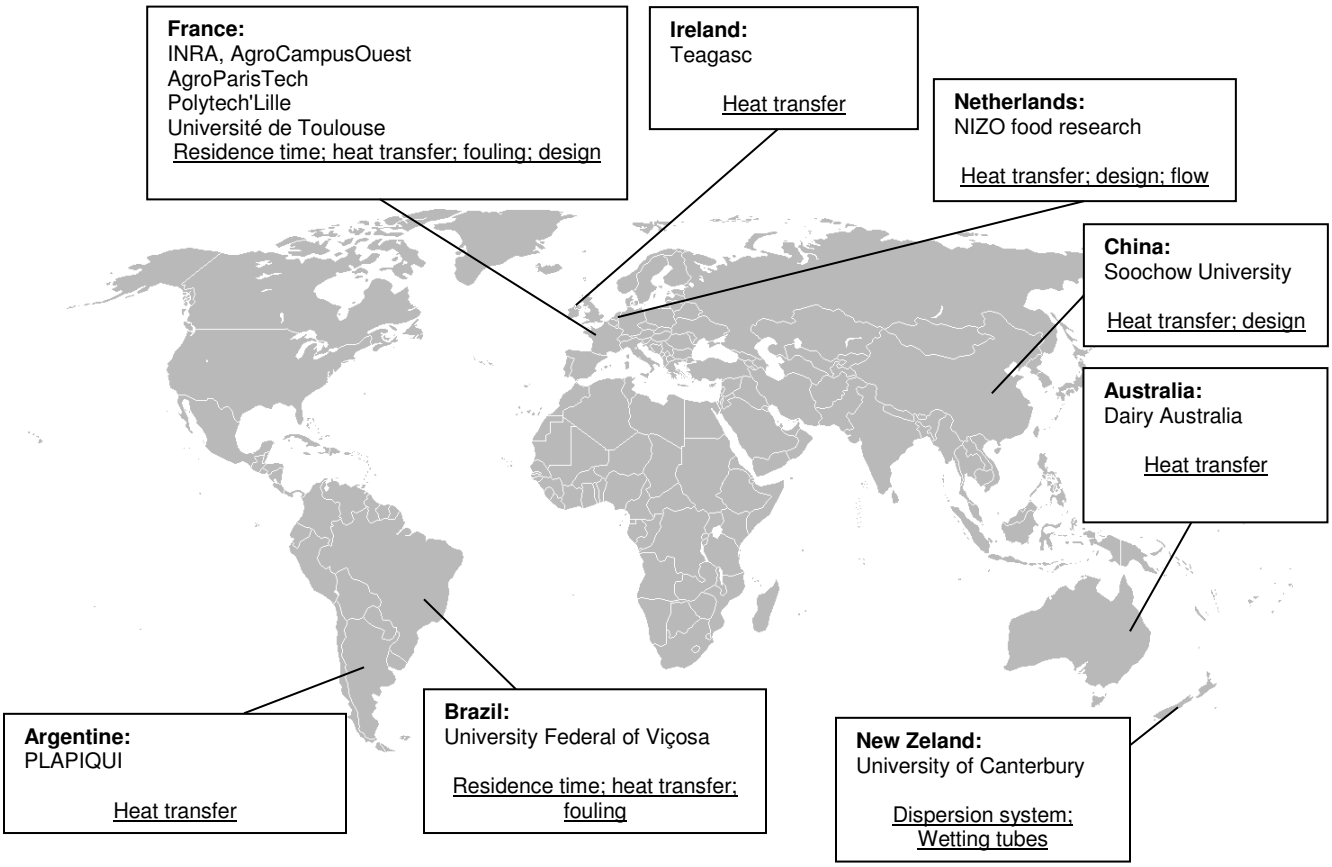

Figure 1.6. Overview of main research teams focusing on vacuum evaporation of dairy products, since 2010.

Chapter 2

LITERATURE REVIEW

This chapter aims to provide a literature background on the use of falling film evaporators in the dairy industry, and the characteristics of this process (energy consumption, product flow, fouling etc.). Many factors contribute to the dynamics of the vacuum evaporation process. In general this process involves heat and mass transfer. Other factors are related to the design of the evaporator (falling film, rising film, plate evaporators, etc.) and to product characteristics (viscosity, composition, surface tension, etc.). The physicochemical characteristics of milk and different designs of evaporators used in the dairy industry are described. The characteristics of dairy concentrates (viscosity, specific heat, enthalpy, etc.) and their flow during concentration in a falling film evaporator are also reported. Finally, the factors influencing fouling during vacuum evaporation are described.

The main aims of this chapter are to:
- summarize the main characteristics of milk and dairy concentrates
- introduce falling film evaporator equipment
- describe the factors that contribute to the dynamics of the operation of FFE

Capítulo 2

REVISÃO DE LITERATURA

Este capítulo tem como objetivo proporcionar o contexto literário sobre o uso de evaporadores de película descendente na indústria de laticínios e as características deste processo (consumo de energia, vazão de produto, fouling, etc.). Em geral, este processo envolve a transferência de calor e massa. Muitos fatores contribuem para a dinâmica do processo de evaporação a vácuo, sendo estes relacionados ao design do evaporador (filme descendente, filme ascendente, evaporadores de placas, etc.) e as características do produto (viscosidade, tensão superficial, composição, etc.). As características físico-químicas do leite e de diferentes designs de evaporadores utilizados na indústria de laticínios são descritos. As características dos concentrados lácteos (viscosidade, calor específico, entalpia, etc.) e seu regime de escoamento durante a concentração em um evaporador de película descendente são também relatados. Finalmente, os fatores que influenciam o fouling durante a evaporação a vácuo são descritos.

Os principais objetivos deste capítulo são:
- resumir as principais características do leite e dos produtos lácteos concentrados
- descrever os evaporadores de película descendente
- descrever os fatores que contribuem para a dinâmica do funcionamento dos evaporadores de película descendente

Table of contents

2.1. Transformation of milk to concentrated dairy products

2.1.1. Classification, composition and structure of milk

Milk is a fluid secreted by mammalian females in order to satisfy the nutritional requirements of their neonates. It constitutes, therefore, a source of energy provided by lipids, lactose, amino acids, vitamins, minerals and water. It also has an important physiological role as it contains enzymes, hormones, antibacterial compounds, proteins and peptides (Fox and McSweeney, 2003). A wide range of factors can intervene in the composition of milk such as race, stage of lactation, health of the animal, season, animal feeding, etc. (Mahaut et al., 2000). Table 2.1 shows the average composition of bovine milk.

Table 2.1. Average composition of bovine milk (Walstra et al., 1999).

Component	Average concentration ($g \cdot kg^{-1}$)
Water	871.0
Fat	40.0
Proteins	32.5
Caseins	26.0
Whey proteins	6.0
Lactose	46.0
Minerals	7.0
Organic acids	1.7
Others	1.5

The average pH value of bovine milk at 20°C is about 6.6 - 6.8. The substances dissolved in milk provide an average water activity of 0.995. Milk density (around 1029 $kg \cdot m^3$ at 20 °C) varies mainly due to the fat content. Although its viscosity is twice that of water, it behaves as a Newtonian fluid (Walstra et al., 2006).

The nitrogen content of milk is about 34.0 $g \cdot kg^{-1}$, divided into three groups: caseins, whey proteins and non-protein nitrogen. Casein and whey proteins differ according to their solubility at pH 4.6 (Croguennec et al., 2008).

Casein represents 80% of the total milk proteins (Cayot and Lorient, 1998; Fox and Brodkorb, 2008; Horne, 2003). Casein in milk exists as large colloidal particles called “casein micelles” (Fox and Brodkorb, 2008). Casein micelles have a relatively wide size distribution, from less than 50 nm to more than 500 nm, with an average diameter of approximately 200 nm (Horne, 2003). In their native state, casein micelles are hydrated particles containing several thousand α_{S1}-, α_{S2}-, β- and κ-casein molecules as well as minerals, mainly colloidal calcium phosphate (CCP) (de Kruif, 1999; Panouillé et al., 2005). In milk at pH 6.7, casein micelles are electronegative, with an isoelectric point (pI) of 4.7. Caseins in the micelle structure are held together by hydrophobic interactions and by the presence of CCP. In physiological conditions, a “hairy layer” of the hydrophilic parts of κ-casein (about 10 nm thick and located at the surface of casein micelles) is responsible for steric and electro-repulsive stabilization of casein micelles, thus producing a balanced colloidal system (Panouillé et al., 2005).

In contrast to caseins, whey proteins are soluble at pH 4.6 in their native form. These proteins are heat-sensitive. The major whey protein constituents are β-lactoglobulin (β-lg) and α-lactoglobulin (α -lg). β-lg is a globular protein with a molecular mass of 18.3 kDa that has a very compact structure due to the presence of many β sheets. In milk at pH 6.7, β-lg is in the form of a dimer held together by non-covalent interactions. This protein has a free sulfhydryl group that is not accessible in the native form of the protein. α-la is a compact globular protein with a molecular weight of 14.2 kDa. This protein has an excellent amino acid profile, being rich in lysine, leucine, threonine, tryptophan and cystine (Kinsella and Whitehead, 1989). Other minor whey proteins are also present in the soluble phase of milk, in particular bovine serum albumin, immunoglobulins and lactoferrin.

Table 2.2. Composition and properties of milk proteins (Cayot and Lorient, 1998; Walstra et al., 2006).

		Concentration in milk ($g \cdot kg^{-1}$)	Molecular weight ($kg \cdot mol^{-1}$)	Number of cystein residues (including free sulfhydryl) (per mol)	Isoeletric point (pI)
Casein (~29 $g \cdot kg^{-1}$)	α_{S1}-Casein	11.1	23.6	0	4.5
	β-Casein	10.4	24	0	4.8
	κ-Casein	3.7	19	2 (0)	5.6
	α_{S2}-Casein	2.9	25.2	2 (0)	5
Whey protein (~5 $g \cdot kg^{-1}$)	β-lactoglobulin	2.5 - 4.5	18.3	5 (1)	5.2
	α-lactoglobulin	1.2 - 1.7	14.2	8 (0)	~ 4.3

Whatever the origin, milk consists of three phases: lipid phase; protein and mineral fraction in the colloidal state and a dispersing aqueous phase containing lactose, soluble proteins, minerals and vitamins (Croguennec et al., 2008). Fig. 2.1 (a) shows a transmission electron microscopy image of raw milk at room temperature in which these three phases can be identified: the lipid phase bounded by a membrane (milk fat globule membrane), casein micelles in suspension and the aqueous phase. The diameter of milk fat globules is between 0.1 µm and 10 µm. The average diameter of the fat globules (about 7 µm) is much larger than that of casein micelles (~ 120 nm) as shown in Fig. 2.1. Fig. 2.1 (b) shows the casein micelles (dark grey) and aqueous phase (light grey).

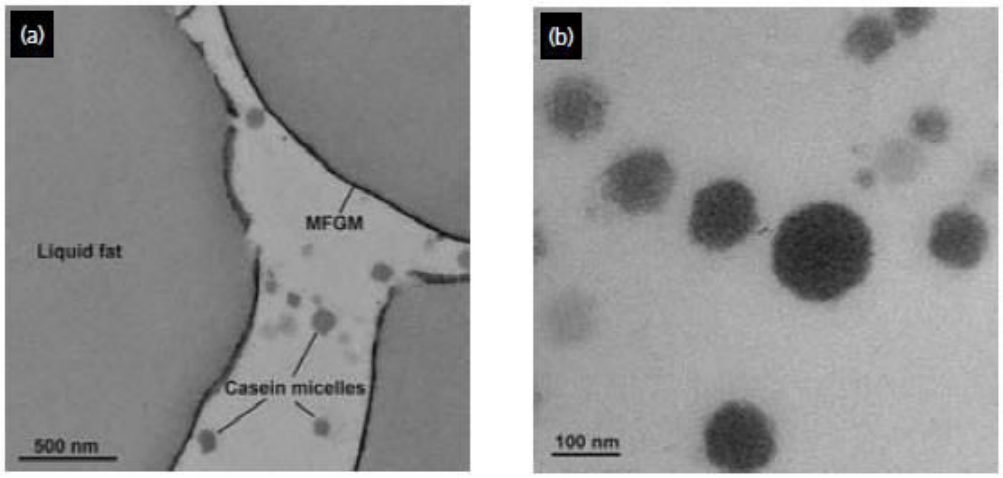

Figure 2.1. Raw milk at ambient temperature observed by transmission electron microscopy, (a) where fat is present and (b) in the absence of fat (Tamine et al., 2007).

The ability of milk to be processed into a variety of products is mainly due to the physicochemical characteristics of its proteins that confer various tecnofunctional properties (gelling, foaming, emulsifying, etc.) (Croguennec et al., 2008). Finally, milk is a system under dynamic equilibrium and several changes may occur on modifying its composition and structure. These changes may be physical (foaming), chemical (oxidation, lipolysis, proteolysis) and microbial (production of acid lactic).

2.1.2. Cracking of milk

Milk is a constituent of many food products. If the milk components are available separately a wider range of functionalities properties such as foaming, emulsifying, etc., can be used for new applications. Fractionated milk components provide a more constant quality of consumer products and the development of new products, such as bio-active peptides. Milk fractionation therefore leads to a more efficient and diverse use of milk. Furthermore, working with concentrated streams may reduce the cost of transport significantly and also have environmental advantages. Membrane separation technology seems a logical choice for the fractionation of milk, because many milk components can be separated on size (Fig. 2.2).

Membranes are already well established for the processing of whey and are gaining popularity in other dairy applications (Daufin et al., 2001). These processes lead to the fractionation of dairy components, i.e. the "cracking" of milk (Fig. 2.3) and whey (Fig. 2.4). Progress is still being made on the extent of fractionation of milk and whey using more specific combinations of membrane filtration and other separation techniques (electrodialysis, ion exchange, and chromatography) and/or chemical treatments (such as acidification or hydrolysis).

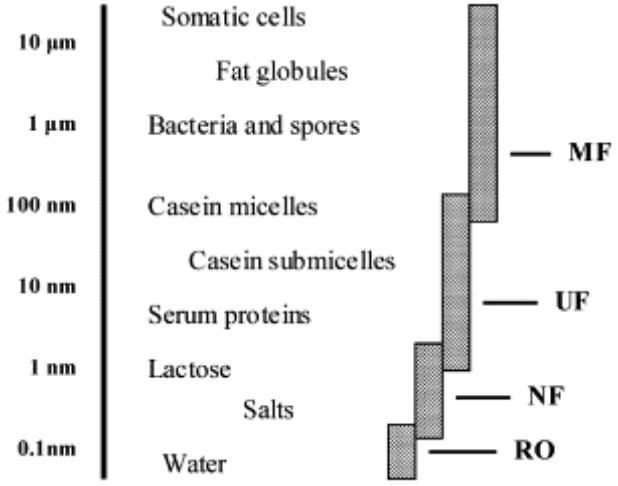

Figure 2.2. Components in milk: size indication and membrane processes. MF= microfiltration, UF = ultrafiltration, NF = nanofiltration, RO = reverse osmosis (Brans et al., 2004).

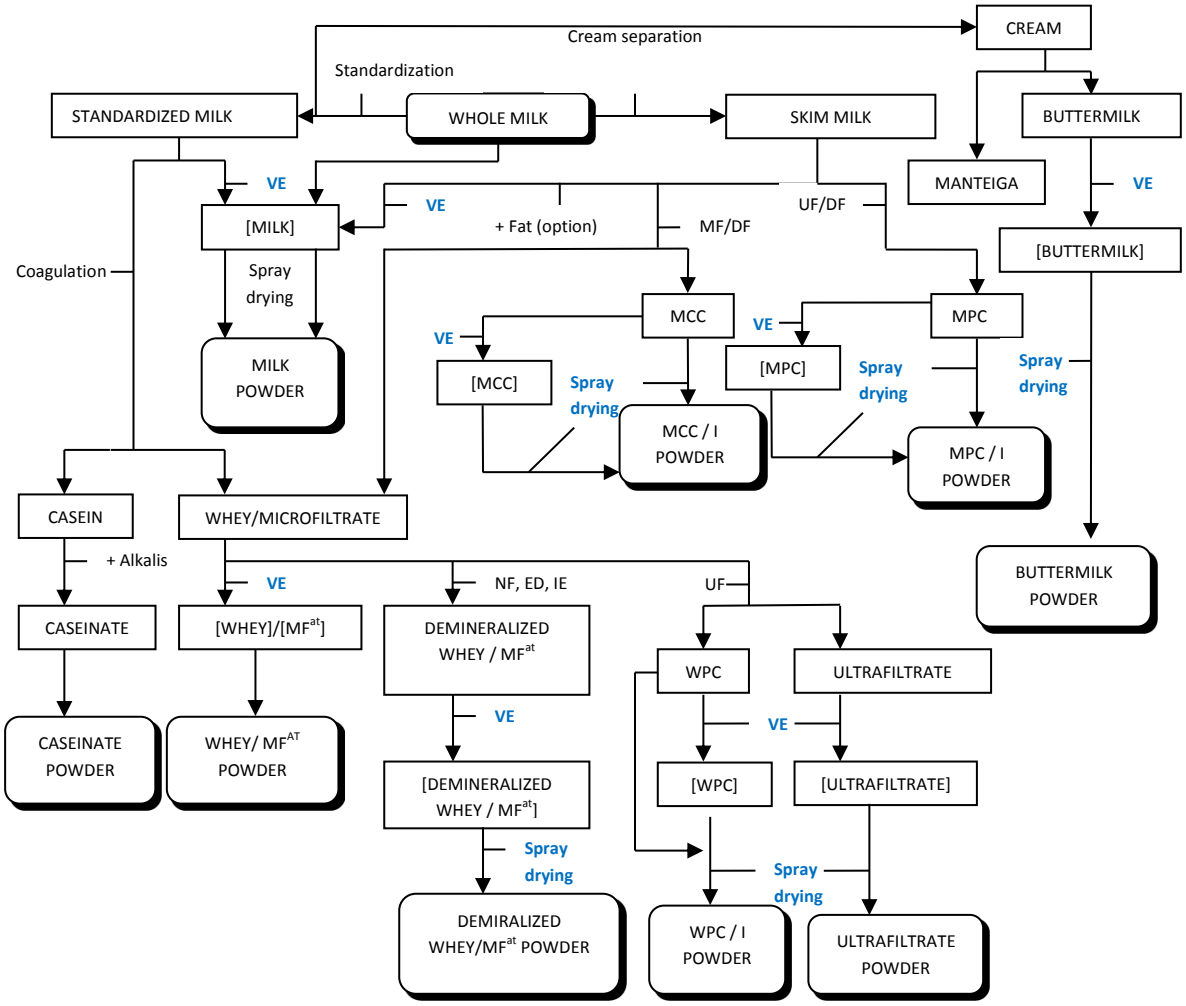

Figure 2.3. "Cracking" of milk featuring the vacuum evaporation and spray drying processes (Schuck, 2002).

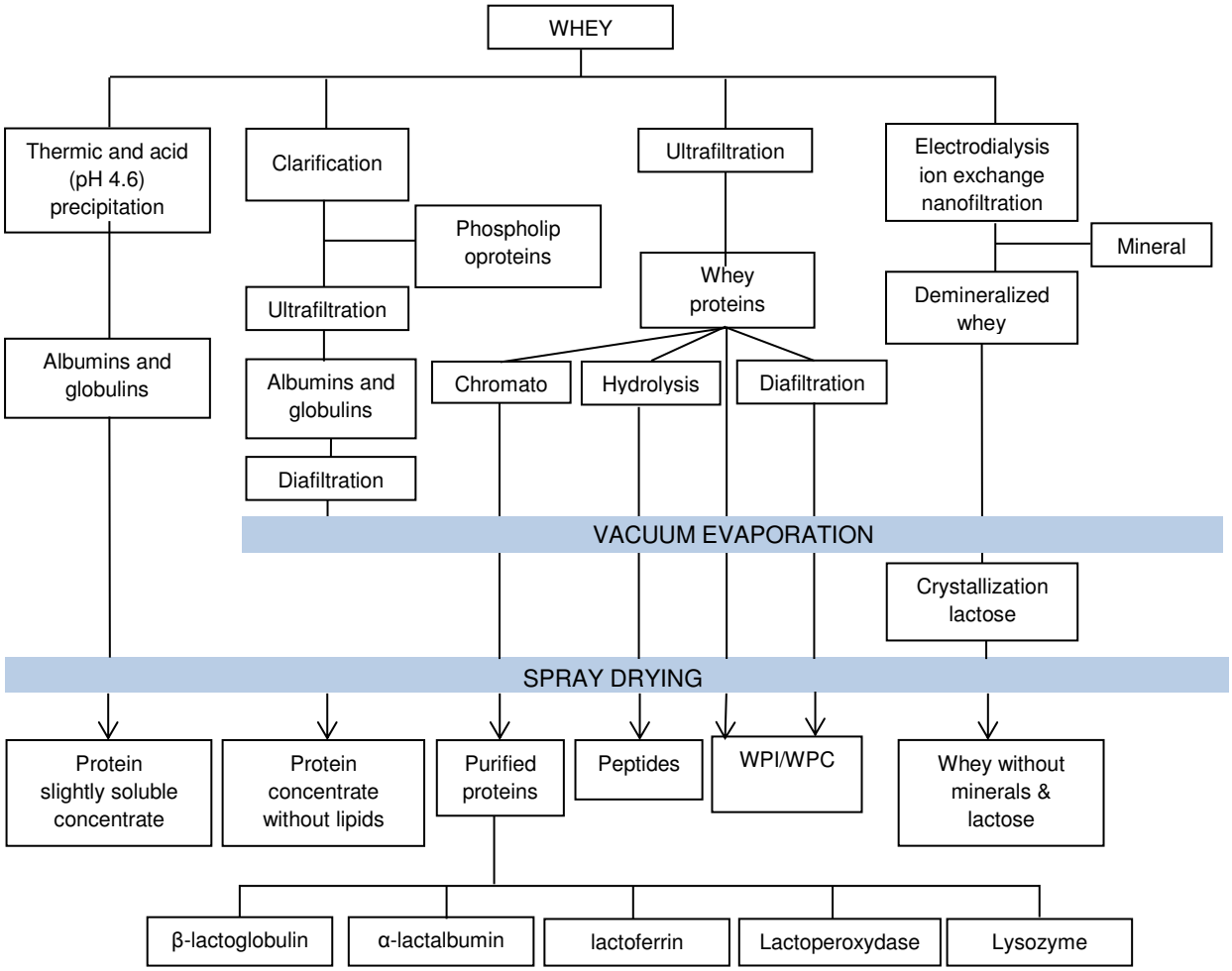

Figure 2.4. Whey cracking. Modified from Lortal and Boudier (2011).

Once the component of interest has been extracted, the solution is very often concentrated and spray dried. The vacuum evaporation process is widely applied in the food industry for the concentration of solutions (Fig. 2.5). Although more energy expensive than membrane concentration processes (Table 2.3), this process yields more viscous products, which is not possible with membrane techniques.

Table 2.3. Energy consumption for various water removal processes.

Processes	Energy Consumption ($kWh \cdot t^{-1}$ removed water or permeate)
Membrane processes	
Ultrafiltration	3 to 4
Nanofiltration	5 to 7
Reverse osmosis	9 to 10
Vacuum evaporation*	100 to 300
Spray drying	1,000 to 2,000
Freeze drying	5,000 to 10,000

* Vacuum evaporator without mechanical vapor re-compression

The vacuum evaporation process is currently used before drying for production of dairy products (Gray, 1981) (Fig.2.5). According to Jebson and Iyer (1991), the cost of the energy required for the evaporation of milk is a major factor determining the production cost of milk powder.

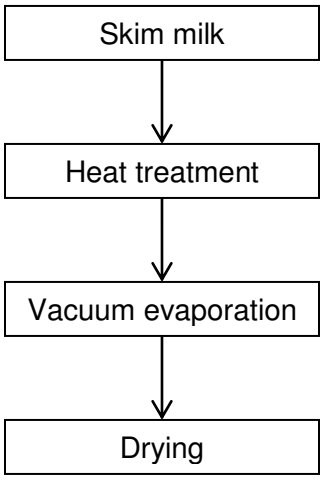

Figure 2.5. Flow diagram of the production of skim milk powder.

2.2. Vacuum evaporation

Evaporation is a process used to remove a liquid from a solution, suspension, or emulsion by boiling off some of the liquid. It is thus a thermal separation or thermal concentration process. The evaporation process is defined as one that starts with a liquid product and ends up with a more concentrated, but still liquid and still pumped concentrate as the main product from the process (Kessler, 1981). There are in fact a few instances where the evaporated, volatile component, is the main product, but these are not discussed in this work. In the food domain evaporation is used for product concentration, volume reduction, water / solvent recovery and crystallization (Bimbenet et al., 2007).

In the field of thermal separation / concentration technology, evaporation plants are widely used for concentration of liquids in the form of solutions, suspensions, and emulsions. The major requirement in the field of evaporation technology is to maintain the quality of the liquid during evaporation and to avoid damage to the product. This may require the liquid to be exposed to the lowest possible boiling temperature for the shortest period of time. In the food industry evaporation is performed at absolute pressures in the order of 0.02 MPa to 0.09 MPa (pressures below atmospheric pressure). The term "vacuum" is therefore used to classify this process.

In the dairy industry, vacuum evaporation is a process used for the production of final (sweetened condensed milk, evaporated milk, etc.) (Gänzle et al., 2008), and intermediate products before any further operations such as crystallization, precipitation, coagulation or drying (infant formulae, whey and milk powders, etc.) (Bimbenet et al., 2007; Schuck, 2002; Zhu et al., 2011).

2.2.1. Evaporators

An evaporator is the device or set of devices used to achieve evaporation. The destination of the vapor emitted is essential in the study of an evaporator. Even if there is no potential use, it is necessary to condense such vapor. The vapor to be condensed is generally used to heat the incoming products. This preheating serves to improve the energy use, and the functional operation of the evaporator, since the liquid enters the evaporator at a temperature close to its boiling temperature (Jeantet et al., 2011).

For vacuum evaporators, the vapor emitted is aspirated into the condenser by a condenser pressure (P_c) lower than the evaporation pressure (P_{ev}). P_c is controlled by the liquid-vapor equilibrium that exists within the condenser. This means that the lowest pressure that can be obtained in an evaporator is imposed by the temperature of the condensation of the product vapor in the condenser. The vacuum pump connected to the condenser is only responsible for evacuating the air out of the plant and for removing the incondensable gases. The amount of gases to be evacuated depends on the amount of gas dissolved in the product and especially of the quality of the vacuum tightness of the system (including pipes, pump seals, etc.) (Bimbenet et al., 2007).

There are two main types of condenser (Fig. 2.6): mixture condensers (the vapor emitted is cooled by mixing with cold water) and wall exchange condensers (tubular heat exchanger) (Kessler, 1981). The vapor can also be condensed by mechanical refrigeration (as in lyophilization) but this very expensive technology is justified only in special cases, i.e. flavor recovery in coffee (Bimbenet et al., 2007).

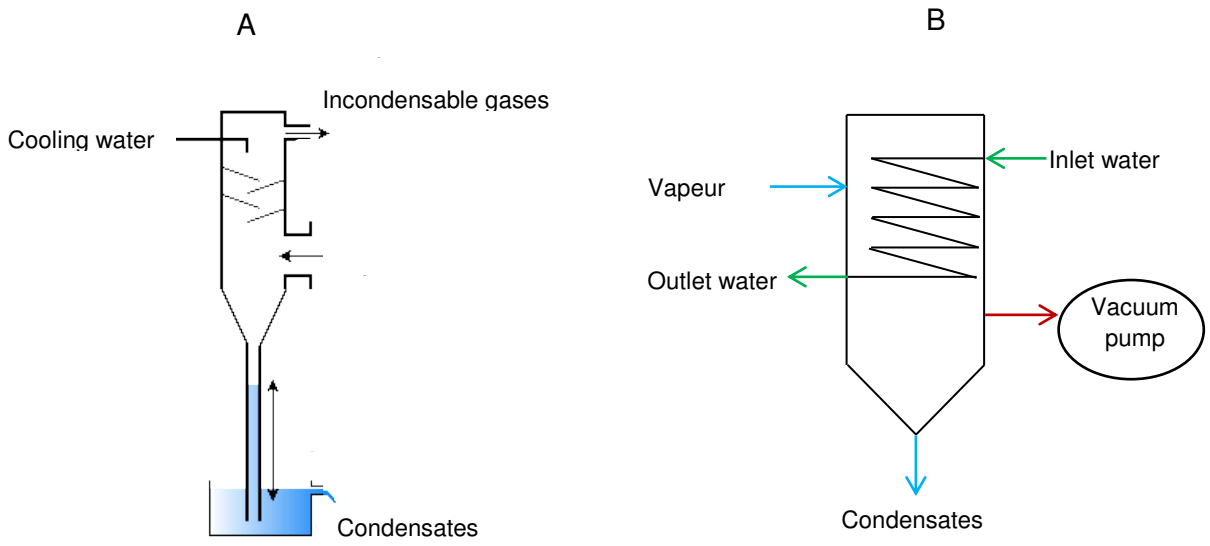

Figure 2.6. Diagram of: (A) mixture condensers, and (B) wall exchange condenser.

While the design criteria for evaporators are the same regardless of the industry involved, two questions always exist: is this equipment best suited for the purpose and is the equipment arranged in the most efficient and economical way? As a result, many types of evaporator and many variations in processing techniques have been developed to take into account different product characteristics and operating parameters. The most common types of evaporators used currently are:

- Rising film evaporators
- Forced circulation evaporators
- Plate evaporators
- Falling film evaporators

Other types of evaporator, include the inclined tube evaporator, forced-circulation evaporator, wiped film evaporator, etc. (Leleu, 1992).

2.2.1.1. Rising film evaporators

These evaporators operate on a "thermo-siphon" principle. Feed enters at the bottom of the heating tubes and as it heats, vapor begins to form (Fig. 2.7). The ascending force of this vapor produced during boiling causes liquid to flow upwards. At the same time vapor production increases and the product is pressed as a thin film on the walls of the tubes (Smith and Hui, 2008).

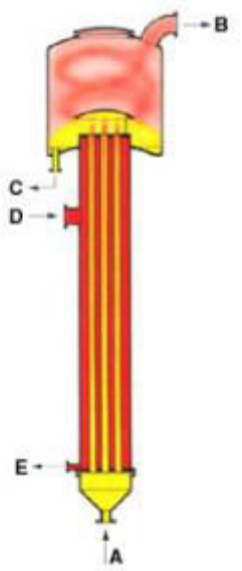

A: Product
B: Vapor
C: Concentrate
D: Heating Steam
E: Condensate

Figure 2.7. Rising Film Evaporator (www.niroinc.com).

This co-current upward movement has the beneficial effect of creating a high degree of turbulence in the liquid. This is advantageous during evaporation of highly viscous products. A large temperature difference is need between the heating and boiling sides of this type of evaporator, otherwise the energy of the vapor flow is not sufficient to convey the liquid and to produce the rising film. The length of the boiling tubes will typically not exceed 7 meters. This type of evaporator is often used with product recirculation, where some of the concentrate

formed is reintroduced back to the feed inlet in order to produce sufficient liquid loading inside the boiling tubes.

2.2.1.2. Forced circulation evaporator

Forced circulation evaporators (Fig. 2.8) are used if boiling of the product on the heating surfaces is to be avoided due to fouling or crystallization. The flow velocity in the tubes must be high, and high-capacity pumps are required. The circulating liquid is heated when it flows through the heat exchanger and then partially evaporated when the pressure is reduced in the separator, cooling the liquid to the boiling temperature (Smith and Hui, 2008).

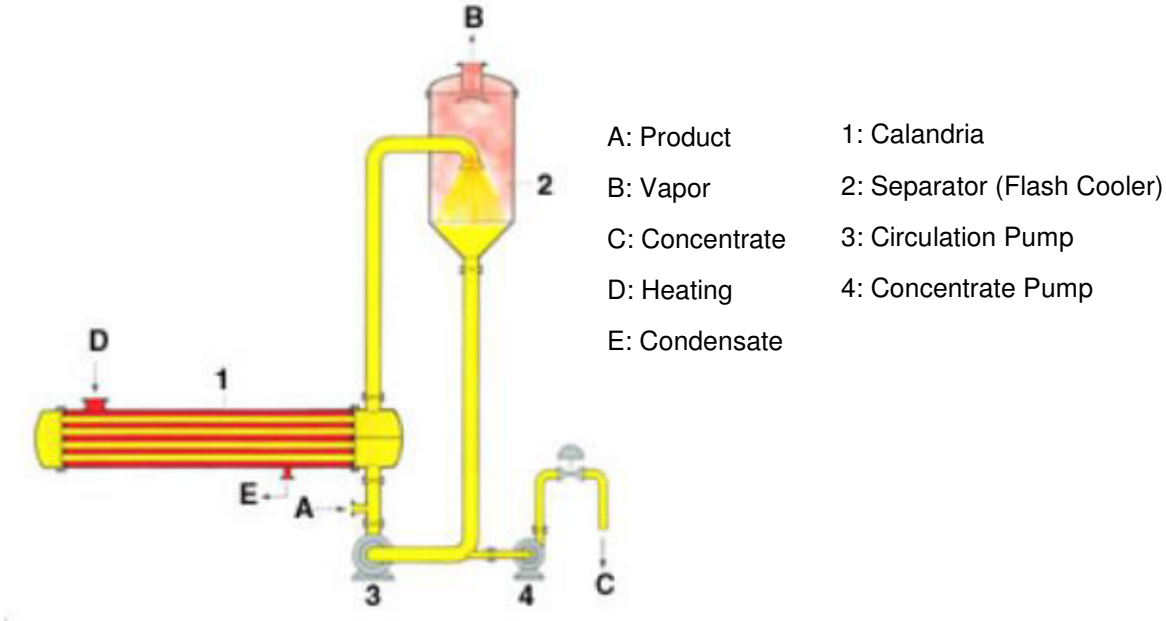

Figure 2.8. Forced circulation evaporator (www.niroinc.com).

The liquid is typically only heated a few degrees for each pass through the heat exchanger, which means the recirculation flow rate has to be high. This type of evaporator is also used for crystallizing applications because no evaporation and concentration take place on the heat transfer surface. Evaporation occurs as the liquid is flash evaporated in the separator / flash vessel. In crystallizing applications this is then where the crystals form, and special

separator designs are used to separate crystals from the recirculated crystal slurry. The heat exchanger can be arranged either horizontally or vertically depending on the specific requirements in each case.

2.2.1.3. Falling film evaporators

The need, for an evaporator capable of functioning with a very small temperature difference between heat steam and product, imposed by shorter process times and operating economy led to the application of the falling film evaporation principle (Gray, 1981). With this arrangement the product is made to flow downwards in a film over the heating surface. The principal driving force is gravity. In contrast to the climbing film evaporators, high heat fluxes and temperature differences are not required to establish the desired flow conditions. The heat transfer surface may be in the form of either tubes or plates, but capacity limitations of the falling film plate evaporator have led to the tubular version being much more widely applied (Gray, 1981). The falling film tubular evaporator is currently the standard type used in the dairy industry.

In falling film evaporators (FFE) (Fig. 2.9), liquid and vapors flow downwards in parallel. The liquid to be concentrated is preheated to boiling temperature. An even thin film enters the heating tubes via a distributor system in the head of the evaporator, flows downward at boiling temperature, and is partially evaporated. This gravity-induced downward movement is increasingly augmented by the co-current vapor flow.

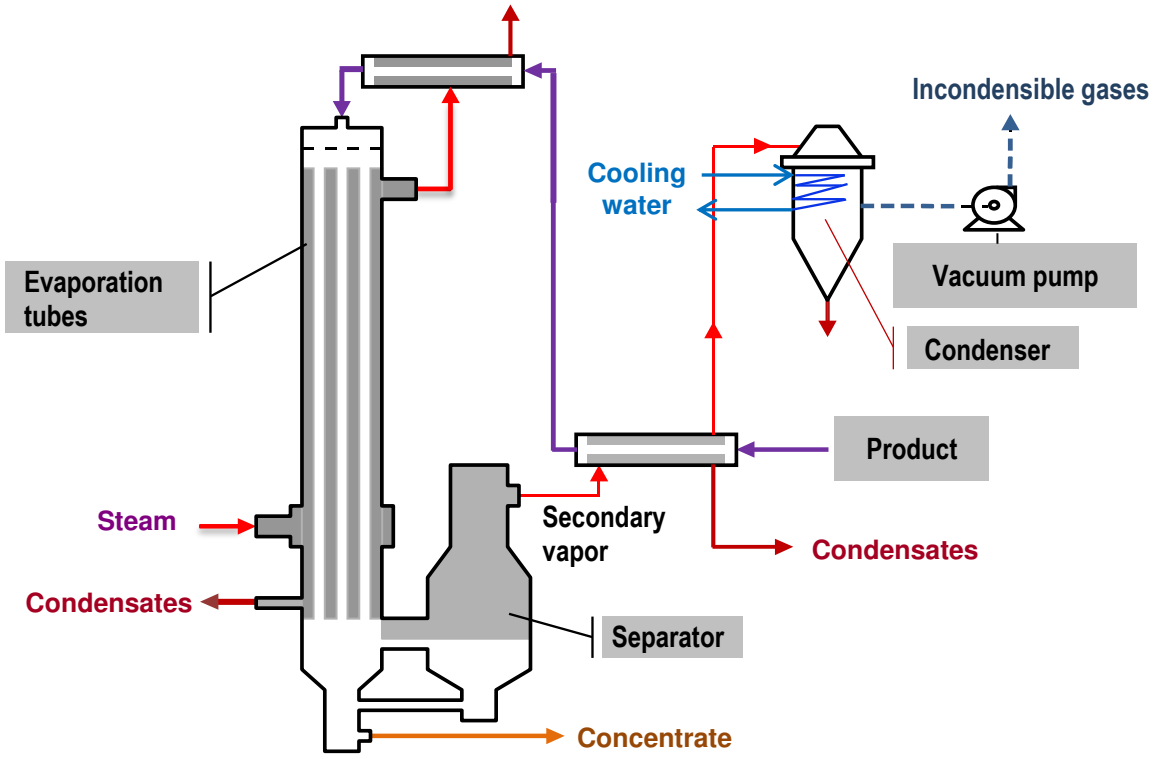

Figure 2.9. Falling film evaporator. Addapted from Jeantet et al. (2011).

However, falling film evaporators must be designed very carefully for each operating condition; sufficient wetting of the heating surface by liquid is extremely important for trouble-free operation of the plant (Morison et al., 2006). Due the low liquid holding volume in this type of unit, the falling film evaporator can be started up quickly and changed to cleaning mode or another product easily. The fact that falling film evaporators can be operated with small temperature differences makes it possible to use them in multiple effect configurations with very low energy consumption.

2.2.2. Energy efficiency

To become even more energy efficient the vapor produced in one falling film evaporator can be used to heat another evaporator operating at a lower pressure and temperature. The first evaporator thus acts as a "boiler" for the second. Similarly, the second serves as a condenser for the first (Fig. 2.10). This way of recycling the water vapor continuously in series is often termed multi-effect evaporation. With *n* evaporators added in series to recycle the water vapor for use in the next evaporator, the energy usage can be decreased by approximately $1/n_{effects}$.

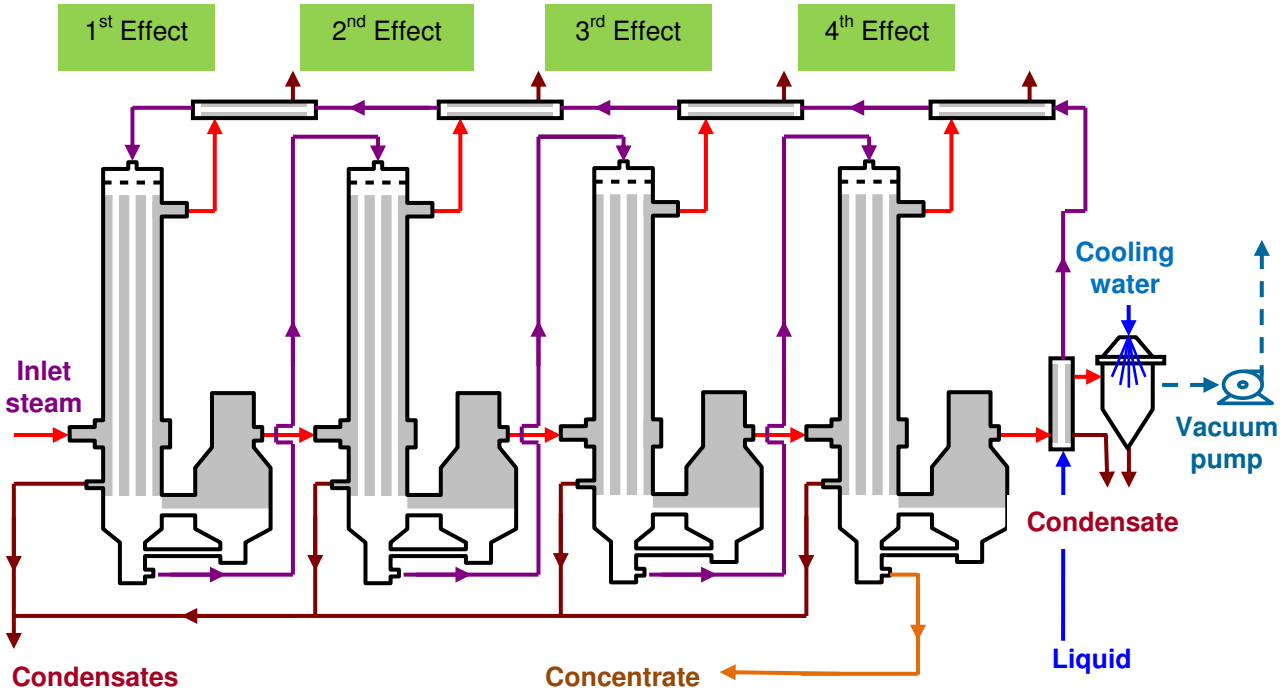

Figure 2.10. Multi-effect evaporator (Jeantet et al., 2011).

The economic optimization of the number of effects is chosen for a minimum total cost of the evaporation process. The main elements of the total cost (TC) are the investment costs (IC); the consumption costs (CC) of heating steam, water, electricity, etc.; and the staff cost (SC). These various costs vary with the number of effects *n* (Fig. 2.11).

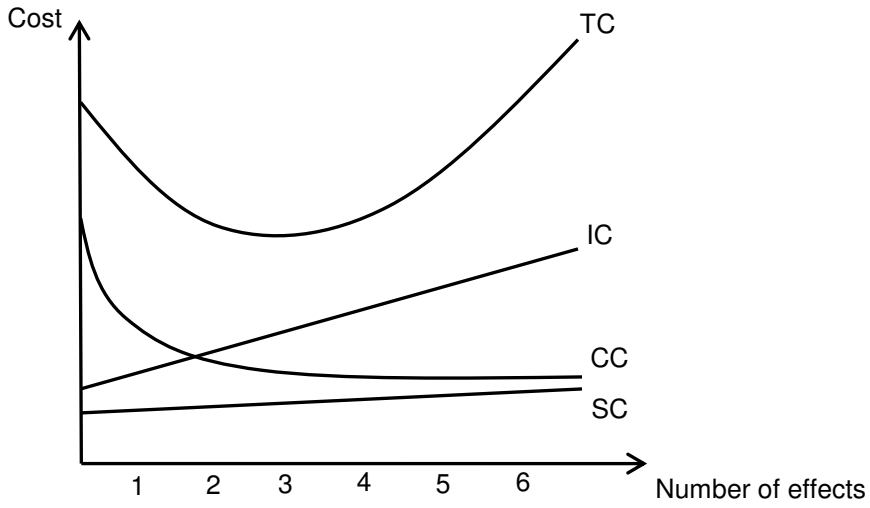

Figure 2.11. Diagram of the cost components of an evaporator as a function of the numbers of effects. IC = investment cost; CC = cost of consumption; SC = staff costs and TC = total cost = IC + CC + SC (Jeantet et al., 2011).

The curve of the total cost (Fig. 2.11) passes through a minimum for a given *n* value. This number rounded to the nearest whole number, is the optimum number of technical and economic effects.

In order to reduce the energy consumption and environmental impact, it is important that evaporators operate at their maximum capacity, which is highly dependent on the overall heat transfer coefficient. This parameter cannot be considered as an intrinsic characteristic of the evaporator, since it also depends on the nature of the product and on their flow conditions (Mafart, 1991). The factors that control heat transfer in the evaporator tubes are important for close monitoring of the evaporation process and for the calculation of the evaporators dimensions (Bouman et al., 1993; Jebson and Iyer, 1991).

2.2.2.1. Heat transfer coefficient

Knowing the heat transfer coefficient is essential to monitor the evaporation process closely. In most dairy factories the total energy usage is known, but often information on the quantities of energy used for individual processes is lacking (Jebson and Chen, 1997).

For all types of evaporator, the evaporation rate depends on the heating power ($\dot{Q}$), which depends on the overall heat transfer coefficient (U), the heat exchange area (A), and the temperature difference between the heating steam and the boiling liquid, Δθ, Eq. 2.1:

$$\dot{Q} = U \cdot A \cdot \Delta\theta \qquad \text{Eq. 2.1}$$

The design, optimization and investment costs of the unit are thus strongly dependent on the predicted value of this variable (Prost et al., 2006).

The inverse overall heat transfer coefficient (1/U) for a given effect is resistance resulting from four resistances in series: the resistance of the heating steam side ($1/h_v$), the resistance of conduction through the wall (e_m/λ_m), the resistance of an eventual fouling layer ($R_{fouling}$) and the resistance of the product ($1/h_p$) (Fig. 2.12, Eq. 2.2).

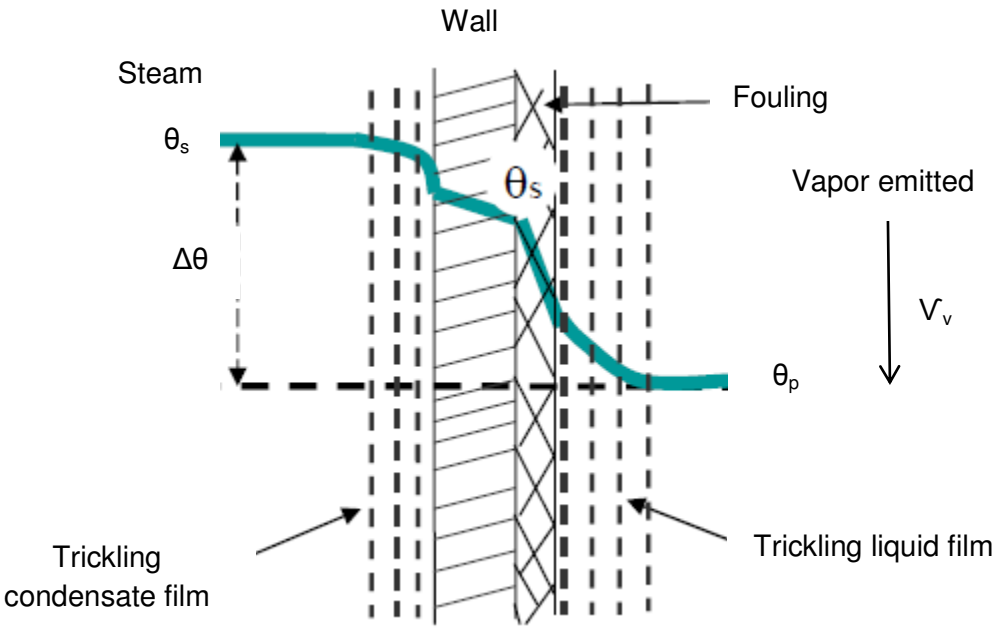

Figure 2.12. Temperature profile between the heating steam (θs) and the boiling product (θp) at a steady regime in a falling film evaporator (Adib, 2008).

Legend: V_v: vapor velocity and Δθ: temperature difference between steam and product

$$\frac{1}{U} = \frac{1}{h_{v-1}} + \frac{e_m}{\lambda_m} + R_{fouling} + \frac{1}{h_p} \qquad \text{Eq. 2.2}$$

where h_{v-1} is the steam heat transfer coefficient ($kW \cdot m^{-2} \cdot °C^{-1}$), λ_m the thermal conductivity of the wall ($kW \cdot m^{-1} \cdot °C^{-1}$), e_m the wall thickness (m), $R_{fouling}$ the thermal resistance of the fouling layer ($kW \cdot m^{-2} \cdot °C^{-1}$) and h_p the product heat transfer coefficient ($kW \cdot m^{-2} \cdot °C^{-1}$)

The heating steam condenses to form a film condensate along the external wall of the evaporator tube. The steam heat transfer coefficient is in the order of 5,000 $W \cdot m^{-2} \cdot °C^{-1}$ to 15,000 $W \cdot m^{-2} \cdot °C^{-1}$. h_{V-1} can be calculated by equations based on the Nusselt number (Eq. 2.3) (Adib et al., 2009), eventually adjusted to take into account of the shape and arrangement of the heating surfaces, the speed of the heat steam, the presence of non-condensable gas, the surface condition of the wall, etc. (Bouman et al., 1993).

$$N_u = 0.693 \cdot R_e^{-\frac{1}{3}}$$ Eq. 2.3

where

$$N_u = \frac{h_{v-1}}{\lambda_m}\left(\frac{\eta^2}{\rho^2 \cdot g}\right)^{\frac{1}{3}}$$ Eq. 2.4

where h_v is the heat transfer coefficient of the condensing steam ($kW \cdot m^{-2} \cdot °C^{-1}$), Re the Reynolds number (-), η the viscosity of the condensate steam (Pa·s), ρ the density of the condensate steam ($kg \cdot m^{-3}$), and g the gravity acceleration ($m \cdot s^{-2}$)

The heat transfer coefficient through the wall, $(\frac{\lambda_m}{e_m})$, is easier to calculate, because the thermal conductivity coefficients of the materials constituting the exchange surfaces are known, as well the wall thickness. These coefficients are generally high, in the order of 10 $kW \cdot m^{-2} \cdot °C^{-1}$ to 20 $kW \cdot m^{-2} \cdot °C^{-1}$, which corresponds to a low thermal resistance, that can often be disregarded.

The potential fouling layer must be taken into account in the calculation of the overall heat transfer coefficient. Fouling of heat transfer surfaces is one of greater problems in heat transfer equipment.

Generally the product heat transfer coefficient, h_p, is the most difficult to predict, and often it is the limiting factor for the heat transfer, especially for viscous concentrates. The heat transfer coefficient for pure water evaporated at Δθ = 10°C is in the order of 6 $kW \cdot m^{-2} \cdot °C^{-1}$ to 15 $kW \cdot m^{-2} \cdot °C^{-1}$. According to many authors (Bimbenet et al., 2007; Miranda and Simpson, 2005; etc.), h_p depends on several factors such as physical properties of the treated product (viscosity η_p, surface tension σ_p, density ρ_p, etc.); process conditions (heat flux, temperature difference Δθ, boiling temperature θ_p); and nature and geometry of the heating surface, (roughness R, etc.). These factors are summarized in Eq. 2.5.

$$h_p = f(\rho_p, \sigma_p, \eta_p, C_{p_p} \ldots \Delta\theta, R, \text{etc.})$$ Eq. 2.5

where σ_p is the product surface tension ($N \cdot m^{-1}$) and Cp_p the product specific heat ($kJ \cdot kg^{-1} \cdot °C^{-1}$)In this work, only the overall heat transfer coefficient U ($kW \cdot m^{-2} \cdot C^{-1}$) (Eq. 2.1) is discussed. For falling film evaporators this coefficient are in order of 1 $kW \cdot m^{-2} \cdot °C^{-1}$ to 8 $kW \cdot m^{-2} \cdot °C^{-1}$ (Bimbenet et al., 2007).

2.3. Thermo-physical properties of dairy concentrates

Estimation of U in all chemical engineering formulas currently available in the literature is connected to thermo-physical properties of products. These thermo-physical properties (η_p, ρ_p, λ_p ...) generally vary with the concentration and temperature of the product, and possibly also as a function of shear rate in the case of a non-Newtonian fluid.

2.3.1. Viscosity of dairy concentrates

The rheological behavior of dairy concentrates changes during the evaporation process due the changes in the product concentration and temperature. It can be modified by the shear rate, expressed by the velocity gradient, $\dot{\gamma}$ (s^{-1}):

$$\dot{\gamma} = \frac{dv}{dx} \qquad \text{Eq. 2.6}$$

Therefore the apparent viscosity, η_a, is used to represent and classify the flow profile of dairy concentrates. This defined as:

$$\eta_a = \frac{T}{\dot{\gamma}} \qquad \text{Eq. 2.7}$$

where T is the shear stress (Pa)

According to the relationship between the shear stress and the shear rate presented in Eq. 2.7, two types of rheological behavior can be distinguished (Fig. 2.13).

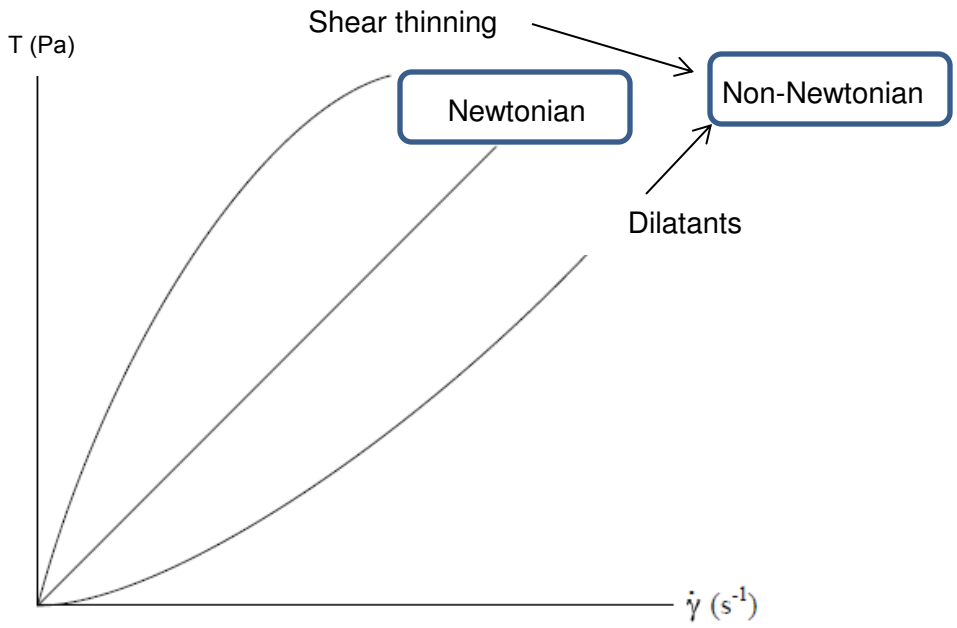

Figure 2.13. Newtonian and non-Newtonian fluids.

For Newtonian fluid the viscosity only depends on the temperature and concentration. On the other hand for the Non-Newtonian fluids the viscosity depends on the shear rate in addition to the temperature and concentration.

2.3.2. Thermal properties of dairy concentrates

Some thermal properties of dairy concentrates can be used for the estimation of heat transfer coefficients and enthalpy balances for an evaporator. These properties are:

• Specific heat C_p ($kJ \cdot kg^{-1} \cdot °C^{-1}$)

At temperature θ, C_p is the amount of heat (in kJ) to be supplied to 1 kg of product, to raise its temperature by 1°C.

• Specific enthalpy: ($kJ \cdot kg^{-1}$)

The specific enthalpy of a solution depends on its temperature and composition. For a solution composed of sugars, salts, proteins and lipids, such as dairy concentrates, the specific enthalpy can be calculated according to Rahman, 2009:

$$H_p = C_p \cdot \theta_p \qquad \text{Eq. 2.9}$$

The specific enthalpy of the water vapor emitted at temperature θ_p of the concentrate is given by the following equation:

$$H_{v-1} = 4.18 \cdot \theta_{sat} + \Delta H_v \qquad \text{Eq. 2.10}$$

• Enthalpy of vaporization: ΔHv ($kJ \cdot kg^{-1}$)

The enthalpy of vaporization, also known as the latent heat of vaporization or heat of evaporation, is the energy required to transform a given quantity of a substance from a liquid into a gas at a given pressure. For example the ΔH_V for pure water at 100°C = 2258 $kJ \cdot kg^{-1}$.

For a food product, the binding of water on the solute will result in a boiling point elevation, i.e. a saccharose solution at 700 $g \cdot kg^{-1}$ of total solids has a boiling point elevation around 2.7°C when concentrated at 80°C (Bimbenet et al., 2007).

• Thermal conductivity λ ($W \cdot m^{-1} \cdot °C^{-1}$):

Thermal conductivity is the property of a material to conduct heat. It can be defined as the quantity of heat transmitted through a unit thickness of a material - in a direction normal to a surface of unit area - due to a unit temperature gradient under steady state conditions. The skim and whole milk thermal conductivity is around $0.563 \cdot 10^{-3}$ $kW \cdot m^{-1} \cdot °C^{-1}$ and $0.537 \cdot 10^{-3}$ $kW \cdot m^{-1} \cdot °C^{-1}$, respectively.

2.4. Flow in falling film evaporators

In FFE a complete film should be maintained inside the tubes over the process time. This requires that the liquid is first distributed to all the tubes to provide sufficient flow. The film must then be maintained down the tubes. Film breakdown (Fig. 2.14) will decrease the efficiency of the process and may cause excessive fouling (Paramalingam et al., 2000).

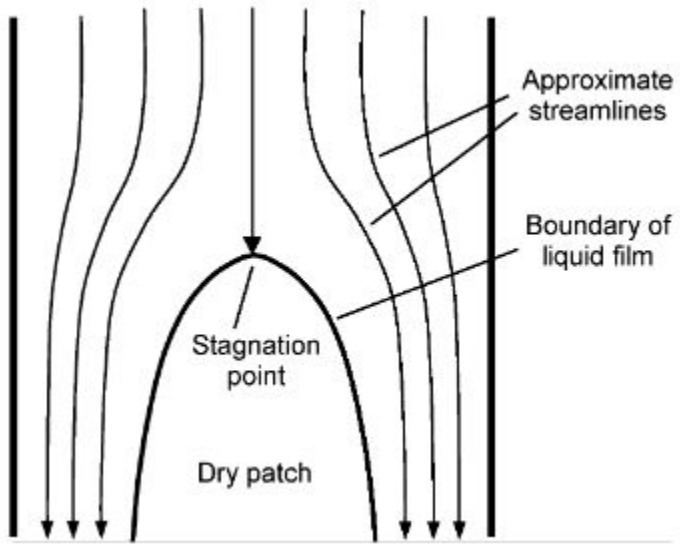

Figure 2.14. Film breakdown (Hartley and Murgatroyd, 1964; Morison et al., 2006).

In an industrial evaporator a distributor system is installed above the top tube sheet. A falling-film distributor (Fig. 2.15) is a critical component in the evaporator, which makes the liquid flow evenly inside the tube and affects the production capacity and service life of the evaporator. Unfortunately, industrial liquid film distributors have certain shortcomings, such as structural complexity, large area, high requirement for production and processing precision, poor uniformity and wettability of falling film (Anurjew et al., 2011; Luo et al., 2011).

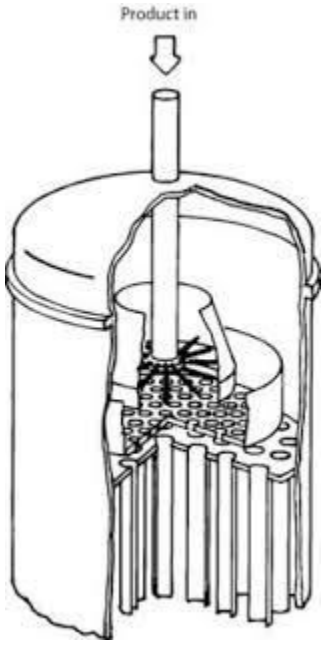

Figure 2.15. Plan of a typical distributor system for a falling film evaporator tube (www.gea.com).

The flow in falling film evaporators is often characterized by using dimensionless numbers. The most important parameter is the film Reynolds number (Re_f), which measures the extent of the inertia relative to viscous effects.

$$Re_f = 4\frac{\Gamma}{\eta} \qquad \text{Eq. 2.11}$$

where Γ is the mass flow rate per unit circumference of the tube ($kg \cdot m^{-1} \cdot s^{-1}$) and η the apparent viscosity of the product (Pa·s).

Γ is measured according to equation 2.12:

$$\Gamma = \frac{\dot{m}}{\pi D} \qquad \text{Eq. 2.12}$$

where $\dot{m}$ is the concentrate mass flow rate ($kg \cdot s^{-1}$) and D the inner diameter of the tube (m).

There are many different classifications of falling film flows in the literature. Grossman and Heath (1984) divided the flow into three regimes, smooth laminar, transition region and fully turbulent flow, where the transition region can in turn be divided into different regions. Numrich (1992) divided the flow into only two regions, the laminar and the turbulent. Bird et al. (1960) established the flow profiles in three regions: laminar, laminar with waves and turbulent. What varies between these different classifications is how the transition from laminar to turbulent flow is handled.

2.4.1. Residence time distribution functions

The residence time distribution (RTD) of fluids passing through a food processing plant can be important for public safety and product quality reasons. It is often assumed for design purposes that either a laminar or plug flow regime exists and that the residence times can be calculated from volume and flow rate (Janssen, 1994). Moreover, in falling film evaporators the product flows in a thin layer in the evaporations tubes, thus making it difficult, to determine plant volume accurately. For such situations, it is necessary to measure the plant RTD directly.

The mathematics and techniques for RTD determination were developed in the field of chemical engineering (Danckwerts, 1953). The most common technique is injecting an inert tracer into the feed stream and measuring the concentration in the product stream over time (Fig. 2.16).

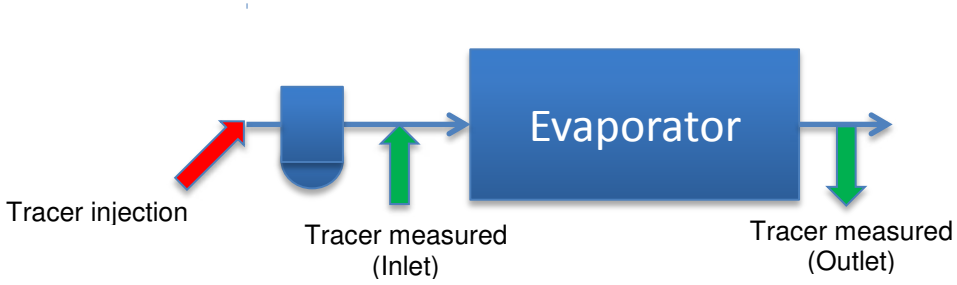

Figure 2.16. Diagram of measurement of tracer for calculation of residence time distribution.

Each element of fluid takes a different route and time through the processing unit. The distribution of these times at the outlet of the unit is called the E-curve or age distribution function, E(t), which characterizes the residence time distribution (RTD) of the process. The simplest way to obtain the E(t) is by the pulse experiment, where a small amount of a non-reactive tracer is injected simultaneously at the unit inlet and its concentration is continuously recorded at the outlet C(t) (Fig. 2.16). The E-curve is then obtained from Eq. (2.13), where C_0 is the total tracer concentration (Levenspiel, 1999).

$$E(t) = \frac{C(t) - C_0}{\int_0^\infty C(t) - C_0 \, dt} \qquad \text{Eq. 2.13}$$

$$\int_0^\infty E(t) dt = 1 \qquad \text{Eq. 2.14}$$

Since the pioneering work of Danckwerts (1953), the RTD theory has been widely developed and is nowadays used in a more general context in order to determine a population balance model (Villermaux, 1982), where the basis of this model is that the number of entities with certain properties in a system is a balanceable quantity. Such properties include size, mass, and age. RTD theory is also used to optimize the process in terms of capital and operation costs (Malcata, 1991). The latter represent an essential step in managing and controlling the quality of food products. Burton et al., (1959) applied the concept of RTD to food engineering in order to calculate the sterilizing effectiveness of a UHT apparatus for milk processing. Baloh (1979) showed that the loss of sugar in pasteurization and evaporation processes of various processing schemes in the sugar industry could be significantly lowered by reducing the mean residence time of sweet juice. Thor and Loncin (1978) established the mechanisms of rinsing (e.g. mass flow rate and shear stress) of a plate heat exchanger by the measurement of RTD, and thereby laid down the basis for optimizing the rinsing of equipment in food engineering. Jeantet et al. (2008) calculated and modeled the RTD for different sections of a spray-dryer tower for skim milk, and described the heat treatment that the product was subjected in this process.

For tube flow, the RTD is associated with the velocity profile and the dispersion flow of the product. Determination of the product RTD is an overall and experimental approach which provides valuable information about the product flow profile in the evaporator, according to the operating conditions. It does not provide a good physical understanding of the operation as computational fluid dynamics does but it integrates the product and process complexity fully.

2.4.2. Residence time distribution models

Ideal flow models such as plug flow, and perfectly mixed tank and laminar flow rarely reflect a real system with enough accuracy. Non-ideal models are usually derived from ideal models to account for deviations implicit in real systems (Torres and Oliveira, 1998). Models with one parameter, such as the well-known dispersion model, are usually more appropriate to represent tubular systems (Levenspiel and Bischoff, 1963). In this section, two single parameter models are presented which have mainly been used to fit the experimental RTD data for food reactors. The dimensionless E-curves of these models are illustrated in Fig. 2.16 and 2.17, where the effects of the model parameter can be observed.

2.4.2.1. Axial dispersion

The axial dispersion model can be used to represent small deviations from plug flow, as well as other non-ideal flow patterns in tubular systems. It has been widely applied to describe the flow in tubes and is the most frequent choice to model flow in holding tubes in aseptic processing (Torres and Oliveira, 1998). The model parameter is the Peclet number, which is defined for tube flow as:

$$P_e = L \cdot \frac{\nu}{D_{ax}} \qquad \text{Eq. 2.15}$$

where L is the tube length (m), ν the mean velocity ($m \cdot s^{-1}$) and D_{ax} the axial diffusion coefficient (-)

This dimensionless number represents the relation between advection (flow) and diffusion. When P_e approaches infinity, negligible dispersion is observed (ideal plug flow). When P_e approaches zero, wide dispersion is observed (perfectly mixed tank) (Fig. 2.17).

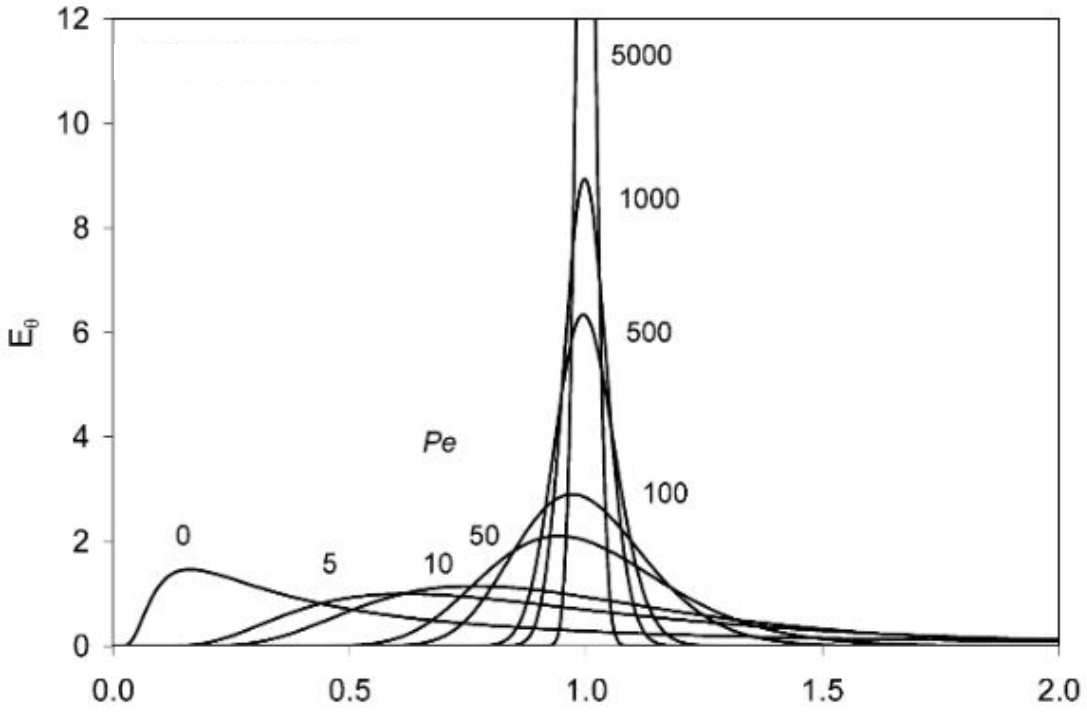

Figure 2.17. Dimensionless E-curves for the axial residence time distribution model (Villermaux, 1993).

The axial dispersion model can be calculated as:

$$E(t) = \sqrt{\frac{P_e+1}{4\cdot\pi\cdot t^3}} \exp\left(\frac{-(P_e+1)\cdot(1-t)^2}{4\cdot t}\right) \qquad \text{Eq. 2.16}$$

2.4.2.2. Extended tanks in series

The extended tanks in series model are based on a series of perfectly mixed tanks and can be used to represent deviations from plug flow and to represent real stirred tanks. The E function for this model is presented in Eq. 2.17, where the parameter being modeled is the number of tanks, N.

$$E(t) = \frac{N\cdot(N\cdot t)^{N-1}}{(N-1)!} \exp(-N\cdot t) \qquad \text{Eq. 2.12}$$

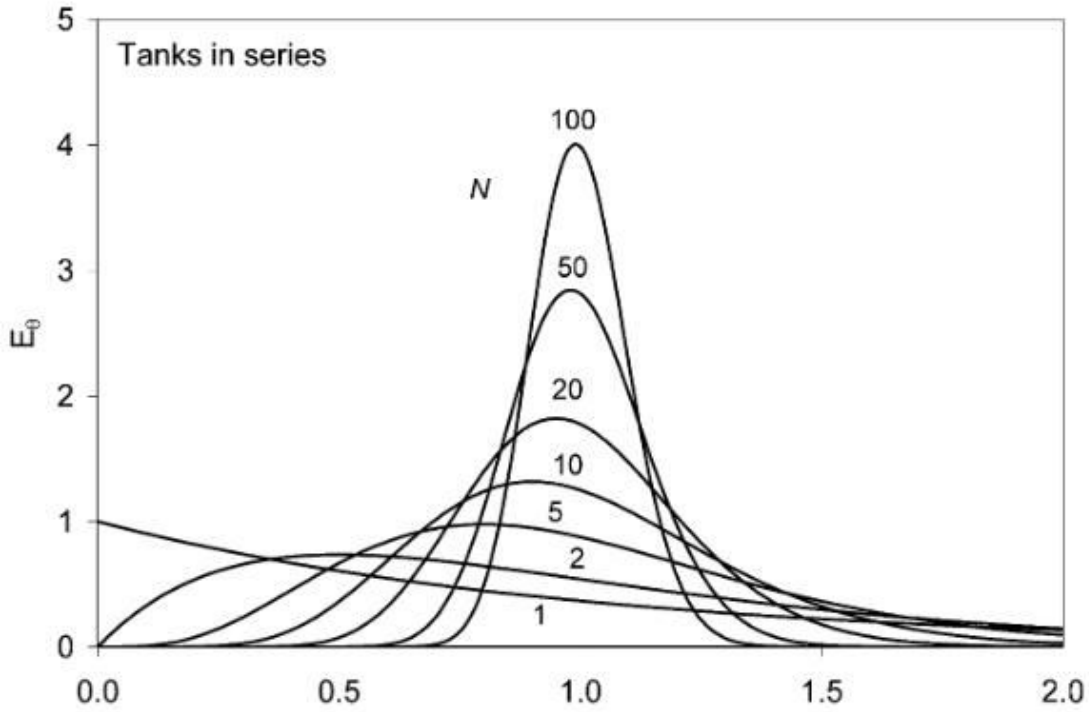

Figure 2.18. Dimensionless E-curves for the tanks in series residence time distribution model (Villermaux, 1993).

2.5. Fouling in falling film evaporators

Fouling is defined as the formation of deposits from the product on heat exchange surfaces which impede the heat transfer. In FFE a fouling layer accumulates on the inner wall of the evaporator tubes during processing (Jeurnink et al., 1996) leading to a decrease in the heat transfer coefficient, increased pressure drop, and the formation of a biofilm, thus impeding the optimal functioning of the evaporator equipment (Langeveld et al., 1990; Visser and Jeurnink, 1997).

Due to fouling that decreases the heat transfer coefficient, most evaporators do not have a constant production capacity. In petrochemical industries, pipe cleaning is carried out once a year, whereas in food-processing industries, it has to be done at least once a day (Ozden and

Puri, 2010). The high frequency of cleaning periods results in a shorter production time and higher consumption of water and cleaning agents, leading to high economic costs and ecological problems (Jimenez et al., 2013).

Milk fouling can be classified in two categories (Burton et al., 1959; Changani et al., 1997; Visser and Jeurnink, 1997): Type A (protein) where fouling takes place at temperatures between 75°C and 110°C, and the deposits are white, soft, and spongy (milk film); and type B (mineral) where fouling takes place at temperatures above 110°C. Type B deposits are hard, compact, granular in structure, and gray in color (milk stone) (Table 2.4).

Table 2.4. Composition of the two milk fouling categories (modified from Bansal and Chen, 2005).

Composition	Milk fouling category	
	Type A	Type B
Proteins ($g \cdot kg^{-1}$)	500 to 700	150 to 200
Minerals ($g \cdot kg^{-1}$)	300 to 400	700 to 800
Fat ($g \cdot kg^{-1}$)	40 to 80	40 to 80

Vacuum evaporators can be considered as heat exchangers in a first approach, where the main mechanism factors likely to generate fouling during the heat treatment of milk are: the formation and subsequent deposition of activated whey protein molecules; the precipitation of minerals as a result of the decreasing solubility of calcium phosphates with increasing temperature; and the temperature difference between the heating surface and the liquid to be heated (Lalande and Tissier, 1985; Paterson, 1988).

During heat treatment, fouling is particularly problematic with concentrated products. Schraml and Kessler (1994), found that fouling during pasteurization of whey products increased to a maximum concentration of 250 $g \cdot kg^{-1}$ of total solids (TS), after which deposition decreased.

The decrease was thought to result from two competing mechanisms: aggregation of whey proteins and crystallization of salts (Fryer et al., 2011).

In general, the ability to transfer heat efficiently remains a central feature in the production of dairy products. Much attention has therefore been paid to improving the understanding of heat transfer mechanisms and the development of suitable correlations and techniques that may be applied to the design of vacuum evaporation. On the other hand, relatively little consideration has been given to the problem of surface fouling in FFE. Most of studies of the fouling and cleaning in the food engineering domain have focused on pasteurization and sterilization processes, where the temperatures are higher than 70°C. Chen and Bala (1998) showed that surface temperatures need to be above 70°C for significant surface fouling of milk to occur, but most milk evaporators parts operate below this temperature (Morison, 2015). Therefore, most of the fouling occurring in milk evaporators should not be assumed to be the same as that occurring in sterilizers and pasteurizers.

Chapter 3

AIMS AND STRATEGY OF THE PHD PROJECT

This chapter describes the aims and the strategy of this PhD project. Based on the progress in dairy powder technology, and the importance of the vacuum evaporation process in terms of energy consumption and final powder quality, this part sets out the research area and outlines the research questions of the project. This study focused mainly on the performance of falling film evaporators during concentration of different dairy products, including skim milk, whole milk, sweet whey and lactic acid whey, at different concentrations. The innovative aspect of this project is the use of a pilot-scale, single-stage falling film evaporator that describes the same process as that of an industrial scale from a hydrodynamic point of view, and the development of a methodology for the calculation and modeling of the residence time distribution functions. The effectiveness of evaporation, the heat transfer coefficient, the extent of fouling formation, the flow behavior and the dispersion of the residence time could thus be identified over the processing time. This PhD project has benefited from close collaboration with GEA (Process Engineering - France), AgroParisTech (Massy – France), Federal University of Viçosa (Brazil) and INRA STLO (Science and Technology of Milk and Eggs) Research laboratory.

The main aims of this chapter are to:
- define the PhD research area and outline the research questions
- introduce the innovative hydrodynamic characterization methodology
- highlight the multidisciplinary aspects of this research

Capítulo 3

OBJETIVOS E ESTRATÉGIA DO PROJETO DE DOUTORADO

Este capítulo descreve os objetivos e a estratégia adotada para a realização deste projeto de doutorado. Com base no progresso das tecnologias para a produção de lácteos desidratados, bem como na importância do processo de evaporação a vácuo em termos de consumo de energia e na qualidade final do pó obtido, esta seção define a área de pesquisa e descreve as questões de pesquisa a serem abordadas pelo seguinte trabalho. Este estudo centrou-se principalmente no desempenho de evaporadores de película descendente durante a concentração de vários produtos lácteos, incluindo leite desnatado, leite integral, soro de leite doce e soro de leite ácido, ambos a diferentes concentrações. O aspecto inovador deste projeto é o uso de um evaporador a vácuo piloto de película descendente que descreve o mesmo processo usado nas indústrias de um ponto de vista hidrodinâmico, e o desenvolvimento de uma metodologia para o cálculo e modelagem das funções de distribuição dos tempos de residência. A capacidade evaporativa, o coeficiente de transferência de calor, a extensão da formação do fouling, o perfil de escoamento e a dispersão dos tempos de residência podem ser portanto identificados ao longo do tempo de processamento. Este projeto de doutorado beneficiou-se da parceria com GEA (Process Engineering - France), AgroParisTech (Massy - França), Universidade Federal de Viçosa (Brasil) e INRA STLO (Ciência e Tecnologia do Leite e ovos - França).

Os principais objetivos deste capítulo são:

- definir a área de pesquisa do doutorado e descrever as questões de pesquisa
- introduzir uma metodologia inovadora para a caracterização hidrodinâmica do processo de evaporação a vácuo
- destacar os aspectos multidisciplinares da pesquisa

Table of contents

3.1. Context of the PhD project

The vacuum evaporation process has an important role in the economic aspects of the world market for dairy powders, which has been considerably expanding as previously stated (Fig. 1.3). Indeed, this process is quasi systematically applied in the dairy industry for the concentration of solutions prior to the drying step: dairy products must be concentrated to a maximum total solids content around 500 g·kg^{-1} to 550 g·kg^{-1}, 550 g·kg^{-1} to 600 g·kg^{-1}, and 200 g·kg^{-1} to 250 g·kg^{-1} for skim milk, whey and whey protein isolates, respectively, as below this value the concentrated product cannot be atomized in the spray-dryer (Schuck, 2002). Besides, the energy used in multi stage evaporators is about 10 times less than that used in a spray-dryer, and evaporation is therefore used to remove the maximum amount of water from the product, while maintaining the physicochemical and microbiological quality of the liquid.

The evaporation process has a major influence on the final powder quality, e.g. an increase in the concentrate viscosity will lead to a decrease in the powder bulk density, and an increase in powder solubility, porosity and wettability, etc. (Fergusson, 1989). However the increase of the concentrate viscosity leads to an increase in the powder bulk density according to Minton (1986). The milk powders properties is also affected by the thermal heat treatment during the evaporation process, as in the spray dryer the thermal effects on the product can be disregarded due to the very low residence time and temperature. The evaporation process can also cause issues with microbiological powder quality, since thermoduric bacteria tend to grow during the vacuum evaporation process (Crossley and Campling, 1957; Murphy et al., 1999).

The control of vacuum evaporators operation is still a challenge due to the complexity of their closed geometry and process - product interactions (e.g. fouling of tubes). The dairy industry already knows the key operating parameters which must be controlled to obtain a concentrate with a specific composition and how to identify irregularities in the production line (e.g. fouling in the evaporation tubes). However, this knowledge is usually obtained empirically,

and therefore there is a lack of information regarding the energy consumption of the vacuum evaporation process, the product flow profile during concentration, the optimal effectiveness of evaporation and which operating parameters need to be monitored to obtain final products of controlled composition. This is why a better understanding of the thermodynamic and hydrodynamic phenomena is needed to determine which operating parameters need to be monitored to improve the performance of evaporators and to control the final properties of the concentrates. Finally, it appears necessary to improve understanding of the effects of the interaction of the product and operating parameters on the performance of falling film evaporators.

It is of note that, there are few scientific papers related to the vacuum evaporation process despite its wide use in the dairy industry. The few available papers focused mainly on calculation of the heat transfer coefficient of different solutions (Ali Adib and Vasseur, 2008; Chun and Seban, 1971; Monnier et al., 2012; Prost et al., 2006), on evaporation process was carried out with industrial equipment, and therefore the initial composition of the product and the operating parameters were not fully controlled (due to large-scale production) (Bouman et al., 1993; Jebson and Iyer, 1991; Jebson and Chen, 1997). Others used laboratory-scale falling film evaporators, where the hydrodynamic profile of the fluids is not the same as that found on an industrial scale (Adib et al., 2009; Luo et al., 2011; Monnier et al., 2012; Park et al., 2004; Pehlivan and Ozdemir, 2012).

An equipment representative of the same process as the industrial scale was therefore needed to study the vacuum evaporation process and to improve understanding of the effects of the operating parameters on the process performance and product quality. These issues are the basis for this PhD framework.

3.2. Aims, objectives and strategy

The main aim of the PhD project was to provide some answers regarding the performance of evaporators during the concentration of dairy products, by means of thermodynamic and hydrodynamic approaches relating the interactions between products properties and operating parameters.

A prototype of a pilot-scale, single-stage falling film evaporator was therefore used to tackle these issues. This equipment was designed according to specifications established by INRA STLO (Science and Technology of Milk and Eggs) Research laboratory, to describe the same process as the industrial scale from a hydrodynamic point of view. As it is possible to perform evaporation at a constant temperature with this pilot evaporator (whereas in industrial scale evaporators temperature evolves over time), the time / temperature / concentration triplet was simplified to a binomial time / concentration approach.

The first stage of this PhD project was therefore to characterize the pilot vacuum evaporator, with instrumentation of the pilot (choice and positioning of the different sensors) and setting of the thermodynamic balances. This information allowed the determination of the operating process range for maximum effectiveness of evaporation of pure water, skim and whole milk (Chapter 5).

After the thermodynamic characterization of the evaporator, hydrodynamic characterization was undertaken (second stage of this PhD project). The hydrodynamic profile of water and skim milk were determined using Reynolds number and residence time distribution (RTD) functions. In addition to provide important information relating to the product flow profile in the evaporator, RTD functions also provided the time that the product spent in the evaporator. As the product temperature in this equipment may be kept constant, the profile

time / temperature can be accessed. These RTD functions were modeled and a physical interpretation of the model was obtained (Chapter 6).

The thermodynamic and hydrodynamic characterization of the evaporation process was performed with other dairy products such as sweet and acid lactic whey. These approaches indicated the fouling formation during concentration in a falling film evaporator (Chapter 7).

3.3. Originality of the research project

The PhD project has had to combine fundamental and experimental information on the "concentration phenomenon" and aspects related to the flow profile during concentration of different dairy products in a falling film evaporator. The project consisted of an experimental study, where the results of which could be used to improve process performance, control and quality in the dairy industry. A prototype pilot vacuum evaporator was characterized and instrumented, which are essential steps for further studies of the interactions between product and process, and process performance as regards the processing time and cleaning efficiency.

Methodology was developed for the measurement of residence time distribution functions of real products in a falling film evaporator. To date this approach has been used in cases where the product composition remained constant before and after the process (e.g. pasteurizers) or with model solutions, which do not represent the complexity of a real solution, such as skim milk. The difficulty for calculation the RTD in the vacuum evaporator equipment is the changes occurring in the product throughout the process, due to increase in the concentration. The product properties and their interactions with the evaporator equipment therefore change over the process time. An approach was also proposed for modeling these RTD functions. Due to thorough understanding of the process, a physical interpretation of the RTD is proposed, which provides important information related to the flow of different dairy products, such as skim milk, sweet whet and lactic acid whey during its concentration in a falling film evaporator.

PART 2

MATERIALS AND METHODS, RESULTS AND DISCUSSION

Chapter 4

MATERIALS AND METHODS

The aim of this chapter is to describe the working of the pilot scale, single stage falling film evaporator, used for carrying out this PhD thesis, and the methodologies used to characterize this process. The initial configuration of the pilot and the improvements made are presented. Different types of sensors to measure temperature, conductivity, flow rate, pressure and heating power were used to characterize and monitor the vacuum evaporation process. Water, skim milk, whole milk, sweet whey and lactic acid whey were used as solutions to be concentrated. The methods for the physicochemical analysis of these products are presented. Enthalpy balances as well as the methodology used to calculate and model the residence time distribution functions are also described.

The main aims of this chapter are to:
- Describe the pilot-scale vacuum evaporator used
- Describe how the experimental runs were carried out
- Describe the physicochemical analyses applied to the concentrated products
- Describe the calculations and model of the residence time distribution functions

Capítulo 4

MATERIAIS E MÉTODOS

O objetivo deste capítulo é descrever o funcionamento do evaporador piloto, único efeito, de película descendente utilizado para a realização deste trabalho de doutorado, e as metodologias utilizadas para a caracterização deste processo. A configuração inicial do piloto e as melhorias realizadas posteriormente neste equipamento são apresentadas. Diferentes tipos de sensores para medida de temperatura, condutividade, vazão, pressão e potência de aquecimento foram usados para caracterizar e monitorar o processo de evaporação a vácuo. Água, leite desnatado, leite integral, soro de leite doce e ácido foram usados como soluções a serem concentradas. Os métodos para as análises físico-químicas destes produtos são apresentados. Balanços entálpicos, bem como a metodologia utilizada para o cálculo e modelagem das funções de distribuição dos tempos de residência são também descritos.

Os principais objetivos deste capítulo são:
- descrever o piloto de evaporação a vácuo utilizado
- descrever como os ensaios experimentais foram realizados
- descrever as análises físico-químicas
- descrever os cálculos e modelagem das funções de distribuição dos tempos de residência

Table of contents

4.1. Pilot vacuum evaporator

A pilot scale, single stage falling-film evaporator (GEA Process Engineering, St Quentin-en-Yvelines, France; Fig. 4.1) was used for the characterization of the vacuum evaporation process. From the hydrodynamic point of view, the working of this equipment is close to that used in the dairy industry, i.e. the product falls in a trickling film along the inner wall of the evaporator tube, with indirect counter-flow contact with primary steam. The equipment consists of three evaporation tubes connected in series (Fig. 4.1), whose the dimensions are shown in Table 4.1.

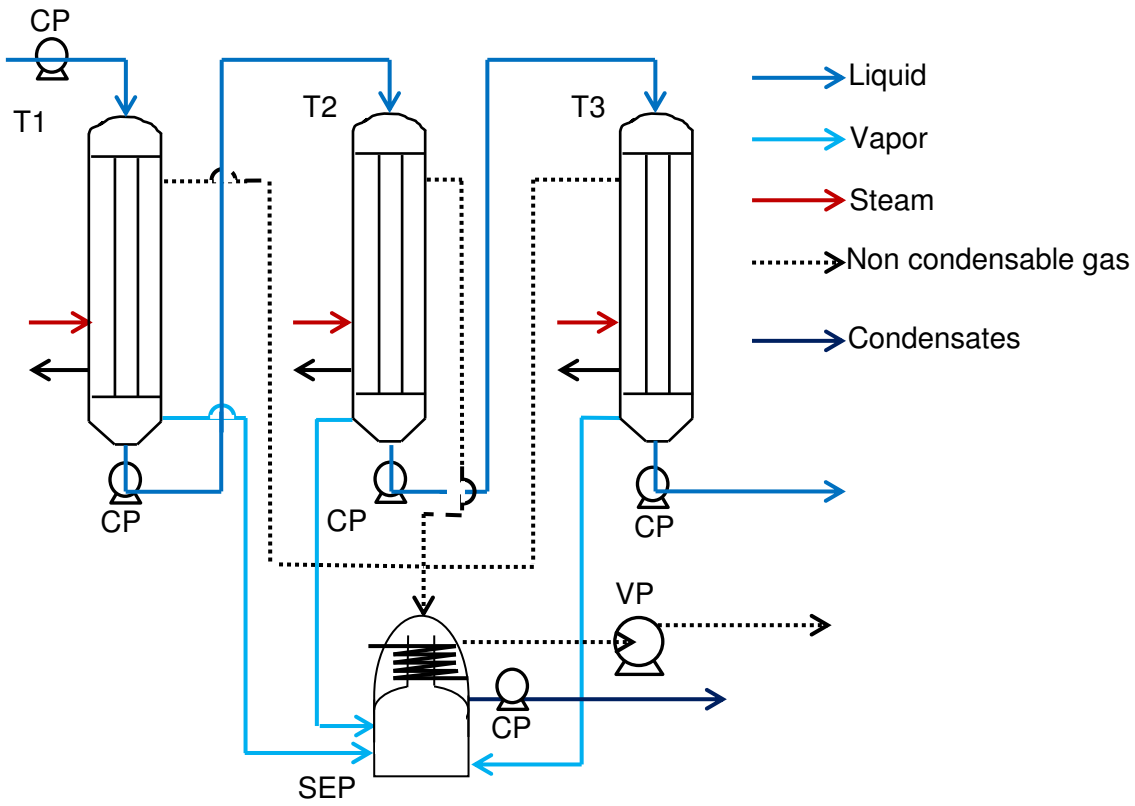

VP: Vacuum pump
SEP: Separator and indirect condenser
CP: Centrifugal pumps

Figure 4.1. Flowsheet of the evaporator.

Table 4.1. Dimensions of the inner side of the three tubes (T1, T2 and T3) in the falling-film evaporator. Wall thickness of each tube is 1 mm.

Tube	D (m)	h (m)	A (m^2)
T1	0.036	4.0	0.452
T2	0.023	4.0	0.289
T3	0.023	4.0	0.289
Total			1.030

Legend: D= diameter; h= height; A= heating surface

The inlet product, concentrate and condensate are circulated by means of five circulation pumps (Fig. 4.1 - CP) (Pompes AB, Maurepas, France) with the same characteristics (centrifugal type, 0.7 kW).

Each evaporation tube is thermally insulated and has an independent electrical heating system (Fig. 4.2) that provides the vaporization energy. As the vapor emitted by the product (secondary vapor) is not used for heating the product in the next tube, this pilot is a single stage evaporator. A level sensor (Fig. 4.2) is used to inject water at maximum temperature of 20°C into the heating systems when the level of water is below the sensor. The aim of this sensor is to ensure that the electric resistances are always immersed in water. The production of steam in this equipment is therefore discontinuous, because from the moment that water is inserted the temperature of the steam side decrease and therefore steam production ceases. The steam production is reestablished when water is heated to steam vaporization temperature. Water can be inserted manually or automatically through a water injection electro valve (Burkert, Triembach

au Val, France). When automatically injection was set the time of water injection is around 30 min of the process time, against around 60 min of process time for manually injection.

Concentration of the solutions was performed at a total heating power of 25.20 ± 0.05 kW (8.40 ± 0.02 kW for each tube), corresponding to the maximum heating power of the equipment.

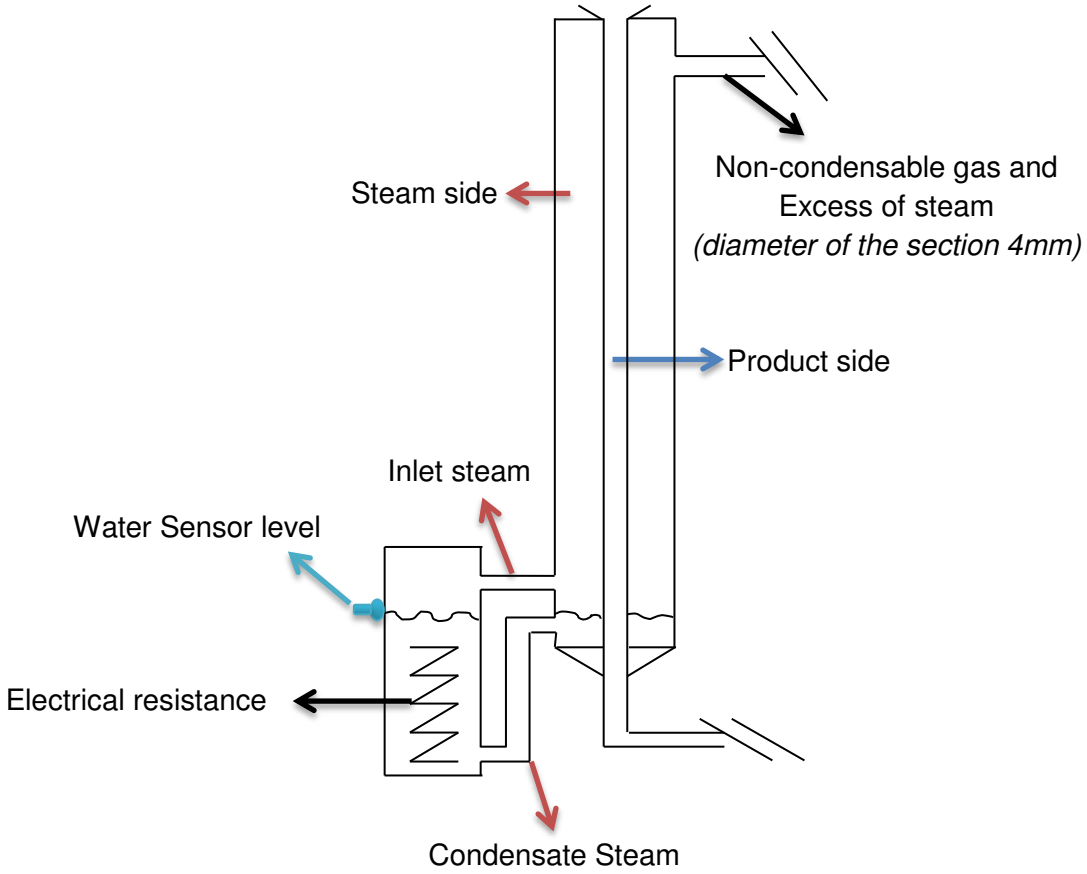

Figure 4.2. Evaporation tube with independent electrical heating system.

The secondary vapor of the three evaporation tubes are separated in a separator with an integrated indirect condenser (coil-type heat exchanger) (Fig. 4.3). As the secondary vapor (product vapor) is condensed in the condenser, the pressure in the system is reduced (P_{total} < 0.1 MPa), which leads to a decrease of the evaporation temperature. The experiments were performed at an absolute pressure (P_{abs}) of 0.02 MPa and thus the evaporation temperature (θ_{ev})

was maintained at 60°C throughout the three tubes. This temperature was the most commonly used for concentration of milk in the first stage of industrial vacuum evaporators. The temperature is controlled by the mass flow rate of the cooling water (ranging between 300 $kg \cdot h^{-1}$ to 800 $kg \cdot h^{-1}$) at a maximum temperature of 20°C. A vacuum pump (Fig. 4.3) (liquid ring type, 1.1 kW power consumption) connected to the condenser is required for the starting phase and to extract the non-condensable gases, which would otherwise accumulate in the condenser.

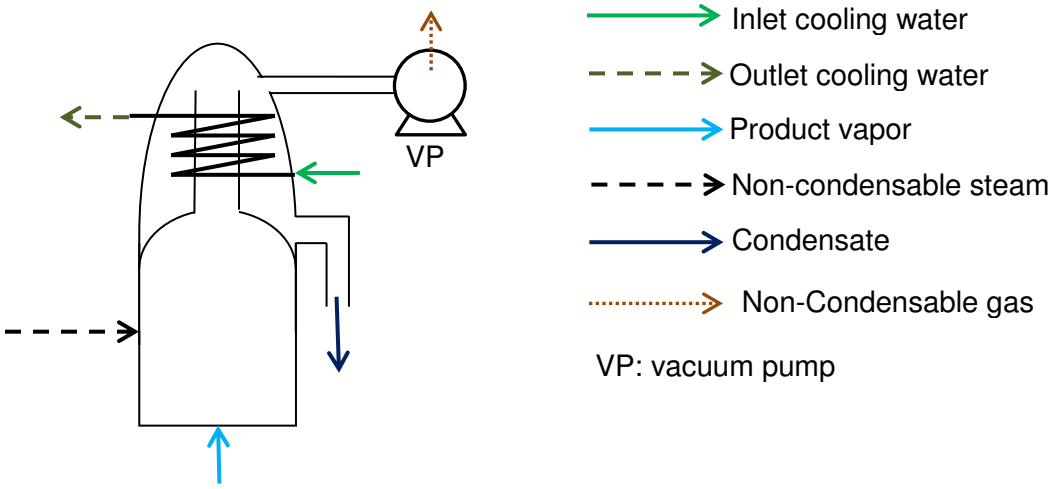

Figure 4.3. Separator integrated with indirect condenser.

4.2. Pilot instrumentation

4.2.1. Acquisition

The initial configuration of the pilot had fifteen temperature probes, one pressure sensor and three flowmeters, as well as one data acquisition system (Endress Hauser, Huningue, France). Fig. 4.4 shows the position of these sensors.

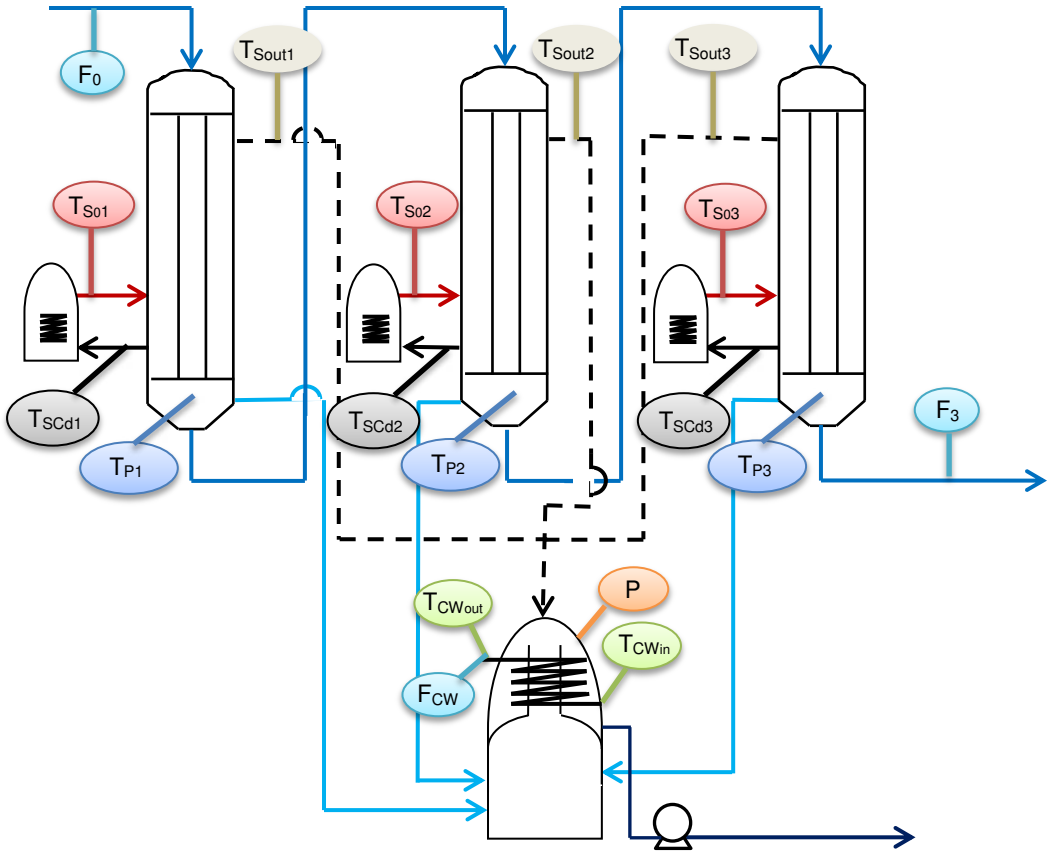

F_0, F_3 and F_{CW}: Flowmeters of inlet product, outlet concentrate and cooling water
T_{S01}, T_{S02} and T_{S03} Inlet steam temperature probes
T_{SCd1}, T_{SCd2} and T_{SCd3}: Steam condensate temperature probes
T_{P1}, T_{P2} and T_{P3}: Product temperature probes
T_{Sout1}, T_{Sout2} and T_{Sout3}: Outlet steam temperature probes
T_{CWIn}, T_{CWOut}: Inlet and outlet cooling water temperature probes
P: Pressure sensor

Figure 4.4. Initial configuration of the evaporator.

Temperature probes (Endress Hauser, Huningue, France) were used to record the temperatures of the product at the bottom of each tube, inlet and outlet steam, condensate steam, and inlet and outlet cooling water. The flow rate of the inlet product, concentrate and cooling water were measured with an electromagnetic flowmeter (Krohne, Romans Sur Isere,

France). The pressure was measured with a pressure sensor (Endress Hauser, Huningue, France) in the condenser, which has the same pressure inside the evaporator tubes.

The product enters at the top of the evaporator tubes and it is dispersed by a plate distributor (Fig. 4.5). The aim of this piece is to ensure that a complete film, with thickness around 1.0 mm to 1.5 mm, is maintained inside the tubes throughout the process time.

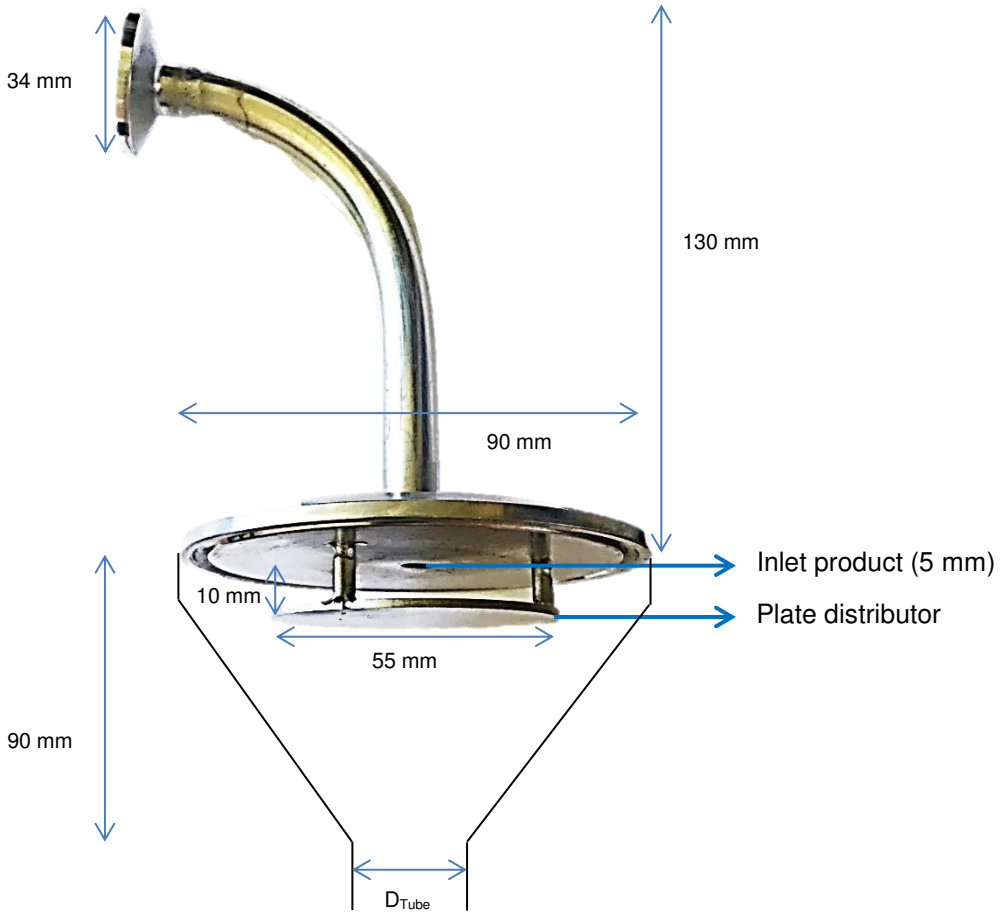

Figure 4.5. Plate distributor.

4.2.2. Additional instrumentation

Some modifications were made on the pilot to improve its instrumentation and to obtain more data about the working of the equipment. Two flowmeters (electromagnetic type - Krohne, Romans Sur Isere, France) and three conductivity probes (Endress Hauser, Huningue, France) were added. A cone-shaped concave distributor system (Fig. 4.6) was also built (to ensure that a complete film was maintained inside the tubes at all times), and a heat exchanger was added in the product inlet line. Fig. 4.7 shows the first evaporator tube with all installed sensors. Aside from the preheater, the other two tubes have the same sensors in similar positions.

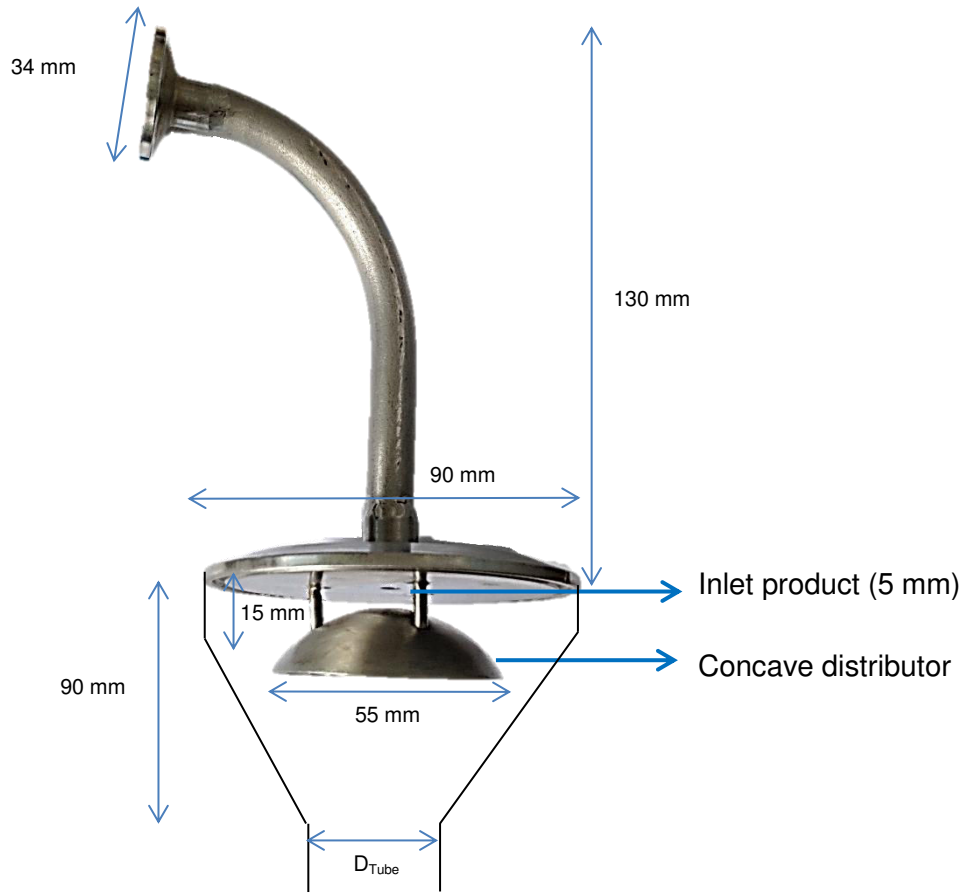

Figure 4.6. Cone-shaped concave distributor.

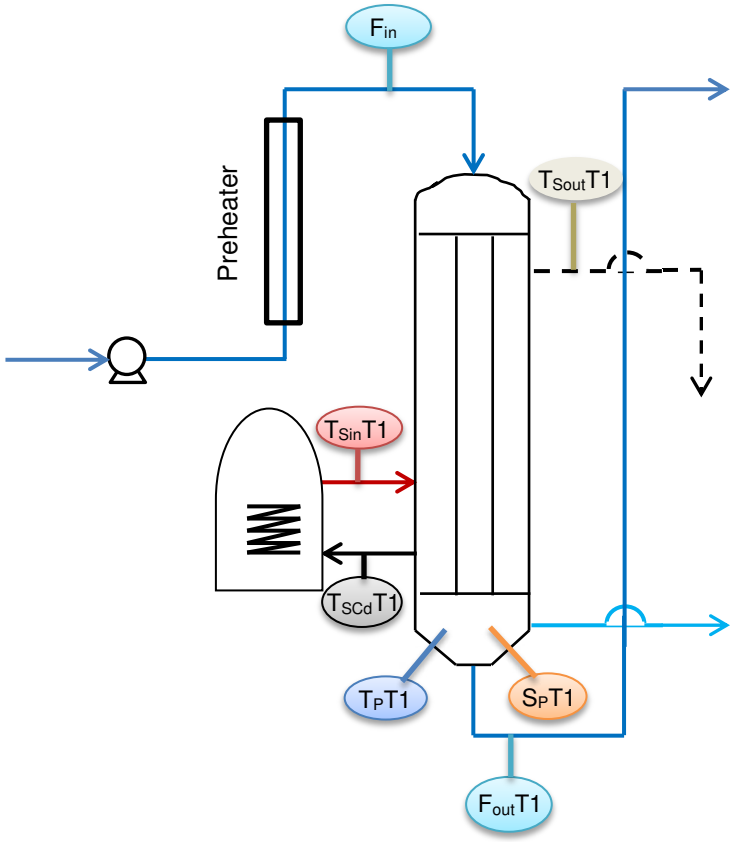

F_{in}: Product inlet flowmeter
$F_{out}T1$: Product outlet flowmeter
$T_{Sin}T1$: Inlet steam temperature probe
$T_{SCd}T1$: Steam condensate temperature probe
$T_{Sout}T1$: Outlet steam temperature probe
T_PT1: Product temperature probe
S_PT1: Product conductivity probe

Figure 4.7. Instrumentation of the first evaporator tube.

4.3. Calibration of the vacuum evaporator sensors

Temperatures, conductivity probes and flowmeters were calibrated when these sensors were installed. The temperature probes were calibrated at two temperatures, 0°C and 80°C. The difference between the reference and the acquisition temperatures was always less than 0.5°C. For calibration of the flowmeters, the volume flow rate of water measured by the control panel system was compared with the mass flow rate measured with a graduated test tube and a chronometer. As the conductivity of the solutions studied was in the order of 0.01 $mS \cdot cm^{-1}$ to 100 $mS \cdot cm^{-1}$, the conductivity probes were calibrated with a standard solution (Hanna Instruments, Inc., Tanneries, France) with conductivity between 0.05 and 200 $mS \cdot cm^{-1}$. The correlation coefficient (R^2) between the measured and the calculated flow rate and conductivity was greater than 0.99.

4.3. Experimental runs

Experimental runs were carried out with water, skim milk, sweet whey and lactic acid whey.

Skim milk was reconstituted from low heat skim milk powder (Lactalis ingredients, Bourgbarré, France). Fresh concentrated sweet whey and lactic acid whey were obtained from an industrial cheese manufacturer in Brittany (France). Before entering the evaporator the products were preheated to the evaporation temperature in a jacketed tank, at the initial evaporator configuration, and in a tubular indirect preheater (Fig. 4.7) after the additional instrumentation. When desired, after passing of the entire product through the three evaporation tubes (Fig. 4.1) (first run – 1R), the entire volume of the product obtained at the end of the first run (still at the evaporation temperature) was reintroduced into the equipment and re-concentrated a second time, again passing through the three evaporation tubes (second run – 2R). This operation could be performed once more (third run – 3R).

The vacuum evaporator was divided in four different sections (Fig. 4.8). ❶ corresponds to the section from the feed to the bottom of the first tube; ❷ the section from the bottom of the first tube to the bottom of the second tube; ❸ the section from the bottom of the second tube to the bottom of the third tube; and ❹ the section from the feed to the evaporator outlet.

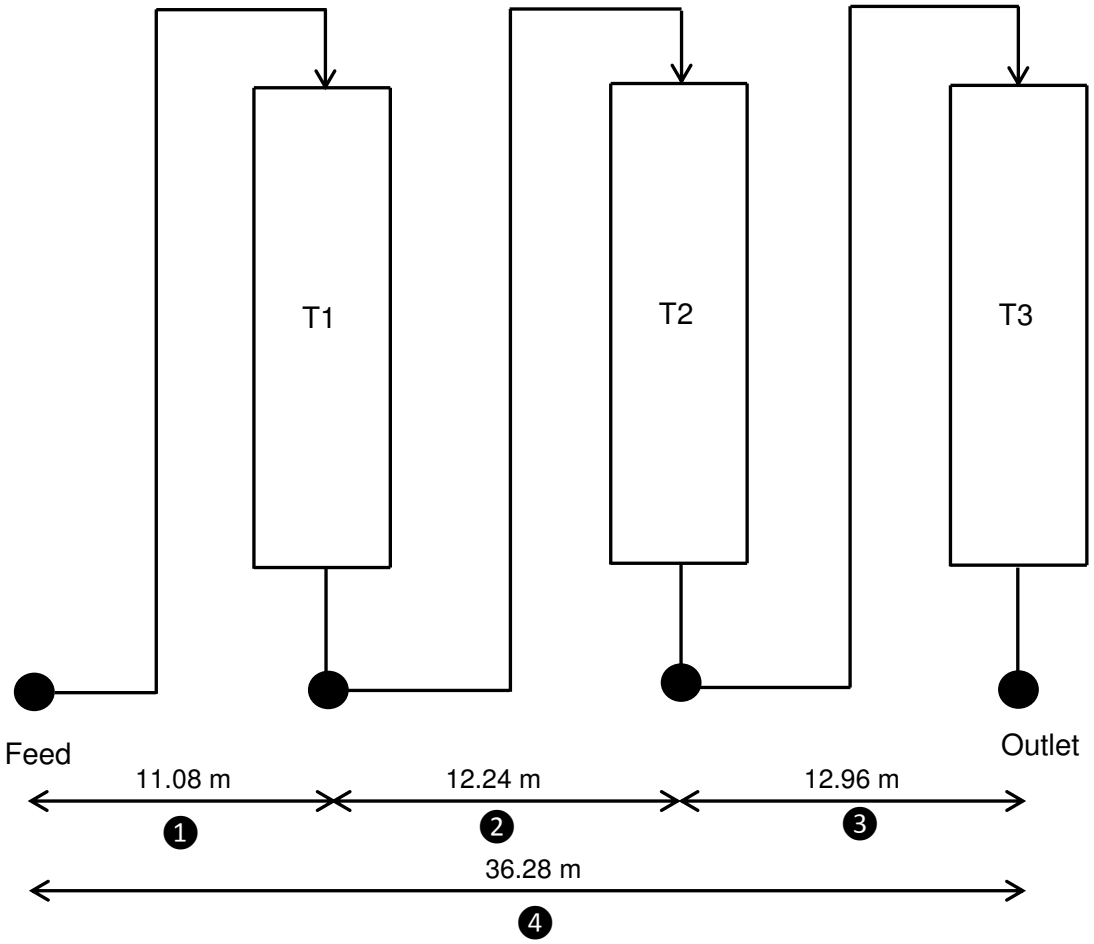

Figure 4.8. Sampling points for determination of local and overall RTD. ❶: measurement from inlet to outlet of tube 1; ❷: measurement from outlet of tube 1 to outlet of tube 2; ❸ measurement from outlet of tube 2 to outlet of tube 3; ❹: overall RTD measurement from inlet to outlet of the falling film evaporator.

4.4. Physicochemical analyses

4.4.1. Total solids

The feed and final total solids content (TS) were calculated according to weight loss after drying 5 g of each sample with sand in a forced air oven at 105 °C for 7 h.

Due the low pressure of the process, it was not possible take a sample of the product at the bottom of the first and second tube without affecting the process parameters (decrease in the pressure process, product flow rate, temperature, etc.). Therefore the TS were calculated at these two points (mass balance) as:

$$TS_{out_i} = \frac{\dot{m}_{in_i} \cdot TS_{in_i}}{\dot{m}_{out_i}} \qquad \text{Eq. 4.1}$$

where $\dot{m}_{in_i}$ is the inlet mass flow rate of the product in tube i, TS_{in_i} corresponding to the total solids of the inlet product at the bottom of tube i, and $\dot{m}_{out_i}$ corresponding to the outlet mass flow rate of the product in tube i.

4.4.2. Viscosity measurement

Viscosity measurements were obtained at the evaporation temperature with a Physica MCR 301 rheometer (Anton Paar, Graz, Austria) using a coaxial aluminum cylinder (inner radius 23.05 mm; outer radius 25 mm; height of rotor 30 mm; gap 5 mm). Shear rates between $10 \cdot s^{-1}$ and $1000 \cdot s^{-1}$ at the evaporation temperature were used for rheological determinations. As the solutions studied behave as a non-Newtonian fluid at high concentrations, apparent viscosity at a shear rate of $100 \cdot s^{-1}$ (η_{100}) was used to make comparisons between the different products. This shear rate value was chosen because it is representative of the value reached in agitation, flow in tubes and other industrial operations (Steffe, 1996). As it was not possible to take samples at the bottom of T1 and T2, calibration curves of apparent viscosity were obtained (η_{100}) as a function of product total solids (Fig. 4.9).

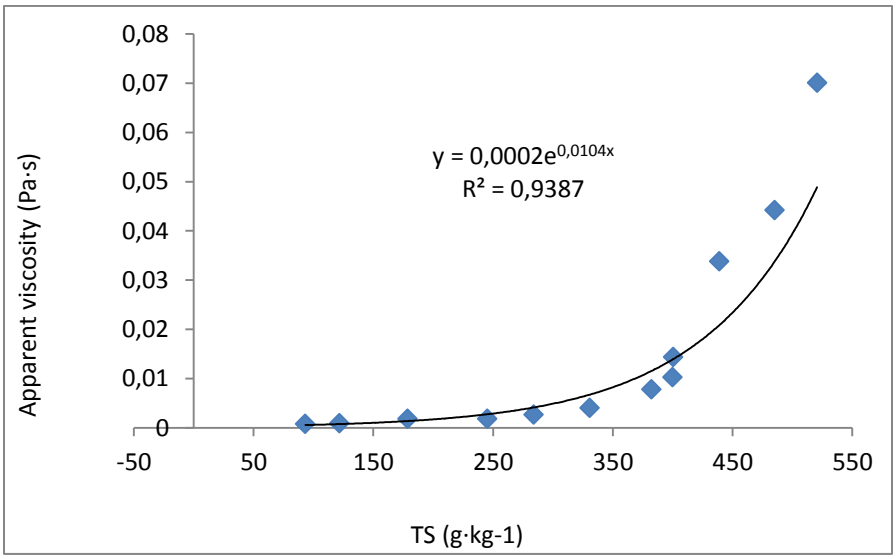

Figure 4.9. Skim milk apparent viscosity (η100) measured at 60°C in function of total solids contents.

4.4.3. Density measurements

A Mettler-Toledo densimeter DE40 (Mettler-Toledo, Columbus, USA) was used to determine the density of the products at 60°C. The product density was used to convert the liquid flow rate (measured by the flowmeters) to mass flow rate.

4.4.4. Conductivity

The conductivity of the product was measured and recorded every second at the bottom of the three tubes (Fig. 4.7 (S_P)) by conductivity-meter (Endress Hauser SAS, Huningue, France).

4.4.5. Protein composition

Non-casein nitrogen (NCN) and non-protein nitrogen (NPN) fractions were determined by the Kjeldhal method (IDF, 1993). Nitrogen content was converted into equivalent protein content using 6.38 as converting factor for NCN and NPN content, respectively. Whey protein content (WPC) was calculated as WPC = NCN·6.38 − NPN·6.38.

4.4.6. Ash content

Ash content was determined by incinerating 5 g of the product in a muffle furnace at 550°C for 5 hours (IDF, 1964).

4.4.7. Calcium concentration

Calcium concentration was determined by atomic absorption spectrometer (Varian 220FS SpectrAA, Les Ulis, France) (Le Graët and Brulé, 1993).

4.5. Mass and enthalpy balance

Fig. 4.10 provides a diagram representing the mass flow rate and the physical characteristics of the fluids in the evaporator. Each fluid is characterized by its mass flow rate ($\dot{m}$ in $kg \cdot h^{-1}$), temperature (θ in °C), pressure (P in MPa) and enthalpy (H in $kJ \cdot kg^{-1}$).

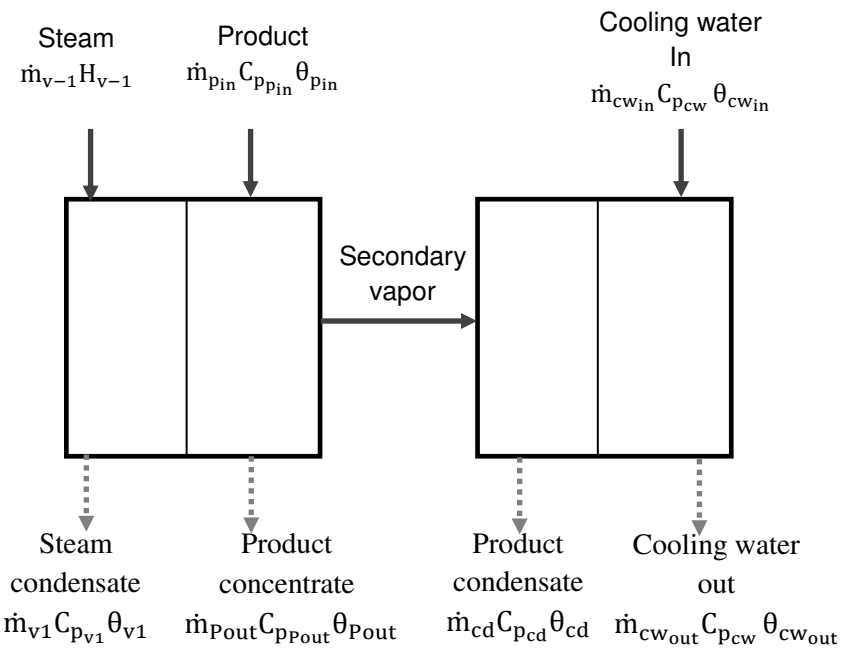

Legend:

C_p = sensitive heat (kJ·kg^{-1}·°C^{-1}) θ = temperature (°C)

H = enthalpy of evaporation (kJ·kg^{-1}) $\dot{m}$ = mass flow rate (kg·h^{-1})

Figure 4.10. Thermodynamic diagram of a single stage vacuum evaporator.

As seen in Fig. 4.10, the overall mass balance was calculated as:

$$\dot{m}_{v-1} + \dot{m}_{p_{in}} + \dot{m}_{cw_{in}} = \dot{m}_{Pout} + \dot{m}_{cd} + \dot{m}_{v1} + \dot{m}_{cw_{out}} \quad \text{Eq. 4.2}$$

In this pilot equipment steam is produced in excess. A part of steam is therefore not used for energy exchanges. This excess of steam goes to the condenser where it is condensed and exits the equipment by the condensates line. The mass of water inserted in the heating systems, therefore used to steam production, may be measured. After working during a given process time without adding water in the heating systems, the mass of remaining water was calculated. The difference between the mass of water inserted and remaining in the heating system is therefore the mass of steam produced in excess. This part of steam is not used to the energy

exchange, and it is therefore not taken into account in the mass and energy balances. Thus the mass of the excess steam is not reported in this thesis. The non-condensable gases from the steam (Fig. 4.1) were transferred to the condenser where they were removed from the system. The mass flow rate of non-condensable gas was considered to be negligible, and therefore it was not taken into account in the calculation of mass and energy balances.

At the outlet of the evaporator, the inlet mass flow rate of the product was a combination of the mass flow rate of product concentrate and the mass flow rate of secondary vapor that was finally converted in product condensate (Fig. 4.10).

$$\dot{m}_{p_{in}} = \dot{m}_{Pout} + \dot{m}_{cd} \quad [4.3]$$

As the condenser was an indirect heat-exchanger, there was no mixing of the condensate and cooling water. Therefore:

$$\dot{m}_{cw_{in}} = \dot{m}_{cw_{out}} \quad [4.4]$$

As the steam entering the evaporator tubes was saturated, it is supposed that its condensation was complete and that all the steam was transformed into the condensate at saturation temperature. Therefore:

$$\dot{m}_{v-1} = \dot{m}_{v1} \quad [4.5]$$

Thus, only the latent heat of vaporization was exchanged:

$$\Delta H_v = (H_{v-1} - H_{v1}) \quad [4.6]$$

where H_{v-1} and H_{v1} are the enthalpy of evaporation ($kJ \cdot kg^{-1}$) of steam and its condensate, respectively.

The heating power Q (kW) applied to the three tubes was used to the production of saturated steam according to:

$$\dot{Q} = \dot{m}_{v-1} \cdot \Delta H_v \qquad [4.7]$$

Equation [4.7] thus makes it possible to calculate the mass flow rate of the steam, whose pressure and temperature are known, as well as the heating power generated by the boilers. Expressing heat loss as $\dot{q}_p$, the enthalpy balance can be written:

$$(\dot{m}_{v-1} \cdot H_{v-1}) + (\dot{m}_{p_{in}} \cdot H_{p_{in}}) + (\dot{m}_{cw_{in}} \cdot H_{cw_{in}}) = (\dot{m}_{Pout} \cdot H_{Pout}) + (\dot{m}_{cd} \cdot H_{cd}) + (\dot{m}_{v1} \cdot H_{v1}) + (\dot{m}_{cw_{out}} \cdot H_{cw_{out}}) + \dot{q}_p \qquad [4.8]$$

Where $\dot{q}_p$ comprises the rate of energy losses and error of measurements and calculation.

By substituting Equations [4.4], [4.5] and [4.6] in Equation [4.8]:

$$\dot{m}_{v-1} \cdot (\Delta H_v) = (\dot{m}_{Pout} \cdot H_{Pout}) + (\dot{m}_{cd} \cdot H_{cd}) - (\dot{m}_{p_{in}} \cdot H_{p_{in}}) + \dot{m}_{cw} \cdot (H_{cw_{out}} - H_{cw_{in}}) + \dot{q}_p \qquad [4.9]$$

The left term of equation 4.9 corresponds to the heating power Q provided by the steam, i.e. the energy provided by the heating system of the evaporator.

4.6. Overall heat transfer coefficient

The overall heat transfer coefficient for each tube was calculated as:

$$Q = U \cdot A \cdot \Delta\theta \iff \Phi = {}^{Q}/_{A} = U \cdot \Delta\theta \iff U = {}^{\Phi}/_{\Delta\theta} \qquad \text{Eq. 4.10}$$

where U is the overall heat transfer coefficient, $kW \cdot m^{-2} \cdot °C^{-1}$; Q the heating power, kW; A the heating surface, m^2; $\Delta\theta$ the mean temperature difference between steam and product concentrate, °C; and Φ the heat flux, $kW \cdot m^{-2}$.

The inlet steam temperature and the product temperature (Fig. 4.7 (T_{S0}, T_P)) were used to the measurement of the $\Delta\theta$.

4.7. Assessment of process efficiency

The energy consumption for evaporation is a key parameter used to assess the efficiency of a plant. As in drying, it can be evaluated from the Specific Energy Consumption (SEC; $kJ \cdot kg^{-1}$ of water evaporated) (Bimbenet et al., 2007), and from the energy efficiency (EE; % - $w \cdot w^{-1}$), that is the ratio between the amount of water evaporated and the amount of steam, expressed as a percentage. EE can also be represented as the ratio between the latent heat vaporization of the steam and of the product. Due to the gradient of temperature between the steam and the product the ratio will not be equal to 1. In an adiabatic process without energy losses EE value is of the order of 99%. SEC and EE are defined by the following equations:

$$SEC = \frac{\dot{m}_{v-1} \cdot \Delta H_v}{\dot{m}_{cd}} \qquad \text{Eq. 4.11}$$

and

$$EE = \frac{\dot{m}_{cd}}{\dot{m}_{v-1}} \qquad \text{Eq. 4.12}$$

4.8. Characterization of the flow

Flow was characterized using an experimental Reynolds number of the film (§ 2.4), and the classification defined by Bird et al. (1960) that established the flow profiles for the falling film in three regions was used:

- Ref < 25: laminar flow;
- 25 < Ref < 1000: laminar flow with waves (wavy-laminar);
- Ref > 1000: turbulent flow.

As Ref was always measured at the bottom of the evaporation tubes, the characterization of the flow behavior in sections ❸ and ❹ was always the same, as both were measured at the bottom of T3.

The maximum flow velocity, corresponding to the velocity of the first fluid elements that arrived at the bottom of the evaporation tube, was calculated according to equation 4.13.

$$\nu_{max} = \frac{\text{length of a section}}{t_{i_{min}}} \qquad \text{Eq. 4.13}$$

where ν_{max} is the maximum flow velocity and $t_{i_{min}}$ the time that the first particles of tracer take to cross a section of the evaporator equipment (Fig. 4.8).

4.9. Residence time distribution functions

4.9.1. Measurement of residence time distribution

RTD were determined experimentally by injecting an inert chemical, molecule or atom, called a tracer, into a reactor at some time, t = 0, and then measuring the tracer concentration in the effluent stream as a function of time. In this study, RTD characterization was based on the follow-up of the concentration of sodium chloride added to the product. The product with 10 g·kg^{-1} of sodium chloride was injected into the evaporator for 30 seconds (Fig. 4.11). The NaCl remains soluble at the concentration used in this study (maximum concentration of 20 g·kg^{-1})

and its concentration did not affect the product viscosity (Huppertz and Fox, 2006), which is the main parameter related to the product flow behavior (Ali Adib and Vasseur, 2008; Monnier et al., 2012; Park et al., 2004). The time that the sodium chloride molecules and the product fluid elements took in the evaporator equipment was therefore considered to be the same.

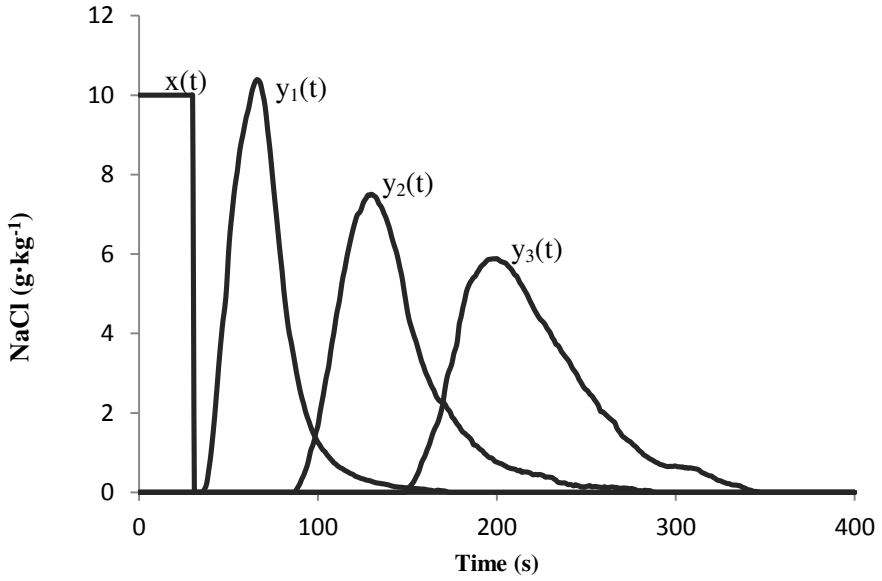

Figure 4.11. Tracer injection x(t) and output signal at bottom of T1 (y1(t)), T2 (y2(t)) and T3 (y3(t)).

As the pilot operates as a continuous process, the products with and without the tracer were put in two different tanks connected to the feed line with a three-way valve, which allowed rapid change in the nature of the feed product. Using this technique the shape of the injection signal could be considered to be a square.

The outlet sodium chloride concentration, measured indirectly by conductivity, was calculated at the bottom of the three evaporation tubes. Calibration curves of product conductivity in relation to product concentration were performed (Fig. 4.12). This was done for all

products in all concentrations obtained in this study. It was then possible to plot the sodium chloride concentrations in the effluent stream as a function of time, ($y_i(t)$) (Fig. 4.11).

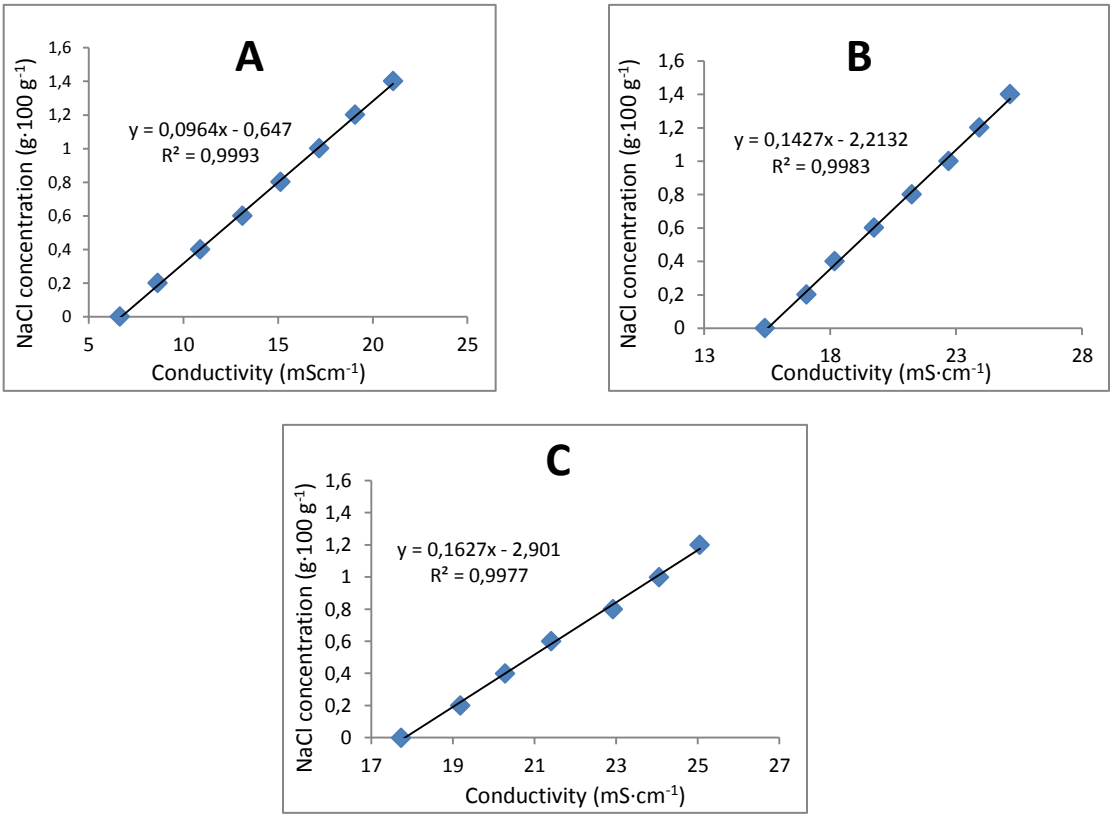

Figure 4.12. Sodium chloride concentration as a function of conductivity: A: Skim milk at 200 g·kg^{-1} of total solids, B: Sweet whey at 363 g·kg^{-1} of total solids and C: lactic acid whey at 364 g·kg^{-1} of total solids.

The RTD signal ($E_i(t)$) was determined in the four different sections of the vacuum evaporator (Fig. 3.8) by numerical deconvolution of the outlet signal (i.e. outlet concentration of NaCl) by the injection signal (i.e. inlet concentration of NaCl). Due to the complexity of the

calculations performed, the MATLAB and Statistics Toolbox Release software (2014b, The MathWorks, Inc., Natick, Massachusetts, United States) was used.

$E_{❶}(t)$ was calculated by numerical deconvolution of y1(t) with the injection signal (x(t)). The sodium chloride concentration measured at the bottom of T1 (y1(t)) was the injection signal for calculating $E_{❷}(t)$. $E_{❷}(t)$ was therefore calculated by numerical deconvolution of y2(t) with y1(t). For $E_{❸}(t)$ the injection signal was y2(t), and thus $E_{❸}(t)$ was calculated by numerical deconvolution of y2(t) with y3(t). (Eq. 4.14, 4.15 and 4.16). The overall RTD from the inlet to the outlet of the evaporator ($E_{❹}(t)$) was calculated by numerical deconvolution of yT3(t) by the injection signal (x(t)) (Eq 4.17).

$$y_{T1}(t) = x(t) \otimes E_{❶}(t) \qquad \text{Eq. 4.14}$$

$$y_{T2}(t) = y_{T1}(t) \otimes E_{❷}(t) \qquad \text{Eq. 4.15}$$

$$y_{T3}(t) = y_{T2}(t) \otimes E_{❸}(t) \qquad \text{Eq. 4.16}$$

$$y_{T3}(t) = x(t) \otimes E_{❹}(t) \qquad \text{Eq. 4.17}$$

Having determined $E_i(t)$ for the different sections of the vacuum evaporator, it was then possible to determine both the residence time of each fluid element and the time at which a certain fraction of the material entering at t = 0 was no longer present in the equipment. The mean residence time, τ, corresponded to the time when 50% of the material entering at t = 0 passed through the equipment. In other words this parameter corresponded to the time for recorded 50% of the inlet sodium chloride molecules at the outlet of the equipment.

4.9.2. Model of the residence time distribution functions

Different models were tested to model the RTD functions for the four different sections of the falling film evaporator. Due to the changes in product composition during the vacuum

evaporation (i.e. increase in product viscosity and changes in the flow profile), the dispersion of the particles in the equipment was more pronounced than in plug flow systems. Therefore the RTD functions were modeled by a set of perfectly mixed reactor tanks in series in order to take into account the flow profile in the evaporator. Each reactor set includes N_i reactor tanks in series, and can be characterized by a mean residence time (τ_i). Its own RTD function is defined by:

$$E_i(t) = \left(\frac{N_i}{\tau_i}\right)^{N_i} \cdot \frac{t_i^{N_i-1} \cdot \exp\left(N_i \cdot t_i / \tau_i\right)}{(N_i-1)!} \qquad \text{Eq. 4.18}$$

The number of tanks in series, Ni, provides information about the dispersion of the fluid elements: a high N value indicates low dispersion of the particles in the reactor (Gutierrez et al., 2010).

Different arrangements of perfectly mixed reactor tanks in series were studied. For this study the model of two reactor sets in parallel (Fig. 3.13) was the most effective to model the experimental RTD functions. The product therefore was considered to pass through two reactor sets, A and B, characterized by two RTD functions $E_a(t)$ and $E_b(t)$. Reactor set C was a combination of these two reactor sets (Fig. 4.13). It was characterized by the function $E_c(t)$, which describes the experimental RTD of the falling film evaporator (Eq. 4.19).

$$E_c(t) = (1-a) \cdot E_b(t) + a \cdot E_a(t) \qquad \text{Eq. 4.19}$$

where a refers to the fraction of feed flow rate going into reactor set A. The three parameters of each reactor set (a_i, τ_i and N_i) were adjusted step by step in order to fit the modeled curve to the experimental curve.

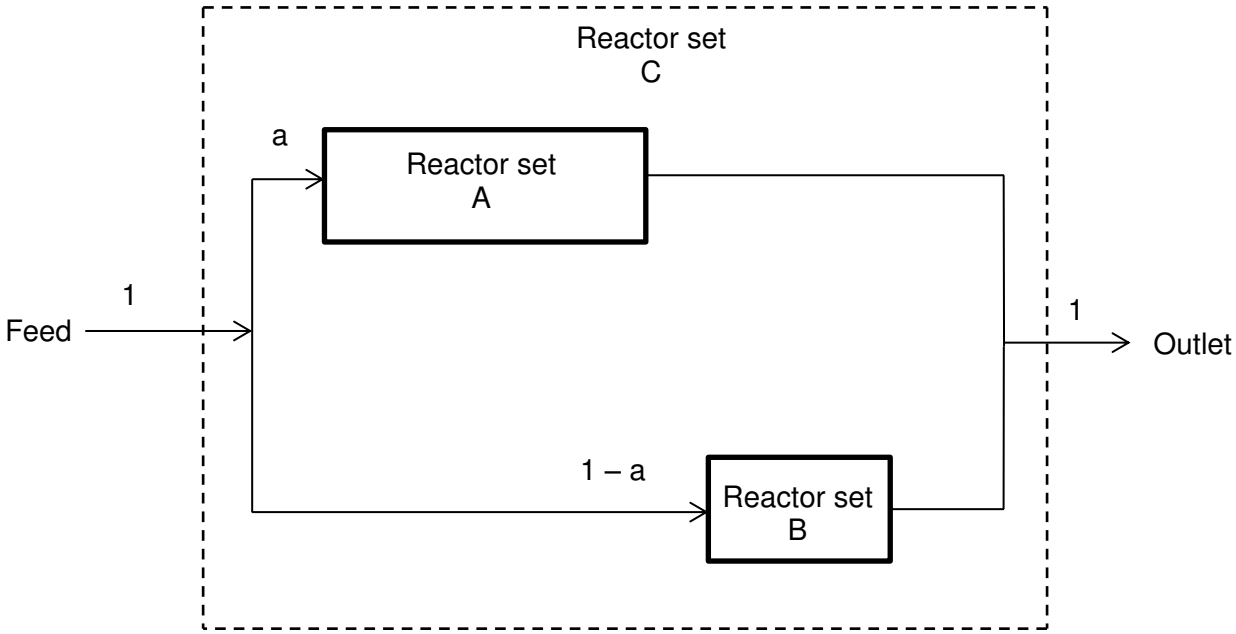

Figure 4.13. Reactor tank sets in series used to model the RTD of FFE for the four sections studied.

Model accuracy was evaluated by calculation of the standard deviation between the model and experimental RTD curves.

Chapter 5

PILOT SCALE INVESTIGATION OF EFFECTIVENESS OF EVAPORATION OF SKIM MILK, WHOLE MILK AND WATER

The aim of the work reported in this chapter was to compare the effectiveness of a pilot scale single stage falling film evaporator in the evaporation of water, skim and whole milk. Using the acquisition instrumentation of the pilot and an inlet mass flow rate of 50 kg·h^{-1}, initially no significant variation ($p < 0.05$) in the evaporation rate or in the energy efficiency for two runs with skim milk were found, but the values were higher than those obtained with the experiments with water. The heat transfer coefficient did not differ according to the product and this result does not explain why the evaporation of SM was more effective than that of water. The results of this Chapter were published in Dairy Science and Technology[1].

After additional instrumentation of the pilot, some problems were identified with the water level sensor of the heating systems and the distributor system of the evaporator tubes. After solving these problems and using the same operating conditions, the difference between the effectiveness of evaporation of water, skim and whole milk was studied. No significant variations were found ($p < 0.05$) in the evaporation rate or in the energy efficiency for the experiments with water, skim milk (two runs – 83.0 g·kg^{-1} to 471.0 g·kg^{-1} of total solids), and during the first run of whole milk (114 g·kg^{-1} to 265 g·kg^{-1} of total solids), but the values were lower in the second run of the whole milk experiments (265 g·kg^{-1} to 545 g·kg^{-1} of total solids), where a poor wetting rate was identified in the evaporator tubes. The experiments were then performed at an inlet mass flow rate of 70 kg·h^{-1}. No significant variations were then found ($p < 0.05$) in the evaporation rate or in the energy efficiency for all runs and products.

The appropriate instrumentation of the vacuum evaporation process allowed identification and correction of the process problems and was necessary to keep an efficient working of evaporators.

The main aims of this chapter are to:

- demonstrate how the process parameters could be used to characterize the evaporation process
- study the effectiveness of evaporation of water, skim and whole milk
- describe the enthalpy balance of the vacuum evaporation process

[1] Accepted as: Silveira, A.C.P., Carvalho, A.F., Perrone, Í.T., Fromont, L., Méjean, S., Tanguy, G., Jeantet, R., Schuck, P., 2013. Pilot-scale investigation of effectiveness of evaporation of skim milk compared to water. Dairy Sci. Technol. 93, 537–549. doi:10.1007/s13594-013-0138-1

Capítulo 5

INVESTIGAÇÃO EM ESCALA PILOTO DA CAPACIDADE DE EVAPORAÇÃO DE LEITE DESNATADO, LEITE INTEGRAL E ÁGUA

O objetivo do trabalho descrito neste capítulo foi o de comparar a capacidade evaporativa da água pura, leite desnatado e leite integral durante a concentração em um evaporador piloto, único efeito, de película descendente. Utilizando a instrumentação da aquisição do piloto e uma vazão mássica de alimentação de 50 kg·h^{-1}, nenhuma diferença significativa ($p < 0,05$) na capacidade evaporativa ou na eficiência energética para as duas passagens de leite desnatado foram identificadas. No entanto esses valores foram superiores aos obtidos pelos experimentos realizados com água pura. O coeficiente de transferência de calor apresentou o mesmo valor para todos os produtos estudados, sendo que este resultado não explica por que a capacidade evaporativa do leite desnatado foi superior ao da água pura. Os resultados apresentados neste capítulo foram publicados na revista Dairy Science and Technology[1].

Após a instrumentação adicional do piloto foram identificados problemas com o sensor de nível de água dos sistemas de aquecimento e com o sistema de distribuição de produto no topo dos tubos de evaporação. Após a reparação destes problemas e utilizando os mesmos parâmetros operacionais, a diferença entre a capacidade evaporativa da água pura, leite desnatado e integral foi novamente estudada. Não houve diferenças significativas ($p < 0,05$) entre a capacidade evaporativa e entre a eficiência energética para os experimentos realizados com água, leite desnatado (duas passagens - 83,0 g·kg^{-1} a 471,0 g·kg^{-1} de sólidos totais), e durante a primeira passagem do leite integral (114 g·kg^{-1} a 265 g·kg^{-1} de sólidos totais), mas esses valores foram inferiores na segunda passagem dos experimentos realizados com leite integral (265 g·kg^{-1} a 545 g·kg^{-1} de sólidos totais), onde uma molhagem ineficiente dos tubos de

evaporação foi identificada. Os experimentos foram então realizadas a uma vazão mássica de alimentação de 70 kg·h^{-1}. Nenhuma diferença significativa foi encontrada ($p < 0,05$) na capacidade de evaporativa ou na eficiência energética para todas as passagens e para ambos produtos utilizados nesse estudo.

A adequada instrumentação do processo de evaporação a vácuo permitiu a identificação e correção de problemas no processo de evapoção e foi necessária para manter um funcionamento eficaz do evaporador.

Os principais objetivos deste capítulo são:

- demonstrar como os parâmetros operacionais do processo podem ser utilizados para caracterizar o processo de evaporação a vácuo
- estudar a capacidade evaporativa da água, leite desnatado e leite integral
- descrever os balanços entálpicos do processo de evaporação a vácuo

Table of contents

5.1. Introduction

Evaporation is a process through which a liquid is brought to its boiling point by external heating, transforming the solvent into vapor that escapes from the surface of the liquid. Such thermal concentration is commonly used for liquid foods (i.e. milk, fruit juice and sugar solutions) to manufacture products such as sweet condensed milk (Gänzle et al., 2008), “dulce de leche” (Hentges et al., 2010), beet or cane sugar, fruit juice (Tonelli et al., 1990) and tomato sauce concentrates (Runyon et al., 1991). Above all, it is an intermediate process in the production of milk, buttermilk and whey powders (Schuck, 2002), infant formula (Zhu et al., 2011), protein isolates (Onwulata et al., 2006), etc.

In order to reduce energy consumption and environmental impact, it is important that evaporators operate at their maximum capacity, which is strongly dependent on the overall heat transfer coefficient. This parameter cannot be considered as an intrinsic characteristic of the evaporator, since it also depends on the nature of the product and on their flow conditions (Mafart, 1991). The factors that control heat transfer in the evaporator tubes are important for close monitoring of the evaporation process and for calculating the dimensions of evaporators (Bouman et al., 1993; Jebson and Iyer, 1991).

As boiling and concentration take place inside the falling-film evaporator, the study of the mechanisms is complex, because both occur simultaneously (Li et al., 2011; Pehlivan and Ozdemir, 2012). Some studies of the evaporation process reported in the literature were carried out on industrial evaporators. In this case, operating conditions such as the configuration of the equipment and the quality of the raw materials were not controlled (Jebson and Iyer, 1991; Jebson and Chen, 1997). In contrast, other studies on laboratory and pilot scales were carried out using model solutions (water, sucrose solutions, etc.) (Luo et al., 2011; Prost et al., 2006) and evaporation systems whose design had been modified from industrial evaporators in order to separate phenomena and facilitate their understanding (Adib et al., 2009; Bouman et al.,

1993). There is, therefore, only limited information on evaporator performance, i.e. the performance of real evaporators working with real products over real concentration steps.

The aim of this study was to compare heat and mass balance using a pilot scale, single stage vacuum falling film evaporator composed of three tubes in series, for the evaporation of skim milk and water. This equipment was designed to study both phenomena (boiling and concentration) occurring during the evaporation of dairy products. The experimental effectiveness of evaporation were compared to theoretical effectiveness with no energy loss. The investigation also involved calculation of the energy used by the evaporator, the overall heat transfer coefficient for each run, and study of the factors influencing the evaporation rate of skim milk compared to water.

5.2. Materials and methods

5.2.1. Pilot vacuum evaporator and experiments

The experiments were performed with the pilot scale, single stage falling-film evaporator equipped with the acquisition sensors (described in Chapter 4.1).

All experiments were performed at the product inlet temperature of 60 °C, an absolute pressure (P_{abs}) of 0.02 MPa, and thus the evaporation temperature (θ_{ev}) was maintained at 60 °C throughout the three tubes. These experiments were taken in triplicate at ambient temperature.

5.2.2. Experimental runs

Experimental runs were carried out with water (maximum hardness of 80 mg $CaCO_3 \cdot kg^{-1}$) and skim milk at two different initial concentrations. All experiments were performed at an inlet mass flow rate of 50.0 ± 0.7 $kg \cdot h^{-1}$ and the results analyzed after 30 min of process time. This short process time was chosen to evite fouling formation. The value of inlet flow rate was

provided by the evaporator manufacturer as a good flow rate for milk concentration. It was therefore used to characterize thermodynamically the evaporation process.

Skim milk was prepared at 100.0 g·kg^{-1} of total solids (TS) from dairy powder (Societé Mayenne, Mayenne, France). It was heated to 60 °C before evaporation. The total process time was around 60 min to avoid fouling formation from 200 kg of product. After the first run (1R) through the evaporator, skim milk was concentrated from 100.0 g·kg^{-1} TS to 240.0 g·kg^{-1} TS. This product, still at 60 °C, was reintroduced into the evaporator where it was re-concentrated (second run (2R)) from 240.0 g·kg^{-1} TS to 520.0 g·kg^{-1} TS (Table 5.1).

Table 5.1. Evaporation rates for skim milk and water, showing inlet and outlet total solids content and viscosities. Average (n=3) ± standard deviation.

Product	Inlet / Outlet TS (g·kg^{-1})	Inlet / Outlet η_{100} (mPa·s)	Evaporation rate [a] (kg·h^{-1})	Error of mass balance [b] (%)
Water	-	0.47 / 0.47	23.5 ± 0.7	1.4
Skim milk first run	100.0 ± 0.5 / 240.0 ± 0.5	1.08 / 2.83	30.0 ± 0.7	1.6
Skim milk second run	240.0 ± 0.5 / 520.0 ± 1.5	2.83/ 23.81	30.0 ± 0.9	4.6

a: $(\dot{m}_{p_{in}} - \dot{m}_{cc})$

b: $\left[\left(\dot{m}_{p_{in}} - (\dot{m}_{cc} + \dot{m}_{cd}) \cdot 100\right)\right] / \dot{m}_{p_{in}}$

Legend: TS: total solids; η_{100}: apparent viscosity

Inlet mass flow rate = 50 kg·h^{-1}
Heating power= 25.2 kW

5.2.3. Physicochemical analyses

Viscosity and total solids were measured as described in chapter 4.4.1 and 4.4.2, respectively.

5.2.4. Enthalpy characterization

Mass and enthalpy balance, overall heat transfer coefficient and assessment of process efficiency were calculated as described in chapter 4.5, 4.6 and 4.7, respectively.

5.2.5. Statistical analysis

Data were analyzed by regression analysis of variance using SAS (2008) software, at the 0.05 level of significance.

5.3. Results and discussion

5.3.1. Mass balance

The initial and final product concentrations before and after the run in the evaporator are presented in Table 5.1. The viscosity of these solutions was also measured (Table 5.1). The viscosity of water remained constant during evaporation, whereas the viscosity of skim milk increased from 1.08 mPa·s to 2.83 mPa·s during the 1R, and its behavior was Newtonian, i.e. its viscosity remained constant whatever the shear rate. In the 2R run the viscosity increased from 2.83 mPa·s at 240.0 $g \cdot kg^{-1}$ of TS to 23.81 mPa·s at 520.0 $g \cdot kg^{-1}$ of TS. At this concentration, the product had a shear thinning behavior, i.e. its viscosity decreased with increasing shear rate. This behavior can be explained as a consequence of increasing the shear rate which induces the asymmetric dispersed molecules to align themselves within the shear planes, causing the frictional resistance to diminish (Tung, 1978; Velez Ruiz and Barbosa Canovas, 1997). The mass balance of the process was effective for all experiments, with a maximum error of 4.6 %, representing the difference between the inlet and outlet mass flow rates (Eq. 4.2). The evaporation rate was calculated by subtracting the inlet flow rate of the product and the outlet flow rate of the product concentrate. This parameter reflects the amount of water evaporated from the product. There was no significant variation ($p < 0.05$) in the evaporation rate for the two runs carried out with skim milk, and it was higher than that obtained for the experiments carried

out with water. To explain these results, the enthalpy balance was calculated and the process efficiency assessed (Table 5.2).

5.3.2. Enthalpy balance

To calculate the energy balance, the vacuum evaporation process was considered as a single system (Fig. 4.10). In other words, we took into account the average temperature of the steam measured in the three tubes (Fig. 4.4 (T_{Sin})) and the sum of the mass of steam condensed on the three tubes. The temperature of the outlet steam (Fig. 4.4 (T_{Sout})), remained constant at 75 °C for all experiments. In this case, it was assumed that all energy exchanged between the steam and the product corresponded to latent heat, and consequently the steam temperature was the same as for the steam condensate (75 °C).The pilot scale evaporator could thus be considered as a full latent heat exchanger.

The enthalpy balance data for the experiments performed with skim milk and water are given in Table 5.2. There was no significant variation ($p < 0.05$) in the enthalpy balance error for the experiments. The difference between the inlet and outlet enthalpy values represented the heat losses $\dot{q}_p$ (Eq. 4.3) by radiation and convection to the surrounding air. Such loss is variable and difficult to measure, depending on factors such as the nature of the steel (state of polish), the temperature difference between the surfaces of the evaporator and ambient air, etc. In industrial single stage evaporators, an allowance is made for heat losses up to 1% (Jebson and Iyer, 1991) but with this pilot scale evaporator, these energy losses were expected to be greater as the scale was reduced.

Table 5.2. Data of enthalpy balance for water and skim milk experiments performed at a total heating power of 25.20 ± 0.05 kW. Average (n=3) ± standard deviation.

Run	Q_1[a] (kW)	Q_{cw}[b] (kW)	Energy Losses[c] (%)	SEC[d] (kJ·kg^{-1} of water)	EE[e] (%)
Water	0.05 ± 0.00	23.64 ± 0.29	6%	3243 ± 102	70%
Milk first run	0.03 ± 0.00	23.40 ± 0.35	7%	3024 ± 93	79%
Milk second run	0.05 ± 0.00	23.64 ± 0.11	6%	2889 ± 97	81%

a: $Q_1 = (\dot{m}_{cc} \cdot H_{cc} + \dot{m}_{cd} \cdot H_{cd}) - \dot{m}_{p_{in}} \cdot H_{p_{in}}$

b: $Q_{cw} = \dot{m}_{cw} \cdot (H_{cw_{out}} - H_{cw_{in}})$

c: Calculated according to Eq. 4.9

d: Calculated according to Eq. 4.11

e: Calculated according to Eq. 4.12

Legend: SEC: specific energy consumption; EE: energy efficiency.

Inlet mass flow rate = 50 kg·h^{-1}

As previously explained, SEC (Eq. 4.11) is a parameter used to evaluate the economic aspects of concentration: the higher the SEC, the greater the cost of the operation. With a single stage evaporator operating at the evaporating temperature used in this study, an optimal value of SEC of about 2358 kJ·kg^{-1} would be expected without energy loss. For the experiments with skim milk, there was no significant variation ($p < 0.05$) in the SEC and this value was lower than the values obtained with water (Table 5.2), in agreement with the evaporation rate (Table 5.1). Energy efficiency was calculated to provide a better evaluation of the process yield (Eq. 4.12). This parameter can be interpreted as the percentage of energy gained from the steam which is used for evaporating 1 kg of product. As expected from the SEC results, there was no significant variation ($p < 0.05$) in the energy efficiency (EE) for the experiments with skim milk, and it was higher than the values obtained for the experiments with water. The average values of the EE

were close to 80 % for experiments with skim milk and 70 % for experiments with water (Table 5.2), the difference from 100% (in a theoretical one stage vacuum evaporator) corresponding to the environmental heat lost, product elevation boiling point, wall thermal resistance, etc.. Experiments conducted with water at other heat fluxes showed similar energy efficiency values, demonstrating that the energy from the steam is always produced in excess in this pilot evaporator, thus leading to a lower energy yield.

5.3.3. Overall heat transfer coefficient

To complement and confirm the results obtained, the overall heat transfer coefficient for each tube and for all three products was calculated. The results are shown in Table 5.3.

Table 5.3. Calculated values of heat transfer coefficient and operating parameters for each tube of the vacuum evaporator. Average (n=3) ± standard deviation.

Product	Tube N°	Φ (kW·m^{-2})^a	$\Delta\theta$ (°C)^b	U [kW·m^{-2}·°C^{-1}]^c
Water	1	18.6	15.1 ± 0.4	1.23 ± 0.04
	2	29.1	15.3 ± 0.4	1.90 ± 0.03
	3	29.1	15.7 ± 0.4	1.85 ± 0.04
Skim milk – 1st run	1	18.6	15.0 ± 0.4	1.24 ± 0.03
	2	29.1	15.0 ± 0.3	1.94 ± 0.02
	3	29.1	15.1 ± 0.3	1.93 ± 0.03
Skim milk – 2nd run	1	18.6	14.9 ± 0.3	1.25 ± 0.02
	2	29.1	14.8 ± 0.3	1.96 ± 0.02
	3	29.1	14.6 ± 0.3	2.00 ± 0.02

a and c: Calculated according to Eq. 4.10

b: $(\theta_{v-1} - \theta_{ev})$

Legend: Φ: heat flux; $\Delta\theta$: temperature difference; U: overall heat transfer coefficient.

Inlet mass flow rate = 50 kg·h^{-1}
Heating power= 25.2 kW

The heating power used in this process was 8.40 ± 0.02 kW for each tube. The diameter of the first tube was greater than the other two (36 mm versus 23 mm). The heat flux in the first tube, calculated according to Eq. 4.10, was therefore lower than in the other tubes. The temperature difference between the steam and the product was the same for all the products ($p < 0.05$). This temperature gap was greater than that applied industrially, which is generally less than 10 °C (Adib et al., 2009).

The overall heat transfer coefficient (U), calculated according to Eq. 4.10, was the same ($p < 0.05$) in the first tube for all products (Table 5.3), i.e. an average value of 1.24 $kW \cdot m^{-2} \cdot °C^{-1}$, whereas it was close to 1.96 $kW \cdot m^{-2} \cdot °C^{-1}$ in the other two tubes. Jebson and Chen (1997) obtained values of U between 0.8 $kW \cdot m^{-2} \cdot °C^{-1}$ and 3.08 $kW \cdot m^{-2} \cdot °C^{-1}$ for whole milk measured from several milk powder factories; Jebson and Iyer (1991) found values of U between 2.00 $kW \cdot m^{-2} \cdot °C^{-1}$ and 3.50 $kW \cdot m^{-2} \cdot °C^{-1}$ for skim milk concentrated in five-effect evaporators; Prost et al. (2006) reported values of U between 2.08 $kW \cdot m^{-2} \cdot °C^{-1}$ and 2.40 $kW \cdot m^{-2} \cdot °C^{-1}$ for water evaporated in the first effect of a third-effect evaporator.

In these experiments, the heat transfer coefficient was the same for the same operating conditions (Φ, $\Delta\theta$, P_{abs}) whatever the product. This result does not explain why the evaporation rate of skim milk was greater than that of water (Table 5.1). It is emphasized that the inverse of U is overall resistance resulting from the addition of four resistance levels in a series, where the limiting resistance is generally the value on the product side between the wall and the evaporated liquid, especially at high concentrations (Jebson and Iyer, 1991; Jebson and Chen, 1997). This value depends on several factors:

- Physical properties of the product treated (viscosity, η_p, density, ρ_p, surface tension, σ_p, etc.),

- Process conditions (heat flux, Φ, temperature difference, $\Delta\theta$, boiling temperature, θ_p...)
- Nature and geometry of the heating surface, (roughness R, etc.).

These three types of parameter influence the values of the heat transfer coefficient of the product side and therefore the values of U.

Thus the behavior of a product and the efficiency of the evaporation process (SEC, evaporation rate, etc.) cannot be predicted with only its overall heat transfer coefficient.

It should be remembered that the evaporation rate is related to the operation conditions (e.g., distribution system, heat flux, etc.) (Morison et al., 2006) and product characteristics, such as viscosity and surface tension (Morison et al., 2006; Paramalingam et al., 2000; Pehlivan and Ozdemir, 2012). Moreover, product viscosity has an impact on the thickness and the residence time distribution of the thin falling film. The flow behavior of the product throughout the evaporator is modified according to its viscosity: a thicker and slower thin film should be formed at the end of the skim milk concentration process compared to water. Therefore the higher level of viscosity might result in a longer residence time of the product in the evaporator and thus a longer time when the product would receive the evaporation energy, thereby increasing the evaporation rate.

5.4. Additional information

An additional instrumentation of the evaporation pilot was performed to improve characterization and understanding of the evaporation process (§ 4.2.2.). The pilot equipment could thus be divided into four different sections (Fig. 4.8), where the evaporation rate of each tube could be assessed (since the inlet and outlet product flow rate of each tube could be measured). With the new information some problems were identified in performing the

experiments, such as a lower wetting rate of the tubes and poor regulation of the water level sensor of the heating system.

5.4.1. Distributor system

The plate distributor system (Fig. 4.5), located at the top of the evaporator tubes, did not disperse the water homogeneously (Fig. 5.1 (A)), and therefore a film breakdown (Fig. 2.14) occurred. Since product film formation did not take place uniformly throughout the evaporator tube, the efficiency of the process decreased. The poor wetting rate of the tubes led to the formation of dry patches in the tubes (Fig. 2.14), and this phenomenon thus contributed to loss in the heat transfer surface. The plate distributor system was then changed to a cone-shaped concave distributor (Fig. 4.6). The water dispersion was more effective with the new distributor system (Fig. 5.1 (B)). Dispersion of skim milk with the plate distributor was better than water dispersion (Fig. 5.1 (C)), possibly related to differences in product properties, especially surface tension and viscosity.

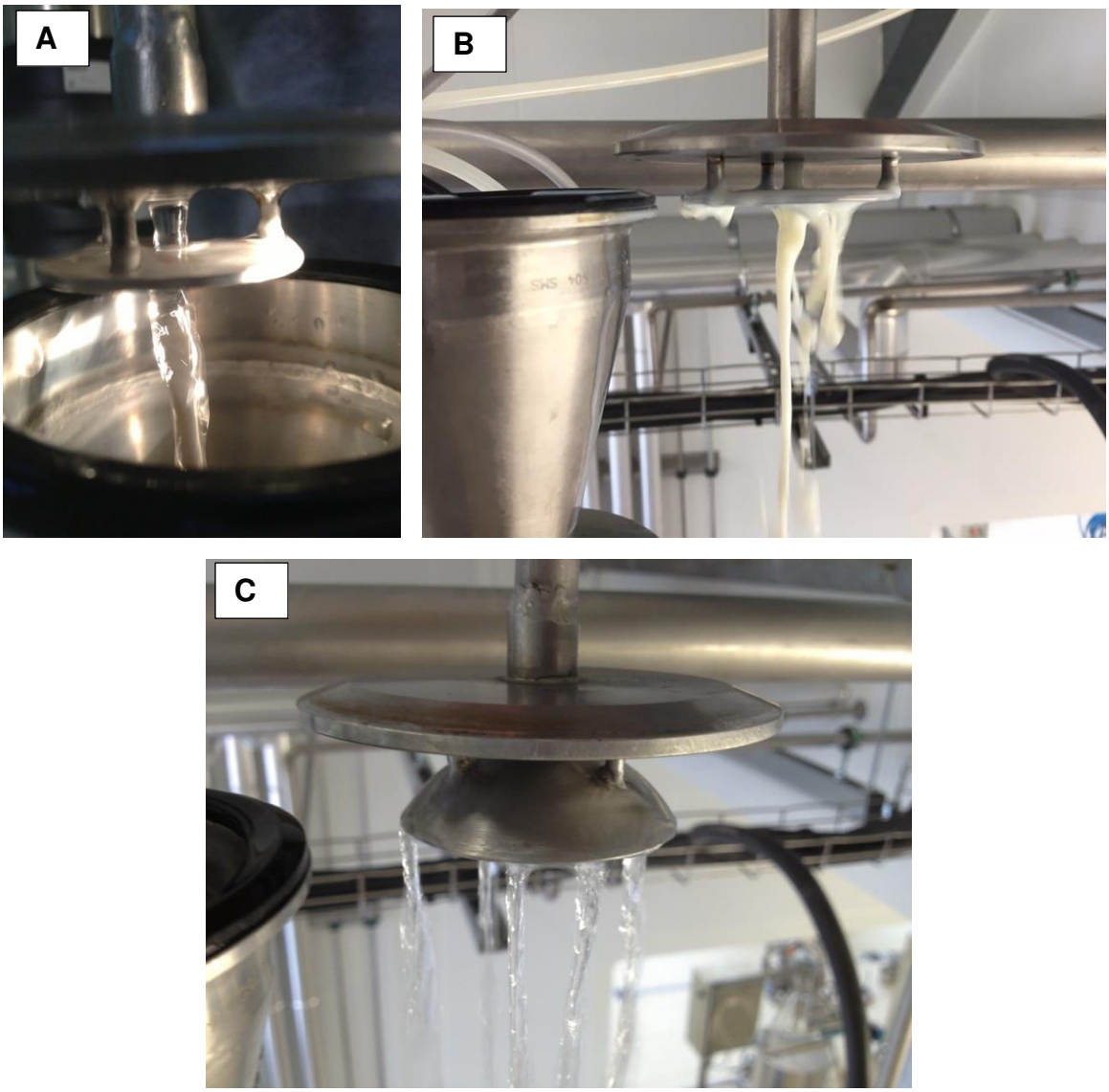

Figure 5.1. Dispersion of water and skim milk with the two distributor systems. (A) plate distributor with water, (B) plate distributor with skim milk at 120 g·kg-1 total solids and (C) cone-shaped concave distributor with water.

5.4.2. Water level sensor of the heating tubes

The water level sensor of the three heating systems (Fig. 5.2) was poorly regulated. A delay of a few seconds in closing the water injection electro valve occurred when fills the heating

systems and an excess of water was therefore injected into the heating system. This excess flowed to the steam side of the evaporator tubes, thus decreasing the heat transfer surface (Fig. 5.2). This problem occurred mainly in the first evaporator tube.

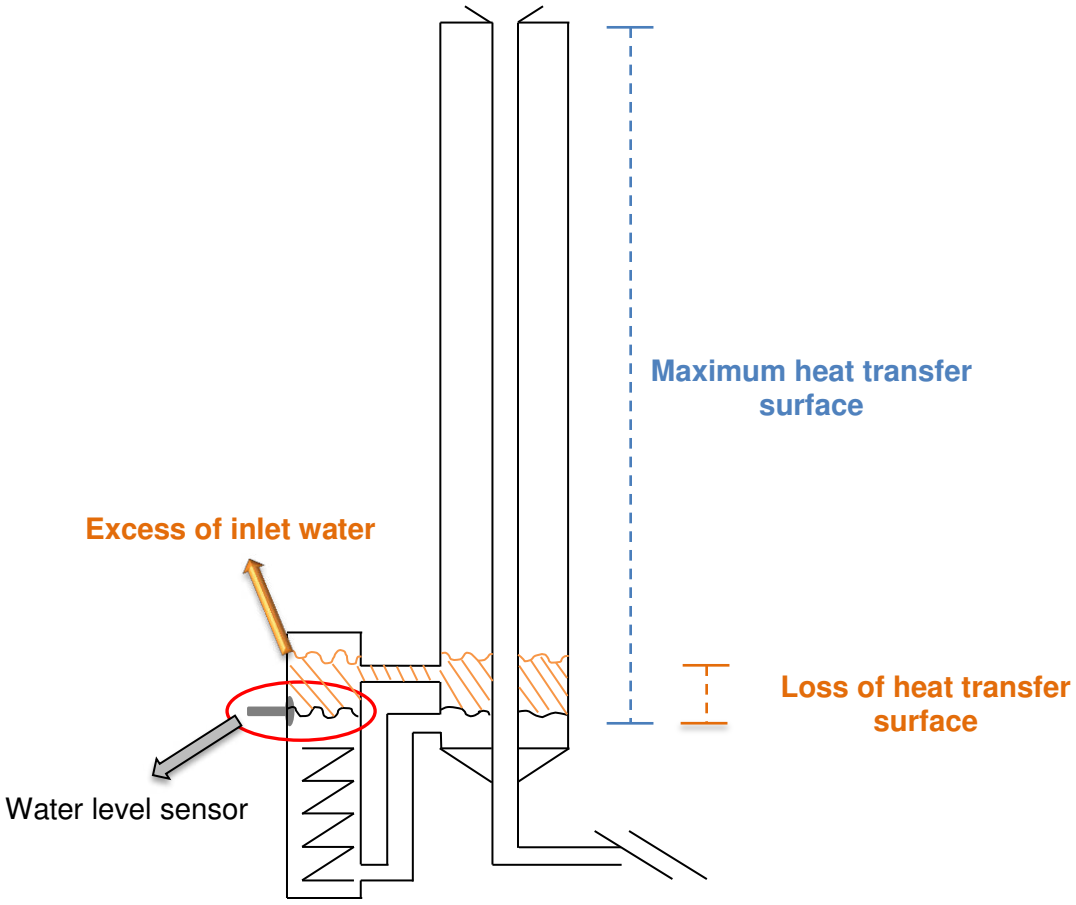

Figure 5.2. Evaporator tube showing the water sensor level and the loss of heat transfer surface due the excess water injected into the heating system.

The experiments with skim milk and water were always performed on the same day, in order to retain the same ambient conditions (same room temperature) and always with water prior to milk. The heating systems were filled with water at the beginning of the experiments and, due to the problem with the water level sensor, a loss of heat transfer surface occurred (Fig. 5.2).

As steam is always produced in excess in this pilot equipment, a part of the steam goes to the condenser (Fig. 4.1). This mass was calculated experimentally as 1.77 kg·h^{-1} of excess steam produced by each heating system, i.e. not used to exchange energy. This steam mass was not used in the calculation of the energy balance. The steam produced in excess was thus condensed in the condenser and extracted by the condensate evacuation pump (Fig. 4.1). A decrease in the water level in the heating system and an increase in the used heat transfer surface therefore occurred over time. The evaporation rate thus increased in relation to the process time, and the heat transfer surface for skim milk experiments was greater than for water experiments (since the experiments with milk were always carried out after water experiments).

These two factors, i.e. poor distribution of water in the evaporator tubes and higher heat transfer surface for skim milk experiments, together explain the lower evaporation rate of water compared to skim milk.

5.4.3. Investigation of the effectiveness of evaporation after improvement of the pilot vacuum evaporator

After regulation of the water level sensor, change in the distributor system and use of manual injection of water into the heating systems, a new characterization of the evaporator process was undertaken. Solutions of water, fresh skim milk and whole milk (26 g·kg^{-1} fat content) were studied to validate the difference in the effectiveness of evaporation. The effects of the inlet mass flow rate of the product at 50 kg·h^{-1} and 70 kg·h^{-1} were also studied. All other operating parameters of the evaporation process were kept constant.

The initial and final product concentrations before and after the runs in the evaporator are presented in Table 5.4.

Table 5.4. Evaporation rates for skim milk, whole milk and water at two different inlet mass flow rates. Total heating power of 25.20 ± 0.05 kW.

Mass flow rate	Product	Inlet / Outlet TS ($g \cdot kg^{-1}$)	Evaporation rate [a] ($kg \cdot h^{-1}$)
50 $kg \cdot h^{-1}$	Water	-	26.9 ± 1.5
	Skim milk first run	83 / 210	27.7 ± 1.7
	Skim milk second run	210 / 471	26.6 ± 2.3
	Whole milk first run	114 / 265	27.9 ± 1.4
	Whole milk second run	265 / 545	25.4 ± 1.5
70 $kg \cdot h^{-1}$	Water	-	27.4 ± 1.7
	Skim milk first run	90 / 152	27.9 ± 1.5
	Skim milk second run	152 / 256	28.3 ± 1.4
	Skim milk third run	256 / 428	27.7 ± 2.3
	Whole milk first run	113 / 188	27.2 ±1.6
	Whole milk second run	188 / 312	27.1 ± 1.2
	Whole milk third run	312 / 513	27.2 ± 1.3

a: calculated as: $(\dot{m}_{p_{in}} - \dot{m}_{cc})$

TS = total solids

For the experiments performed at an inlet mass flow rate of 50 $kg \cdot h^{-1}$, skim milk (SM) and whole milk (WM) were concentrated in two runs in the evaporator, reaching final concentrations of 471 $g \cdot kg^{-1}$ and 545 $g \cdot kg^{-1}$ of TS, respectively.

There was no significant difference ($p < 0.05$) in the evaporation rates between the first and second runs of skim milk, the first run of whole milk, and water experiments. Nonetheless the second run of whole milk presented a lower evaporation rate ($p < 0.05$) compared to the other solutions and runs studied.

The water evaporation rate calculated before and after the additional instrumentation of the pilot evaporator increased from 23.5 ± 0.7 $kg \cdot h^{-1}$ to 26.9 ± 1.5 $kg \cdot h^{-1}$ (at the inlet mass flow rate of 50 $kg \cdot h^{-1}$), reaching similar values to those of the skim milk experiments (27.2 ± 1.5 $kg \cdot h^{-1}$)

under the same operating conditions. These results demonstrated that the difference in the evaporation rate between water and skim milk, calculated before the additional instrumentation and configuration of the equipment, was due to the problems with the water sensor level and the distributor system.

There was no significant variation ($p < 0.05$) in the enthalpy balance error (Table 4.5) for the experiments performed with water, the two runs of skim milk and the first run of whole milk, although the value was higher in the second run of whole milk experiments. The lower evaporation rate of the second run of whole milk might be explained by the poor wetting rate of the tubes, which might cause a film breakdown (Fig. 2.14) and increase in energy loss.

Table 5.5. Data of enthalpy balance for water, skim milk and whole milk experiments performed at a total heating power of 25.20 ± 0.05 kW, and two different inlet product mass flow rates.

Inlet Mass Flow Rate	Run	Q_1[a] (kW)	Q_{cw}[b] (kW)	Energy Losses[c] (%)	SEC[d] ($kJ \cdot kg^{-1}$)	EE[e] (%)
50 $kg \cdot h^{-1}$	Water	0.00 ± 0.00	19.7 ± 1.0	10.6 ± 0.6	2826 ± 48	83 ± 1
	Skim milk first run	-0.01 ± 0.00	20.1 ± 0.9	10.7 ± 2.0	2811 ± 63	83 ± 1
	Skim milk second run	- 0.01 ± 0.00	19.5 ± 0.8	11.7 ± 1.3	2965 ± 56	79 ± 2
	Whole milk first run	0.01 ± 0.00	19.5 ± 1.1	11.1 ± 0.9	2735 ± 58	86 ± 2
	Whole milk second run	0.03 ± 0.01	19.2 ± 1.3	13.8 ± 2.4	3011 ± 62	78 ± 2
70 $kg \cdot h^{-1}$	Water	-0.01 ± 0.01	20.0 ± 0.9	10.2 ± 1.5	2815 ± 48	83 ± 1
	Skim milk first run	0.00 ± 0.01	20.3 ± 0.8	9.0 ± 0.6	2770 ± 41	85 ± 1
	Skim milk second run	0.01 ± 0.01	20.9 ± 0.9	8.8 ± 1.1	2784 ± 46	84 ± 1
	Skim milk third run	0.03 ± 0.01	20.9 ± 0.7	7.3 ± 1.4	2749 ± 47	85 ± 2
	Whole milk first run	0.00 ± 0.01	20.2 ± 0.9	8.1 ± 0.7	2784 ± 48	84 ± 1
	Whole milk second run	0.01 ± 0.01	20.3 ± 0.9	9.4 ± 0.7	2828 ± 66	83 ± 2
	Whole milk third run	0.04 ± 0.01	20.7 ± 0.8	8.0 ± 1.2	2838 ± 37	82 ± 1

a: $Q_1 = (\dot{m}_{cc} \cdot H_{cc} + \dot{m}_{cd} \cdot H_{cd}) - \dot{m}_{p_{in}} \cdot H_{p_{in}}$

b: $Q_{cw} = \dot{m}_{cw} \cdot \left(H_{cw_{out}} - H_{cw_{in}}\right)$

SEC = specific energy consumption; EE = energy efficiency.

An increase in the inlet steam temperature was observed in the second run of whole milk experiments (Fig. 5.3). A poor wetting rate of the inner surface of the tubes, and therefore dry patches and fouling formation (§ 2.4) might be related to the temperature increase. The inlet mass flow rate of 50 kg·h^{-1} was thus not sufficient to ensure a minimum wetting rate for the surface of the tubes when the solution to be concentrated had a high viscosity/total solids values.

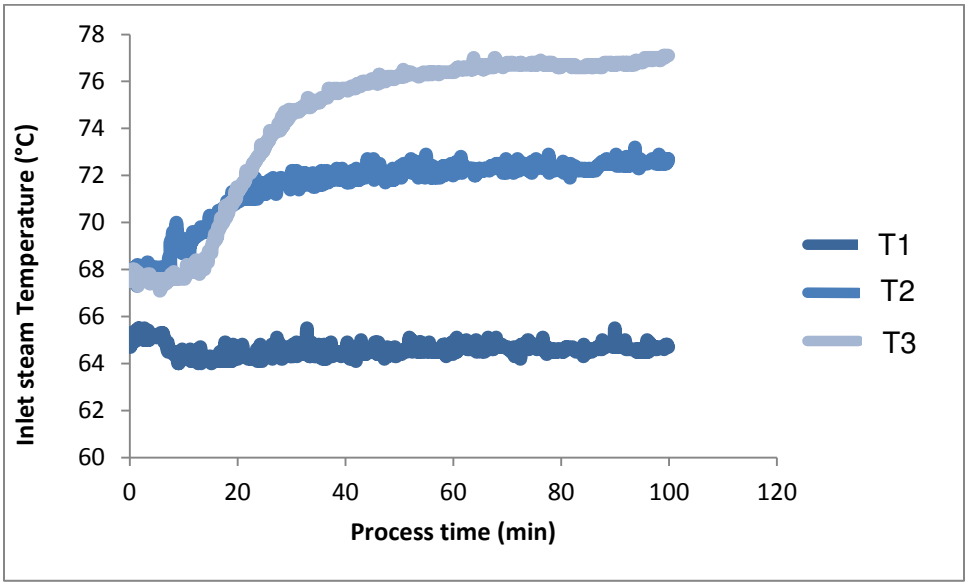

Figure 5.3. Inlet steam temperature in function of the process time for the experiments with whole milk at inlet mass flow rate of 50 kg·h^{-1}.

To ensure a minimum wetting rate of the three evaporation tubes the experiments were performed at an inlet mass flow rate of 70 kg·h^{-1}, where the solutions of skim and whole milk were concentrated in three runs in the evaporator. As the heating power was constant for the two inlet mass flow rates studied (25.20 ± 0.05 kW), the evaporation rate for all solutions and

runs at 70 kg·h^{-1} was the same ($p < 0.05$) (27.4 ± 0.5 kg·h^{-1}) as that of skim milk in the two runs, whole milk in the first run and water at 50 kg·h^{-1}.

Since there was no difference in the evaporation rate of any of the solutions studied at the inlet mass flow rate of 70 kg·h^{-1}, the increase in the inlet mass flow rate (50 kg·h^{-1} to 70 kg·h^{-1}) was effective to ensure a good wetting rate of the evaporator tubes.

The energy loss, SEC and EE were constan, (8.5 ± 1.2 %, 2795 ± 32 kJ·kg^{-1} and 89 ± 1 %, respectively), for all solutions and runs conducted at 70 kg·h^{-1}.

5.5. Conclusion

The effectiveness of a pilot scale single stage falling-film evaporator for the evaporation of water and skim milk was studied, for which a wide range of information was required, i.e. information related to the operating conditions as well as information related to the product.

It was first demonstrated that the evaporation rate of skim milk was greater than that of water in the same operating conditions. Certain conclusions were drawn to explain this phenomenon, such as influence of product viscosity, product dispersion in the tubes, residence time etc.

Some modifications were performed on the pilot evaporator to improve the understanding of its working. These modifications revealed that there was no difference in evaporation rate between the first and second runs of skim milk, water and first run of whole milk. The second run of whole milk showed a lower evaporation rate, where a problem in the wetting rate of the tubes was identified.

At the mass flow rate of 70 kg·h^{-1} there was no difference in the evaporation rate, energy loss, SEC and EE for any of the solutions studied. This inlet mass flow rate showed sufficient efficiency to ensure a good wetting rate of the evaporator tubes.

Improve understanding of the process combined with suitable instrumentation of the vacuum evaporator equipment proved to be effective in identifying and solving problems in this process. Further studies of the evaporation process are needed to investigate the influence of the product residence time distribution and the flow profile in order to improve the working and understanding of evaporators.

Chapter 6

FLOW REGIME ASSESSMENT IN FALLING FILM EVAPORATORS USING RESIDENCE TIME DISTRIBUTION FUNCTIONS

The aim of this chapter is to describe the flow regime, and characterize and model the residence time distribution (RTD) functions of a falling film evaporator (FFE). Experimental runs were carried out with skim milk at 60 kg·h^{-1}, 70 kg·h^{-1} and 80 kg·h^{-1} and water at 70 kg·h^{-1} of feed mass flow rates. Flow was characterized using experimental Reynolds number (Re_f). The RTD function in the FFE was measured in four sections of the vacuum evaporator equipment. These RTD functions were modeled by a combination of perfectly mixed reactor tanks in series. In this study, the turbulent and wavy-laminar flow regime had the same mean residence time, otherwise when the flow regime changed from wavy-laminar to laminar, the mean residence time increased. The flow was analyzed as a main and a minor retarded flow, where two layers of product flowed through the evaporator tubes. The future of this work consists of extending the RTD approach to other products and operating conditions in the evaporator device. The results of this chapter were published in Journal of Food Engineering[1].

The main aims of this chapter were to:
- determine experimentally the RTD functions of a pilot-scale falling film evaporator
- model these RTD functions
- identify the flow regime of the process

[1]Silveira, A.C.P., Tanguy, G., Perrone, Í.T., Jeantet, R., Ducept, F., de Carvalho, A.F., Schuck, P., 2015. Flow regime assessment in falling film evaporators using residence time distribution functions. J. Food Eng. 160, 65–76. doi:10.1016/j.jfoodeng.2015.03.016

Capítulo 6

DETERMINAÇÃO DO REGIME DE ESCOAMENTO EM EVAPORADORES DE PELÍCULA DESCENDENTE UTILIZANDO FUNÇÕES DE DISTRIBUIÇÃO DOS TEMPOS DE RESIDÊNCIA

O objetivo deste capítulo é descrever o regime de escoamento e de caracterizar e modelar as funções de distribuição dos tempos de residência (DTR) de um evaporador de película descendente (EPD). Ensaios experimentais foram realizados com leite desnatado a vazão mássica de alimentação de 60 kg·h^{-1}, 70 kg·h^{-1} e 80 kg·h^{-1} e com água a 70 kg·h^{-1}. O escoamento foi caracterizado usando o número de Reynolds experimental (Re_f). A função DTR foi medida em quatro diferentes seções do equipamento de evaporação a vácuo. Estas funções foram modelizadas através de uma combinação de reatores em tanques perfeitamente agitados em série. Neste estudo, o regime de escoamento turbulento e laminar-ondulado tiveram o mesmo tempo de residência médio, no entanto quando o regime de escoamento alterou-se de laminar-ondulado para laminar o tempo de residência médio aumentou. O escoamento foi analisado como sendo duas camadas de produto fluindo uma sobre a outra através dos tubos de evaporação. As perspectivas deste trabalho consistem em estender a abordagem de DTR para outros produtos e condições operacionais do equipamento de evaporação. Os resultados deste capítulo foram publicados na revista Journal of Food Engineering[1].

Os principais objetivos deste capítulo são:

- determinar experimentalmente as funções de DTR de um evaporador de película descendente
- modelar as funções de DTR
- identificar o regime de escoamaento durante o processo de evaporação a vácuo

Table of contents

6.1. Introduction

Concentration by vacuum evaporation is used to decrease the volume and weight of the product, which subsequently reduces the cost of packaging, storage and transport and facilitates the conservation of the concentrate by lowering the water activity (Bouman et al., 1993; Prost et al., 2006; Bimbenet et al., 2007). This process is used for the production of final (sweetened condensed milk, evaporated milk, etc.) (Gänzle et al., 2008), and intermediate products before any further operations such as crystallization, precipitation, coagulation or drying (infant formulae, whey and milk powders, etc.) (Schuck, 2002; Bimbenet et al., 2007; Zhu et al., 2011).

Falling film evaporators (FFE) are widely used in the chemical and food industries for their ability to process heat-sensitive products. The evaporator device is called "falling film" because the liquid falls in a trickling film along the inner wall of the tube. This type of device allows higher heat transfer coefficients, therefore lower residence times can be achieved in comparison with other designs of evaporator (Bimbenet et al., 2007). However, industrial control of this process often relies on an empirical understanding of the phenomena involved, which then results in a time and cost consuming development phase to establish optimal operating conditions when the final product quality must be changed or a new type of product processed.

As boiling and concentration occur simultaneously inside the FFE, the study of the mechanisms is complex (Li et al., 2011; Pehlivan and Ozdemir, 2012); indeed, the rates of enzymatic and chemical changes depend on solute concentration, product temperature and time, and it is therefore necessary take into account these three parameters in order to control thermal damage of constituents and process-dependent properties (product physicochemical properties and product end-properties).

Moreover, the few scientific papers available on the topic of vacuum evaporation in food and chemical domains mainly focus on the calculation and optimization of the heat transfer

coefficient (Chun and Seban, 1971; Mafart, 1991; Jebson and Iyer, 1991; Bouman et al., 1993; Chun and Park, 1995; Jebson and Chen, 1997; Silveira et al., 2013), and there is a lack of research and information concerning the characterization of the flow regime and of the residence time distribution (RTD) functions of the product, E(t), during concentration in FFE. Moreover, RTD is a powerful approach to characterizing the mixing phenomena and flow regime in chemical reactor systems, which allows comparison with ideal reactors.

Determination of the product RTD is an overall and experimental approach which provides valuable information about the product flow regime in the evaporator, according to the operational conditions. It does not provide a good physical understanding of the operation as computational fluid dynamics does but, on the other hand, it integrates the product and process complexity fully.

Computational fluid dynamics (CFD) allow study of the consequences of modifications in operating conditions (temperature, flow rate) and process configuration with regard to particle characteristics (temperature, water content) and trajectories in the dryer (Ducept et al., 2002; Verdurmen et al., 2002). Nevertheless a numerical simulation of a real evaporator process is not accessible in practice: complex geometry (evaporation tubes, pipelines, pumps, etc.), presence of water and vapor, pressure alterations, etc. The experimental CFD is too complex, and hardly representative of the evaporation process. The experimental RTD allows, in a relatively simple way, to have valuable information about the product and process complexity fully.

Since the pioneering work of Danckwerts (1953), the RTD theory has been widely developed, and is nowadays used in a more general context in order to determine a population balance model (Villermaux, 1982), where the basis of this model is that the number of entities with certain properties in a system is a balanceable quantity. Such properties include, size, mass, and age. RTD theory is also used to optimize the process in terms of capital and operation costs (Malcata, 1991). The latter represent an essential step to managing and controlling the quality of

food products. Burton et al., (1959) applied the concept of RTD to food engineering in order to calculate the sterilizing effectiveness of an UHT apparatus for milk processing. Baloh (1979), showed that the loss of sugar in pasteurization and evaporation processes of various processing schemes in the sugar industry could be significantly lowered by reducing the mean residence time of sweet juice. Thor and Loncin (1978), established the mechanisms of rinsing (e.g. mass flow rate and shear stress) of a plate heat exchanger by the measurement of RTD, and thereby laid down the basis for optimizing rinsing equipment in food engineering. Jeantet et al. (2008), calculated and modelled the RTD for different sections of a spray-dryer tower for skim milk, and described the intensity of the heat treatment that the product was subjected to during this process.

No studies have been published on the characterization and modeling of RTD in falling film evaporators for concentration of food products. Understanding both RTD and kinetics of product temperature along its flow in the equipment should pave the way for further prediction of chemical changes (e.g. protein denaturation) that occur during this processing step. The aim of this study was first to characterize RTD functions of a pilot falling film evaporator experimentally, and then to model these RTD functions and identify the flow regime of the process.

6.2. Materials and Methods

6.2.1. Pilot vacuum evaporator

The experiments were performed with the pilot scale, single stage falling film evaporator with the additional instrumentation (described in Chapter 4.2.2) without the preheater. The product was heated at the evaporation temperature in a jacketed tank before entering the equipment.

All experiments were performed at an absolute pressure (P_{abs}) of 0.02 MPa, and thus the saturation temperature of evaporation was maintained at 60 °C throughout the three tubes.

6.2.2. Experimental runs

Experimental runs were carried out with skim milk at three different feed mass flow rates (60 kg·h-1, 70 kg·$h^{-1}$and 80 kg·h^{-1}).

Skim milk was recombined at 100 g·kg^{-1} of total solids (TS) from skim milk powder (Lactalis ingredients, Bourgbarré, France). It was concentrated in three runs in the evaporator equipment. The inlet and outlet TS of skim milk concentrates at the bottom of the three evaporations tubes for the three feed mass flow rates and runs studied are shown in Table 6.1. The total process time was around 60 min to avoid fouling formation from 200 kg of product.

The conductivity of skim milk concentrates exceeding 520 g·kg^{-1} of TS could not be measured reliably due to their high viscosity. Therefore, for the feed mass flow rate of 60 kg·h^{-1}, the TS of the product exiting the second run at 389 g·kg^{-1} (Table 6.1) were diluted to 283 g·kg^{-1} of TS and re-introduced into the evaporator for the third run. This dilution was undertaken to limit the concentration to 520 g·kg^{-1} of TS at the end of the third run.

In total, 27 experiments were performed, at three feed mass flow rates and in three runs. The experimental conditions are summarized in Table 6.1.

Table 6.1. Operational and skim milk properties at the bottom of each evaporation tube for the three feed mass flow rates and runs studied. T1: Evaporation tube 1, T2: Evaporation tube 2, T3: Evaporation tube 3, 1R: first run, 2R: second run, 3R: third run. Heating power of 25.20 ± 0.05 kW.

Feed mass flow rate		80 kg·h^{-1}			70 kg·h^{-1}			60 kg·h^{-1}		
Evaporation tubes		**T1**	**T2**	**T3**	**T1**	**T2**	**T3**	**T1**	**T2**	**T3**
1R	Γ (kg·s^{-1}·m^{-1})	0.170 ± 0.000	0.235 ± 0.000	0.199 ± 0.001	0.147 ± 0.001	0.192 ± 0.001	0.159 ± 0.000	0.125 ± 0.000	0.162 ± 0.001	0,127 ± 0.001
	TS (g·kg^{-1})	108 ± 1	123 ± 4	145 ± 2	114 ± 2	133 ± 4	161 ± 2	123 ± 2	149 ± 5	195 ± 3
	ρ (kg·m^{-3})	1024 ± 0.5	1031 ± 0.6	1040 ± 0.7	1027 ± 1.0	1035 ± 1.1	1047 ± 0.5	1031 ± 0.8	1042 ± 2.2	1062 ± 1.5
	η_{100} (10^{-3} Pa·s)	0.7 ± 0.1	1.0 ± 0.1	1.0 ± 0.1	0.7 ± 0.1	1.0 ± 0.1	1.1 ± 0.1	0.9 ± 0.0	1.0 ± 0.0	1.6 ± 0.1
	Re_f	971	940	796	891	844	643	555	648	317
2R	Γ (kg·s^{-1}·m^{-1})	0.171 ± 0.000	0.238 ± 0.001	0.199 ± 0.001	0.148 ± 0.001	0.193 ± 0.000	0.159 ± 0.001	0.127 ± 0.000	0.163 ± 0.001	0.130 ± 0.000
	TS (g·kg^{-1})	165 ± 3	187 ± 4	240 ± 3	188 ± 4	221 ± 5	264 ± 1	234 ± 4	290 ± 1	389 ± 5
	ρ (kg·m^{-3})	1049 ± 0.8	1058 ± 1.7	1081 ± 0.5	1059 ± 1.8	1073 ± 2.1	1091 ± 0.9	1078 ± 1.5	1103 ± 1.4	1145 ± 2.1
	η_{100} (10^{-3} Pa·s)	1.2 ± 0.0	1.5 ± 0.0	2.6 ± 0.1	1.5 ± 0.0	2.1 ± 0.0	3.4 ± 0.1	2.5 ± 0.0	4.4 ± 0.0	12.3 ± 0.1
	Re_f	570	635	306	421	406	213	203	148	42
3R	Γ (kg·s^{-1}·m^{-1})	0.177 ± 0.001	0.240 ± 0.000	0.206 ± 0.000	0.149 ± 0.000	0.197 ± 0.000	0.161 ± 0.001	0.128 ± 0.001	0.165 ± 0.000	0.138 ± 0.001
	TS (g·kg^{-1})	254 ± 2	298 ± 3	350 ± 1	305 ± 4	365 ± 5	434 ± 6	331 ± 1	417 ± 2	516 ± 4
	ρ (kg·m^{-3})	1087 ±0.9	1106 ± 1.5	1128 ± 2.3	1109 ± 1.1	1135 ± 0.9	1164 ± 1.6	1120 ± 1.8	1157 ± 1.6	1200 ± 0.7
	η_{100} (10^{-3} Pa·s)	3.0 ± 0.1	4.8 ± 0.0	5.9 ± 0.1	5.2 ± 0.1	9.6 ± 0.0	33.0 ± 0.1	6.7 ± 0.1	16.5 ± 0.0	68.3 ± 0.1
	Re_f	236	200	139	125	91	23	76	40	8

Γ = mass flow rate per unit circumference; TS = total solids; ρ = density; η_{100} = apparent viscosity at 100 s^{-1}; Re_f = Reynolds number of the film.

6.2.3. Physicochemical analyses

Viscosity, total solids, density and conductivity were measured as described in chapter 4.4.1, 4.4.2, 4.4.3 and 4.4.4, respectively.

6.2.4. Characterization of the flow

Flow was characterized as described in chapter 4.8.

6.2.5. Measurement of residence time distribution

Residence time distributions functions were calculated and modeled as described in 4.9.

6.3. Results and Discussion

6.3.1. Product and flow characterization

Although the mass flow rate of product was higher in T1 compared to the other two tubes, the value of Γ at the bottom of T1 was always lower than those at the bottom of T2 and T3 for the same feed flow rate because of a higher inner diameter (0.036 m for T1 instead of 0.023 m for T2 and T3 (Table 4.1)). As tubes T2 and T3 had the same diameter, Γ at these points depended only on the mass flow rate of the product (Eq. 3.12). Due to evaporation, the mass flow rate of the product at the bottom of T2 was always higher than that at the bottom of T3: $\Gamma_{T2} > \Gamma_{T3}$. For the experiments conducted at 80 $kg \cdot h^{-1}$, the Γ increased from 0.170 $kg \cdot s^{-1} \cdot m^{-1}$ to 0.177 $kg \cdot s^{-1} \cdot m^{-1}$ at the bottom of T1 / 1R and T1 / 3R, respectively (Table 6.1), evidencing a decrease in the evaporation rate when the concentration of the inlet product increased from 108 $g \cdot kg^{-1}$ to 254 $g \cdot kg^{-1}$ of TS. Compared to other tubes and runs, the increase in the product concentration caused an increase in the Γ, and therefore a decrease in the evaporation rate, as the concentrate mass flow rate increased. These results are in agreement with those of (Morison and Broome, 2014).

The concentration of the product at the bottom of the three evaporation tubes for the three feed mass flow rates and runs studied is shown in Table 6.1. At 80 $kg \cdot h^{-1}$ the skim milk concentration at the end of the third run of the evaporation process was 350 $g \cdot kg^{-1}$ compared to 434 $g \cdot kg^{-1}$ and 516 $g \cdot kg \cdot g^{-1}$ at feed mass flow rates of 70 $kg \cdot h^{-1}$ and 60 $kg \cdot h^{-1}$, respectively. As the evaporation parameters, and in particular the heating power, were kept constant (except for the feed mass flow rate) the energy transferred to the product was the same, and therefore the concentration of the product at the bottom of the evaporator tubes increased according to the decrease in feed mass flow rate.

Density increased proportionately with TS of the skim milk concentrates, whereas viscosity increased exponentially from approximately 365 $g \cdot kg^{-1}$ of TS, which is consistent with the results of (Chong et al., 2009). The apparent viscosity, η_{100}, of skim milk concentrate at 516 $g \cdot kg^{-1}$ of TS was $68.3 \cdot 10^{-3}$ $Pa \cdot s$. This value, that was higher than that found by (Silveira et al., 2013), might be explained by the time that the product remained at 60°C before measurements. Indeed at higher concentration, the viscosity of the milk concentrate increased with time, a phenomenon known as age thickening (Westergaard, 2004). Thus the residence time of the product during concentration in the FFE may affect the viscosity of the concentrate (Baldwin et al., 1980). Viscosity is an important parameter to be monitored for optimal atomization in a spray-dryer (Schuck, 2002; Westergaard, 2004).

The values of Re_f are shown in Table 6.1. Re_f varied between 971 and 8, points corresponding to the maximum and minimum flow rates and product concentration at 80 $kg \cdot h^{-1}$ at bottom of T1 / R1 and at 60 $kg \cdot h^{-1}$ at the bottom of T3 / 3R. In this study, Re_f decreased as the product passed through the evaporation tubes, decreasing its flow rate and increasing its viscosity. These two factors thus led to a lower Re_f at the bottom of the third tube compared to the first and second tubes for the same feed mass flow rate.

The flow regimes at the bottom of the evaporation tubes are presented in Table 6.2. Almost all products presented a wavy laminar profile, except T3 / 3R at 70 $kg \cdot h^{-1}$ and 60 $kg \cdot h^{-1}$ for which a laminar flow was deduced from Re_f.

Table 6.2. Flow behavior, average and minimum residence time of particles of skim milk in falling film evaporators. Measurements performed at three inlet mass flow rates and three runs for each. 1R = first run, 2R = second run, 3R = third run. Heating power of 25.20 ± 0.05 kW.

Feed mass flow rate		80 kg·h^{-1}				70 kg·h^{-1}				60 kg·h^{-1}			
Section (Figure 2)		❶	❷	❸	❹	❶	❷	❸	❹	❶	❷	❸	❹
1R	t_{min} (s)	33 ± 1	44 ± 2	57 ± 1	134 ± 1	36 ± 1	52 ± 2	59 ± 2	146 ± 2	41 ± 2	51 ± 1	74 ± 2	171 ± 2
	v_{max} (m·s^{-1})	0.33 ± 0.01	0.29 ± 0.01	0.23 ± 0.01	0.27 ± 0.02	0.31 ± 0.00	0.23 ± 0.00	0.22 ± 0.01	0.25 ± 0.02	0.27 ± 0.02	0.24 ± 0.01	0.17 ± 0.02	0.21 ± 0.02
	τ (s)	54 ± 2	56 ± 2	72 ± 2	178 ± 2	55 ± 1	62 ± 2	73 ± 1	186 ± 1	67 ± 2	74 ± 2	95 ± 2	229 ± 2
	Flow behaviour	W.L.	W.L.	W.L.	W.L.	W.L.	W.L.	W.L.	W.L.	W.L.	W.L.	W.L.	W.L.
2R	t_{min} (s)	33 ± 1	43 ± 1	57 ± 2	133 ± 2	36 ± 2	52 ± 1	59 ± 1	145 ± 1	42 ± 1	50 ± 1	75 ± 1	175 ± 2
	v_{max} (m·s^{-1})	0.33 ± 0.01	0.28 ± 0.01	0.23 ± 0.01	0.27 ± 0.02	0.31 ± 0.00	0.23 ± 0.00	0.22 ± 0.01	0.25 ± 0.02	0.26 ± 0.01	0.24 ± 0.02	0.17 ± 0.02	0.21 ± 0.02
	τ (s)	53 ± 2	57 ± 2	72 ± 1	179 ± 1	54 ± 1	61 ± 1	73 ± 1	186 ± 1	68 ± 2	72 ± 2	94 ± 2	231 ± 2
	Flow behaviour	W.L.	W.L.	W.L.	W.L.	W.L.	W.L.	W.L.	W.L.	W.L.	W.L.	W.L.	W.L.
3R	t_{min} (s)	32 ± 2	43 ± 1	58 ± 1	135 ± 2	36 ± 1	52 ± 1	60 ± 2	147 ± 2	42 ± 2	51 ± 1	76 ± 2	172 ± 2
	v_{max} (m·s^{-1})	0.35 ± 0.01	0.28 ± 0.01	0.22 ± 0.01	0.27 ± 0.02	0.31 ± 0.00	0.23 ± 0.00	0.22 ± 0.01	0.25 ± 0.02	0.26 ± 0.01	0.24 ± 0.01	0.17 ± 0.02	0.21 ± 0.02
	τ (s)	51 ± 2	58 ± 1	71 ± 2	179 ± 1	55 ± 1	63 ± 2	**77 ± 1**	**196 ± 2**	69 ± 2	75 ± 2	**106 ± 1**	**246 ± 2**
	Flow behaviour	W.L.	W.L.	W.L.	W.L.	W.L.	W.L.	**L.**	**L.**	W.L.	W.L.	**L.**	**L.**

t_{min} = minimum time ; v_{max} = maximum velocity; τ = mean residence time; L. = Laminar; W.L. = Wavy-laminar.

6.3.2. RTD characterization

To improve understanding of the path of the skim milk fluid elements in the evaporator, and thereby improve the characterization of the flow in the FFE, the residence time distribution (RTD) function was maintained. The RTD curves in the third run at a feed mass flow rate of 70 $kg \cdot h^{-1}$ are presented in Fig. 6.1. All curves had the same surface area. The experimental RTD curves at 80 $kg \cdot h^{-1}$ and 60 $kg \cdot h^{-1}$ presented similar shapes. For all feed mass flow rates and runs studied, a more highly concentrated product led to a lower peak on the curves and greater dispersion of the fluid elements.

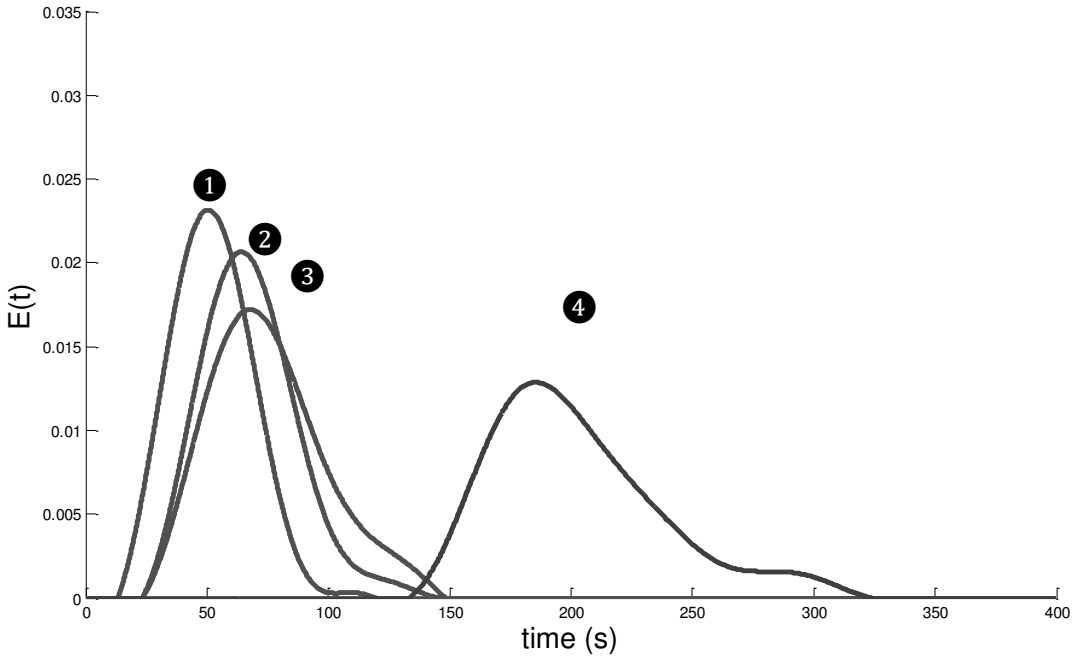

Figure 6.1. Residence time distribution curves of skim milk in FFE at feed mass flow rate of 70 $kg \cdot h^{-1}$ and 3R. ❶: measurement from inlet to outlet of tube 1; ❷: measurement from outlet of tube 1 to outlet of tube 2; ❸ measurement from outlet of tube 2 to outlet of tube 3; ❹: overall RTD measurement from inlet to outlet of the falling film evaporator.

The times that the first fluid elements took to arrive at the bottom of the evaporation tubes (t_{min}) after tracer injection are shown in Table 6.2 for the different sections studied. t_{min} was the same for each section and feed mass flow rate, wherever the run. Only the feed flow rate and the distance covered by the product in the evaporator influenced this parameter. The distance covered by the product of section ❸ was greater than section ❷, which in turn was greater than section ❶. Section ❹ represented the sum of the other three (Figure 4.7). The product flow velocity was lower in section ❸, as the product flow decreases due the evaporation.

The maximum flow velocity, v_{max}, defined as the ratio of the length of a section over t_{min} for the product cover the section and calculated at the bottom of the tubes, is shown in Table 6.2. v_{max} was 0.33 ± 0.01 $m \cdot s^{-1}$, 0.31 ± 0.00 $m \cdot s^{-1}$ and 0.26 ± 0.01 $m \cdot s^{-1}$, for T1 in the experiments conducted at 80 $kg \cdot h^{-1}$, 70 $kg \cdot h^{-1}$ and 60 $kg \cdot h^{-1}$, respectively. v_{max} was 0.31 ± 0.00 $m \cdot s^{-1}$, 0.23 ± 0.00 $m \cdot s^{-1}$, 0.22 ± 0.00 $m \cdot s^{-1}$ at 70 $kg \cdot h^{-1}$ for T1, T2 and T3, respectively, and v_{max} of section ❹ represented approximately the mean maximum velocity (0.25 $m \cdot s^{-1}$) of the three sections. In this study, v_{max} decreased as the product passed through the evaporation tubes. This was mainly due to the reduction in the mass flow rate due to product evaporation.

The mean residence time, τ, for a given section was the same for experiments conducted at a feed mass flow rate of 80 $kg \cdot h^{-1}$. At 70 $kg \cdot h^{-1}$and 60 $kg \cdot h^{-1}$, τ was higher in R3 for sections ❸ and ❹. The increase in τ was assumed to be associated with a higher viscosity of the product, which in turn, is a key parameter for determining the flow regime. Higher liquid film dispersion contributed to a higher mean residence time of the product. When the flow regime changed from wavy-laminar to laminar flow, τ was increased. For the experiments conducted in this study, the laminar flow regime has a mean residence time above that of wavy-laminar flow, hence the lower mean velocity.

The evaporation rate decreases due the increase in the energy losses, possibly due to an increase in the product concentration, a decrease in the heat transfer coefficient, a change in flow regime, a boiling delay phenomenon (i.e. product having a high boiling point due to greater concentration of solutes), etc. When the evaporation rate decreased, the mass flow rate of the product concentrate decreased less compared to high evaporation rate, which also increased the flow velocity and therefore decreased the residence time of the product. Measurement of the mean residence time was not sensitive to detect a decrease in the mean residence time when the evaporation rate decreased very slightly.

It is of note that, one dimensionless number, Re_f was used for determining the flow regime. In this work Re_f described not only the flow regime, but also the mean residence time of the product in the FFE. Where $Re_f < 25$, in sections ❸ and ❹, in 3R at 70 $kg \cdot h^{-1}$ and 60 $kg \cdot h^{-1}$, the flow behaviour changed from wavy-laminar to laminar flow and the mean residence time of the product increased from 73 s to 77 s, 186 s to 196 s, 94 s to 106 s and 231 s to 246 s, compared with 2R in the same section, where $Re_f > 25$. In these experiments, to minimize heat treatment (time/temperature), which is an important factor in controlling final product quality, the flow regime of skim milk in FFE should be in the wavy-laminar region, $Re_f > 25$. This can be achieved by changing the operational parameters, i.e. mass flow rate, heating power, etc. In a recently work Gourdon et al. (2015) showed that the flow behavior of whole and skim milk in FFE, was affected by total solids contents, flow rates and driving temperature differences.

All experimental RTD curves for section ❹ presented shoulder areas at the end of passage through the FFE. These shoulders were also observed from section ❷ in the 2R at a feed mass flow rate of 80 $kg \cdot h^{-1}$ and 70 $kg \cdot h^{-1}$, and from section ❶ in the 2R, at a feed mass flow rate of 60 $kg \cdot h^{-1}$.

Fig. 6.2 shows the models and experimental curves for the 3R of experiments conducted at a feed mass flow rate of 60 kg·h^{-1}. For modelling the results of RTD, two reactor sets were used in parallel. This model represents two different flows, where a main and minor flow was represented by the reactor set A and B, respectively. The parameters used for modelling each reactor set and the standard deviation between model and experimental RTD for all sections, runs and feed mass flow rates are presented in Table 6.3.

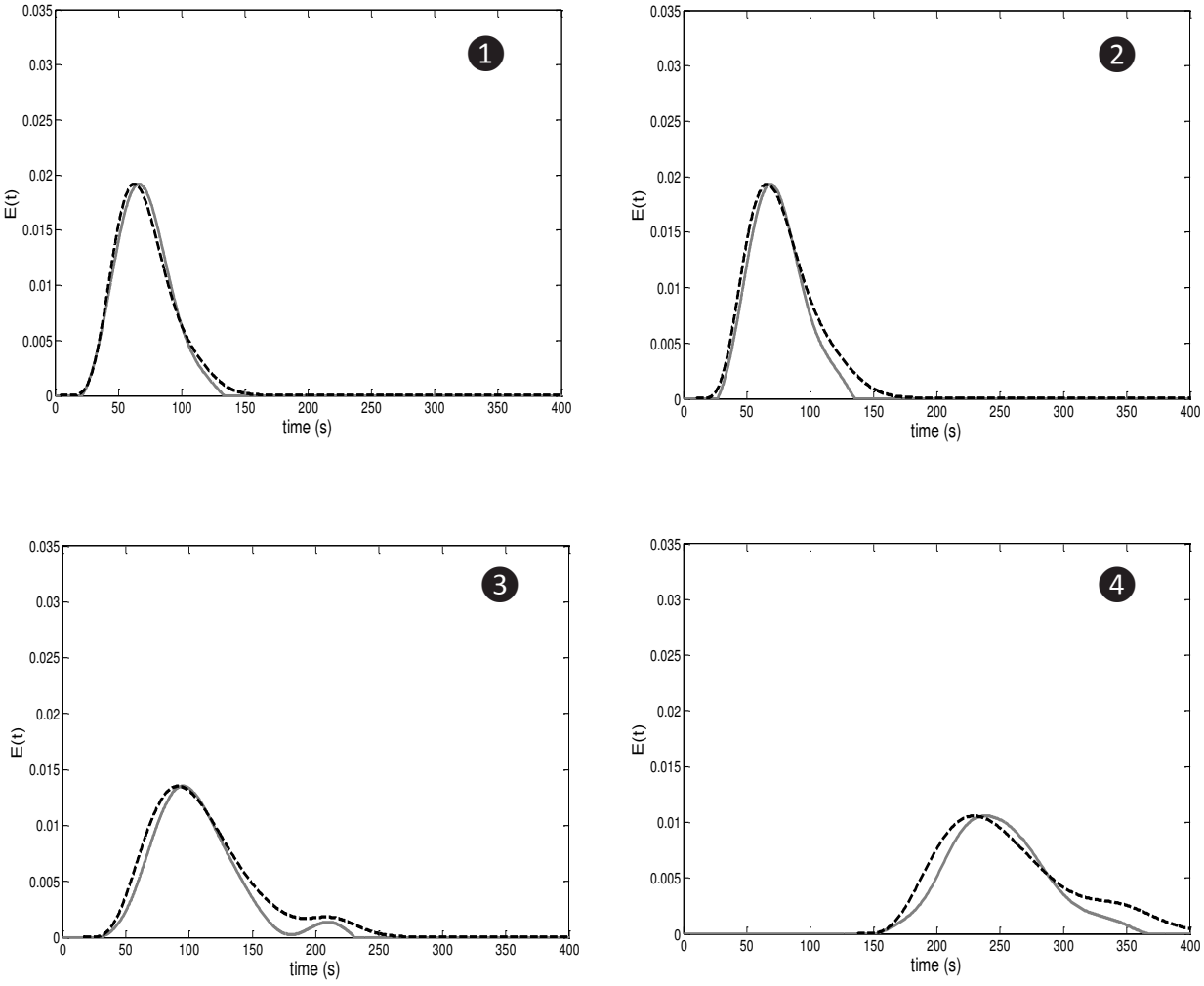

Figure 6.2. Experimental (full line) and model (dotted line) curves of residence time distribution of skim milk in FFE, at 3R for experiments performed at inlet mass flow rate of 60 kg·h^{-1}. ❶: measurement from inlet to outlet of tube 1; ❷: measurement from outlet of tube 1 to

outlet of tube 2; ❸ measurement from outlet of tube 2 to outlet of tube 3; ❹: overall RTD measurement from inlet to outlet of the falling film evaporator. Experimental curves calculated according Eq. 4.8, 4.9, 4.10 and 4.11. Model calculated according Eq. 4.12.

Table 6.3. Model parameters and standard deviation of the model compared with the experimental curves of RTD for skim milk experiments. 1R: first run, 2R: second run, 3R: third run. ❶: measurement from inlet to outlet of tube 1; ❷: measurement from outlet of tube 1 to outlet of tube 2; ❸ measurement from outlet of tube 2 to outlet of tube 3; ❹: overall RTD measurement from inlet to outlet of the falling film evaporator.

	Feed mass flow rate	80 kg·h^{-1}				70 kg·h^{-1}				60 kg·h^{-1}			
	Section (Figure 2)	❶	❷	❸	❹	❶	❷	❸	❹	❶	❷	❸	❹
1R	a	0.999	0.999	0.999	0.960	0.999	0.999	0.999	0.945	0.999	0.999	0.999	0.930
	τ_a	50	47	58	60	51	53	59	60	57	65	79	91
	τ_b	50	47	58	120	51	53	59	145	57	65	79	199
	N_a	14	14	11	10	14	13	11	5	11	11	10	8
	N_b	14	14	11	80	14	13	11	80	11	11	10	60
	Standard deviation	0.002	0.006	0.008	0.014	0.004	0.005	0.006	0.012	0.003	0.003	0.006	0.009
2R	a	0.999	0.991	0.990	0.955	0.999	0.950	0.980	0.940	0.975	0.975	0.975	0.927
	τ_a	49	50	59	75	50	53	59	63	61	63	77	92
	τ_b	49	50	104	175	50	98	100	181	123	113	137	208
	N_a	13	11	10	9	13	11	10	5	10	8	9	7
	N_b	13	90	60	110	13	85	60	40	110	80	100	115
	Standard deviation	0.002	0.004	0.006	0.010	0.003	0.003	0.005	0.009	0.002	0.003	0.005	0.008
3R	a	0.980	0.980	0.960	0.950	0.980	0.960	0.955	0.937	0.975	0.960	0.950	0.925
	τ_a	51	51	57	69	51	61	61	71	66	65	89	111
	τ_b	97	97	109	159	101	101	116	169	113	115	199	214
	N_a	12	11	10	8	11	10	7	5	9	7	6	6
	N_b	100	100	100	40	110	30	80	100	80	50	117	70
	Standard deviation	0.002	0.004	0.006	0.012	0.002	0.003	0.004	0.010	0.002	0.005	0.003	0.008

A = fraction of flow rate going into the Ea(t); τ_a = mean residence time of $E_a(t)$; τ_b = mean residence time of $E_b(t)$; N_a = number of tanks in series of $E_a(t)$; N_b = number of tanks in series of $E_b(t)$.

The accuracy and reproducibility of the model was satisfactory, considering the very low standard deviations obtained (Table 6.3).

In this model, $E_a(t)$ describes the path of between 94.0 % and 99.9 % of product fluid elements. Na could therefore be used to describe the dispersion in the residence time of the skim milk in FFE. A more highly concentrated product required a smaller number of tanks in series, corresponding to greater dispersion of the product. Among the 27 skim milk concentrations studied, the product with the lowest concentration, located at the bottom of T1 / 1R at 80 $kg \cdot h^{-1}$, had a value of N_a = 14. This value decreased when the product was concentrated. The value of the product with greater concentration at the bottom of T3 / 3R at 60 $kg \cdot h^{-1}$, was Na = 6. Function $E_b(t)$, described a small fraction of the fluid elements and served to explain the shoulder curves in the experimental RTD functions (Figures 6.2 and 6.3).

When the shoulders in the RTD curves did not occur, 99.9% of the product fluid elements passed through reactor set A, and the values of τi and N_i were the same for both reactor sets. From the moment that the shoulders were observed, the product fluid elements going to reactor set A decreased and N_b and τ_b increased, showing an increase in the fluid elements that passed through reactor set B. These fluid elements represented 0.9 % to 7 % of total skim milk fluid elements that entered the evaporator. At a feed mass flow rate of 80 $kg \cdot h^{-1}$, the fluid elements that passed through reactor set A decreased from 99.1 % to 96.0 % at T1 / R2 and T3 / R3, respectively. For section ❸ at T3 / R3, 4.0 %, 4.5 % and 5.0 % of fluid elements passed through reactor set B for the feed mass flow rates of 80 $kg \cdot h^{-1}$, 70 $kg \cdot h^{-1}$ and 60 $kg \cdot h^{-1}$, respectively.

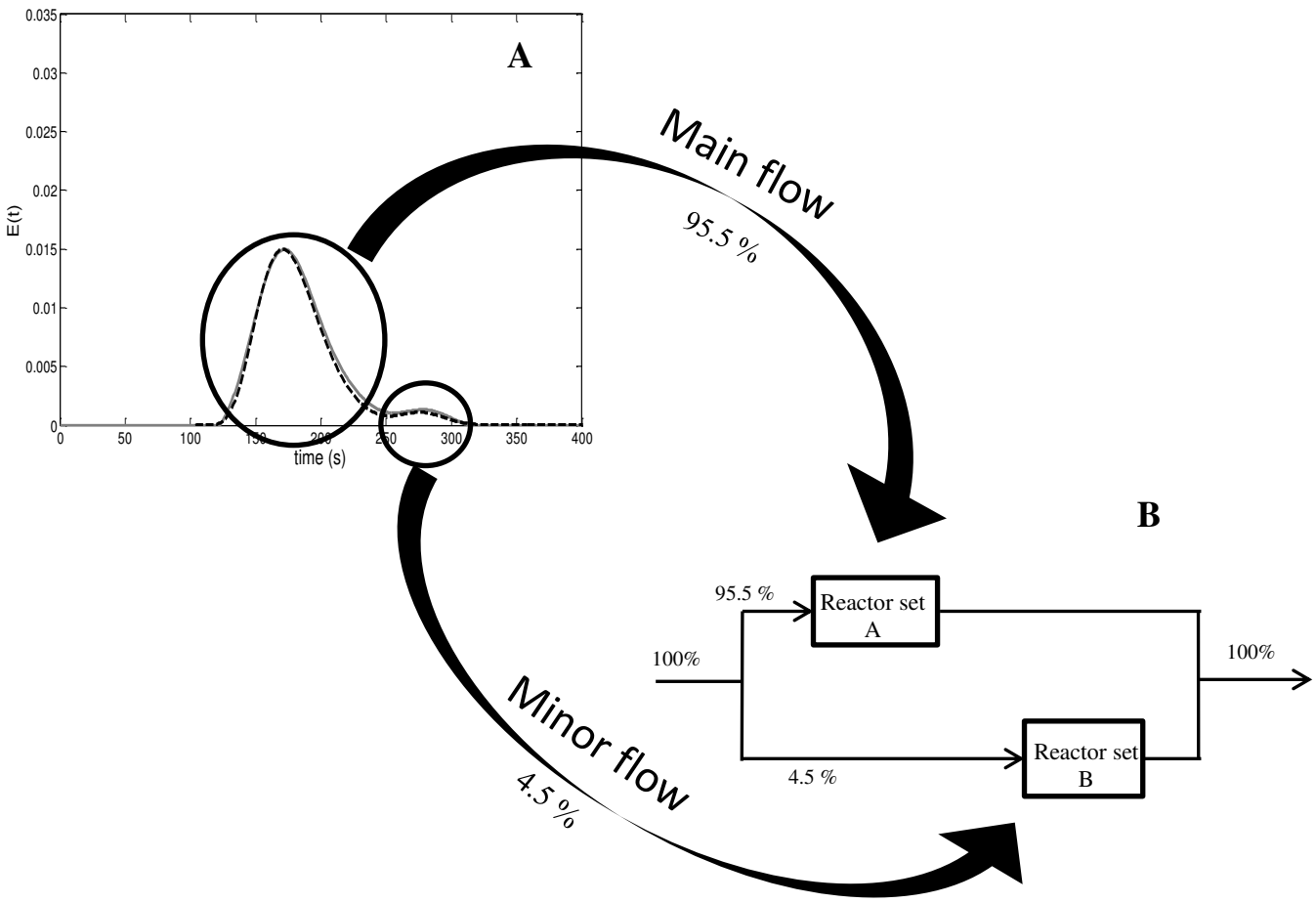

Figure 6.3. Residence time distribution (RTD) model of skim milk in FFE at section ❹ and 2R, at feed mass flow rate of 80 kg·h^{-1}. A: Experimental (full line) and model (dotted line) curves of residence time distribution. B: Tanks in series reactor sets used for modelling the RTD of FFE, showing the fraction of the product fluid elements that passed through reactor sets A and B.

In section ❹ the shoulders were always present in the RTD curves, even if they were not present in the RTD curves of previously sections. It may be due to sensitivity of the model to detecting a small quantity of the fluid elements passing through reactor set B. The quantity of product passing through reactor set A decreased from 96 % to 92.5 % for section ❹, at T3 / R3

at feed mass flow rates of 80 kg·h^{-1} and 60 kg·h^{-1}, respectively. Comparison of different sections showed that the fluid elements going to reactor set A decreased when the product concentration increased, and thus an increase in the shoulders at the end of RTD curves was observed.

As mentioned before, the model used in this study takes into account a main and a minor flow. For the experiments when the shoulders in the RTD curves were noted, the minor flow should be considerate as a retarded flow (Fig. 6.3), due to the high mean residence time presented. These two different flows possibly flow in two layers:

- One representing a small proportion of the fluid elements, demonstrated by reactor set B, where the layer of product flows in contact with the walls of the evaporation tubes; and

- One layer flowing over the first, in the center of the evaporation tubes, representing a greater proportion of the product fluid elements, demonstrated by reactor set A.

Increased viscosity in the FFE results in increased film thickness (Gray, 1981), that could be caused by an increase in the flowing fluid elements in contact with the surface of the evaporation tubes. This layer would be decelerated by friction forces, surface tension, viscosity, etc. and thus present a longer residence time. On the other hand, the majority of the product may flow in a superimposed layer, where the above deceleration forces have a minor influence, thus contributing to a higher flow velocity and shorter residence time.

6.4. Additional information

The RTD functions of water during the process of vacuum evaporation in FFE were also measured.

The t_{min} and v_{max} (Table 6.4) of the experiments conducted with water had similar values (37 s, 52 s, 60 s and 149 s, for sections ❶, ❷, ❸ and ❹, respectively) to those obtained in the

experiments conducted with skim milk in the same operating conditions (inlet mass flow rate of 70 kg·h^{-1}), demonstrating that the viscosity did not influence these parameters.

The experiments with water had a higher value of Re_f in comparison with skim milk experiments (Table 6.1 and 6.4). This increase in the values of Re_f may have been due to the low viscosity of water ($0.46 \cdot 10^{-3}$ Pa·s – Table 5.1), since the evaporation rate and therefore the flow rate at the bottom of the tubes remains constant for the experiments with water and milk (§ 5.4.3). The flow profile for water experiments was therefore characterized as turbulent (Re_f > 1000 – § 4.8).

The mean residence time of the water particles in the evaporator equipment had the same values as that of skim milk experiments when compared to the same section in the 1R and 2R. This parameter only changed when the flow profile changed from wavy-laminar to laminar flow. Therefore only the laminar flow profile affected the mean residence time of the particles during concentration in the FFE.

Table 6.4. Flow behavior, average and minimum residence time of particles of water in falling film evaporators. Measurements performed at the inlet mass of 70 kg·h^{-1} and heating power of 25.20 ± 0.05 kW.

Section (Fig. 3.14)	❶	❷	❸	❹
t_{min} (s)	37 ± 2	52 ± 3	60 ± 2	149 ± 3
v_{max} (m·s^{-1})	0.30 ± 0.00	0.24 ± 0.02	0.22 ± 0.01	0.24 ± 0.02
τ (s)	55 ± 1	63 ± 2	73 ± 1	184 ± 2
Re_f	1257	1671	1371	1371
Flow behavior	T.	T.	T.	T.

T = Turbulent

6.5. Conclusion

The Ref provided information about the mean residence time of the skim milk flow in the FFE. The mean residence time of the product was higher when the flow regime was characterized as laminar flow. The flow behavior of water experiments was characterized as turbulent flow. The flow velocity in wavy-laminar and turbulent conditions was the same, but this parameter was higher than in the laminar conditions. For the same operating parameters, water experiments in turbulent flow had the same mean residence time that skim milk flowing in wavy-laminar conditions

The RTD approach provided greater understanding of the flow in FFE. The concentration affected the dispersion of flow in the FFE but not the time required for the first particles to exit from the evaporator: the more concentrated the product, the greater the dispersion of its particles. The change in t_{min} was affected by the mass flow rate and section (distance covered by the product).

Some RTD curves exhibited shoulders at the ends. This phenomenon characterized a part of the product that followed another path in the FFE. The flow is comprised of two different flows. The minor flow represented by reactor set B, was in contact with the inner surface of the tube and had a longer mean residence time. The second flow, demonstrated by reactor set A and representing the main fraction of product, flowed over the first layer, and had a shorter mean residence time compared to the first layer.

The model with two reactor sets in parallel was effective in modelling the RTD curves. This model allowed calculation of the amount of product that took different paths in the FFE, and helped to improve understanding of the flow of skim milk in FFE.

The future of this work involves combining the RTD approach with different products and operating conditions in the evaporator. These parameters can be accessed either by modelling

or by measurement, and will make it possible to describe the time/temperature history of the product, and to establish further correlations with changes in constituents and operating parameters.

Chapter 7

APPLICATION OF RESIDENCE TIME DISTRIBUTION APPROACH TO DIFFERENT DAIRY PRODUCTS TO INDICATE FOULING DURING CONCENTRATION IN A FALLING FILM EVAPORATOR

The aim of this chapter is to use the residence time distribution approach to indicate fouling caused by the concentration of dairy products in a falling film evaporator (FFE), such as skim milk (SM), sweet whey (SW) and lactic acid whey (LAW). The extent of fouling was determined by measuring the heat transfer coefficient (U), energy efficiency, outlet mass flow rate and mean residence time of the concentrates. The heat transfer coefficient and the mean residence time of the SM concentrate did not change during the 420 min experiment. However, these two parameters gradually decreased with time for the experiments with SW and LAW. When fouling occurred, both the heat transfer coefficient and the mean residence time decreased, due to a decrease in the evaporation rate. No significant loss of SM components was identified after evaporation. However, a decrease in mineral content was observed for SW experiments over the processing time. This chapter demonstrates how to apply RTD on different dairy products and relate several operating parameters, such as steam and product temperature, product flow and conductivity, etc., to indicate fouling formation in a falling film evaporators. The results of this Chapter will be submitted at Journal of Dairy Science[1].

The main aims of this chapter are to:
- Use the RTD approach to indicate fouling in falling film evaporators
- Relate the operating parameters to dairy fouling

[1] To be Submitted in October 2015 in the Journal of Dairy Science: Silveira, A.C.P., Tanguy, G., Perrone, Í.T., Jeantet, R., Fromont, L., Le Floch-Fouéré, C., de Carvalho, A.F., Schuck, P., Residence time distribution functions - application at different dairy products to indicate fouling during concentration in a falling film evaporator.

Capítulo 7

APLICAÇÃO DA METODOLOGIA DE DISTRIBUIÇÃO DOS TEMPOS DE RESIDÊNCIA NO MONITORAMENTO DO FOULING DURANTE A CONCENTRAÇÃO DE DIFERENTES PRODUTOS LÁCTEOS EM UM EVAPORADOR DE PELÍCULA DESCENDENTE

O objetivo deste capítulo é usar a metodologia do cálculo da distribuição dos tempos de residência para monitorar a formação de fouling causados pela concentração de produtos lácteos em um evaporador de película descendente (EPD), tais como leite desnatado, soro de leite doce e soro de leite ácido. A extensão da formação do fouling foi determinada através do cálculo do coeficiente de transferência de calor, eficiência energética, vazão mássica e tempo de residência médio dos concentrados no evaporador a vácuo. O coeficiente de transferência de calor e o tempo de residência médio do leite desnatado não se alteraram durante todo o tempo de processamento (420 min). No entanto, estes dois parâmetros diminuiram gradualmente em função do tempo para os experimentos realizados com soro de leite doce e ácido. Quando ocorre a formação de fouling, tanto o coeficiente de transferência de calor quanto o tempo de residência médio diminuem, devido a uma diminuição na capacidade de evaporação. Não foram identificadas perdas significativa dos componentes do leite desnatado antes e após a evaporação. No entanto, uma diminuição na composição mineral do soro de leite ácido foi observado. Este capítulo demonstra como aplicar DTR a diferentes produtos lácteos e como relacionar vários parâmetros operacionais, como temperatura do vapor primário e do produto, vazões mássicas e condutividade dos produtos, etc., para indicar a formação de fouling em evaporadores de película descendente. Os resultados do presente capítulo será enviado em outubro de 2015 para publicação no Journal of Dairy Science[1].

Os principais objetivos deste capítulo são:

- usar a metodologia de DTR para indicar a formação de fouling em evaporadores de pelicula descendente
- relacionar diferentes parâmetros operacionais ao fouling de produtos lácteos

Table of contents

7.1. Introduction

Falling film evaporators (FFE) are widely used in the chemical, refrigeration, petroleum refining, desalination and food industries (Kouhikamali et al., 2014). Their appeal is mainly due to the high heat transfer coefficient, low evaporation temperature and small temperature differences between the product and the steam (Silveira et al., 2015). FFE is a commonly used method in the dairy industry for the production of final (sweetened condensed milk, evaporated milk, etc.; Gänzle et al., 2008) and intermediate products before any further operations such as crystallization, precipitation, coagulation and drying (infant formulae, whey and milk powders, etc.) (Bimbenet et al., 2007; Schuck, 2002; Zhu et al., 2011). Unfortunately a fouling layer accumulates on the inner wall of the evaporator tubes during processing, impairing optimal functioning of the equipment (Jeurnink et al., 1996), and resulting in a decrease in the heat transfer coefficient, an increased pressure drop and the formation of a biofilm (Langeveld et al., 1990; Visser and Jeurnink, 1997).

Because of the decrease in the heat transfer coefficient that results from fouling, most evaporators do not have a constant production capacity. In petrochemical industries, pipe cleaning is carried out once a year, whereas in food-processing industries, it has to be done at least once a day (Ozden and Puri, 2010). The high frequency of cleaning periods results in shorter production times and higher consumption of water and cleaning agents, increasing economic costs and need to address ecological issues (Jimenez et al., 2013).

Vacuum evaporators are heat exchangers, in which the major factors likely to generate fouling during the heat treatment of milk are the formation and the subsequent deposition of denatured whey protein molecules, the precipitation of minerals as a result of the decreasing solubility of calcium phosphates with increasing temperature, and the temperature difference between the heating surface and the liquid to be heated (Lalande and Tissier, 1985; W. R. Paterson, 1988).

Fouling during heat treatment is particularly problematic with concentrated products. Schraml and Kessler (1994) reported that during pasteurization of whey products, fouling increased to a maximum concentration of 250 $g \cdot kg^{-1}$ of total solids (TS), after which deposition decreased. The reason for the decrease was thought to result from two competing mechanisms: aggregation of whey proteins, which is a second order reaction and crystallization of salts, manly calcium phosphate (Fryer et al., 2011).

Most studies on fouling and cleaning in the area of food engineering relate to pasteurization and sterilization processes, where temperatures are greater than 70°C. Chen and Bala (1998) showed that surface temperatures need to be above 70°C for significant surface fouling of milk to occur, but most milk evaporator parts operate below this temperature (Morison, 2015). Most of the fouling in milk evaporators should therefore not be assumed to be the same as the fouling reported in the case of sterilizers and pasteurizers.

The progress made towards the reduction of fouling in FFE has been largely empirical. The aim of this study was therefore to demonstrate how to monitor the formation and extent of fouling in FFE using operating process data and how the formation of fouling contributes to modification of the process parameters and product quality.

7.2. Materials and Methods

7.2.1. Pilot vacuum evaporator

The experiments were performed with the pilot scale, single stage falling film evaporator with the additional instrumentation (described in Chapter 4.2.2).

All experiments were performed at an absolute pressure (P_{abs}) of 0.02 MPa, and thus the saturation temperature of evaporation was maintained at 60 °C throughout the three tubes.

7.2.2. Experimental runs

Experimental runs were carried out from a single experiment with concentrated solutions of skim milk (SM), sweet whey (SW) and lactic acid whey (LAW), at a feed mass flow rate of 70 $kg \cdot h^{-1}$.

SM was reconstituted at 235.1 $g \cdot kg^{-1}$ of total solids (TS) from skim milk powder (Lactalis ingredients, Bourgbarré, France). Fresh concentrated SW and LAW were obtained from an industrial cheese manufacturer in Brittany (France) at 252.2 $g \cdot kg^{-1}$ and 257.7 $g \cdot kg^{-1}$, respectively. The products were heated at 60°C in a preheater (Fig. 4.7) before entering the evaporator.

The outlet concentrates were collected and analyzed after 30 min, and then every 90 min (120 min, 210 min, 300 min and 390 min) during the evaporation process. For SM experiments the total process time was 420 min. For LAW and SW experiments, due the high levels of fouling deposits on the temperature and conductivity probes, the evaporator had to be stopped for manual cleaning of the probes. After cleaning the probes, the evaporator was re-started, and the operating conditions reestablished before resubmitting the product. Two stops of 60 minutes each were made for SW experiments, and one of 60 minutes and another of 30 minutes for LAW experiments.

7.2.3. Chemical composition

The feed and final total solids (TS), whey protein and ash content were determined according to section 4.4.1, 4.4.5 and 4.4.6, respectively.

7.2.4. Enthalpy characterization

The overall heat transfer coefficient (U) was used to predict the extent of fouling in the last tube of the evaporator equipment. This parameter was calculated only for the last tube because the mass flow rate of the product was lowest at this point, leading to a lower wetting rate of the tubes and higher concentration, viscosity and resistance to heat transfer (Morison et

al., 2006). It could therefore be expected that the formation of fouling should be greater than in the other two tubes.

Mass and enthalpy balance, overall heat transfer coefficient and assessment of process efficiency were calculated as described in chapter 4.5, 4.6 and 4.7, respectively.

7.2.5. Measurement of residence time distribution

Residence time distributions functions were calculated and modeled for the inlet to the outlet of the evaporator equipment (section ❹) as described in 4.9.

7.3. Results and Discussion

The total heat transfer coefficient was used to estimate the extent of fouling in the FFE, as described in Bermingham et al. (1999). Fig. 7.1 shows the evolution of U as a function of time for the three concentrated solutions studied. The blanks in the values of U for SW and LAW experiments corresponded to stops during the evaporation process to clean the conductivity and temperature probes (Fig. 4.7) and restarting of the evaporator.

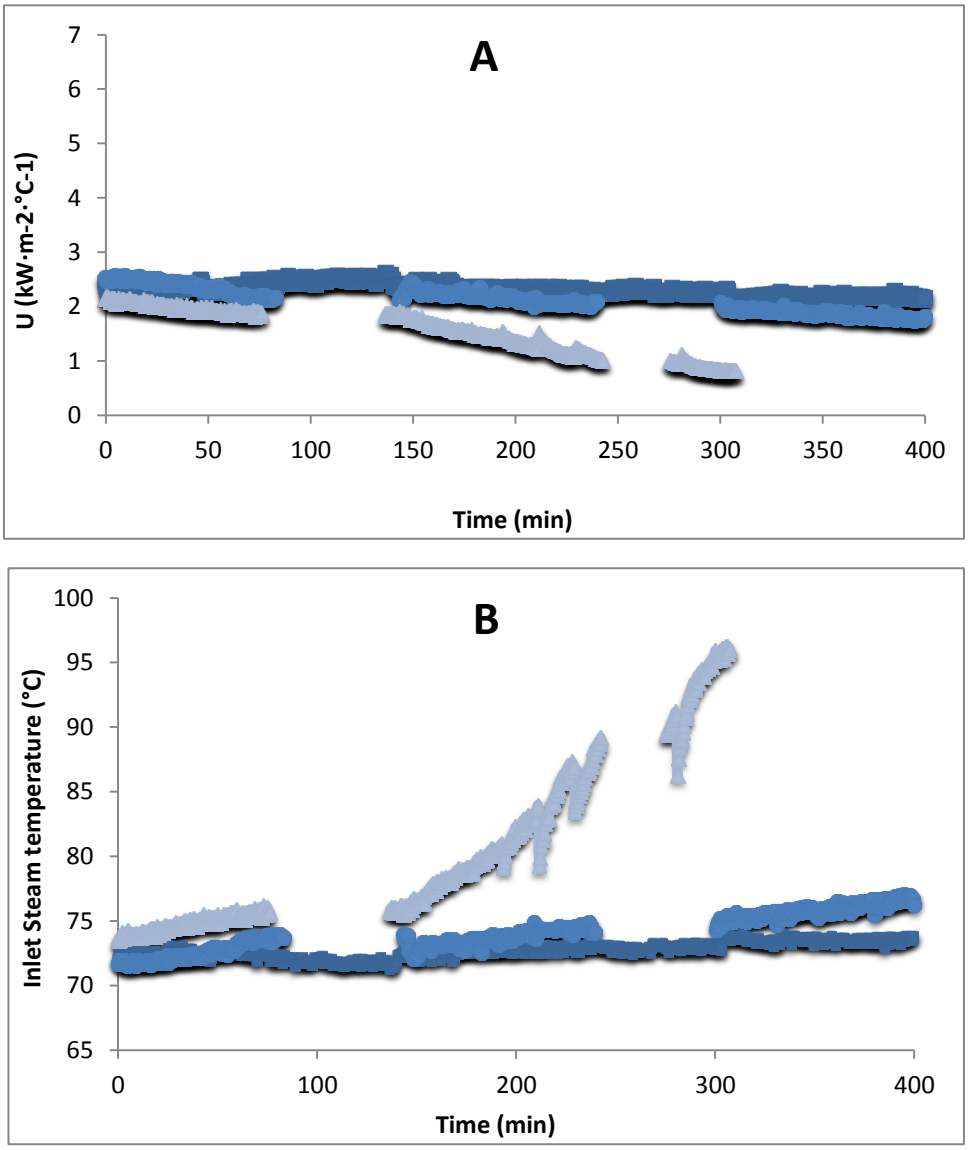

Fig. 7.1. Heat transfer coefficient (A) and inlet steam temperature (B) of skim milk (■), sweet whey (●) and lactic acid whey (▲) as a function of time. Blank spaces between U values correspond to stops of the evaporator to clean probes. U values measured in the third evaporator tube. Product inlet mass flow rate at 70 kg·h^{-1} and Heating power of 25.20 ± 0.05 kW.

At the beginning of the process (time = 0) the evaporator was clean and therefore the U values corresponded to the heat transfer coefficient for a clean surface. The values of U, calculated according to Eq. 4.4, were: 2.33 kW·m^{-2}·°C^{-1}, 2.52 kW·m^{-2}·°C^{-1}, and 2.11 kW·m^{-2}·°C^{-1},

for SM, SW and LAW, respectively. Jebson and Chen (1997) obtained values for U between 0.8 $kW \cdot m^{-2} \cdot °C^{-1}$ and 3.08 $kW \cdot m^{-2} \cdot °C^{-1}$ for whole milk measured in several milk powder factories; Jebson and Iyer (1991) found values for U between 2.00 $kW \cdot m^{-2} \cdot °C^{-1}$ and 3.50 $kW \cdot m^{-2} \cdot °C^{-1}$ for skim milk concentrated in five-effect evaporators. The small difference between the values of U for the three solutions studied at t = 0 may therefore be considered negligible on the scale of the experimental reproducibility. Moreover, the U values at the beginning of the process were similar whatever the dairy product to the mean value of 2.00 $kW \cdot m^{-2} \cdot °C^{-1}$ reported by Silveira et al. (2013) for the same equipment.

The value of U for the SM experiments remained constant during the 420 min of the evaporation process, which indicated that no fouling was present. Reconstituted milk results in less fouling than fresh milk, possibly explained by the fact that the materials which are responsible for forming the deposits on the heat exchanger surface has been partially removed during powder manufacture or are less active (e.g. denatured proteins already aggregated, or calcium phosphates already precipitated) after this step. For example, calcium concentration and ion activity is reduced by 9% and 11%, respectively (Jeurnink et al., 1996). Each of these factors may have contributed to the absence of fouling in SM experiments.

For SW and LAW experiments, U gradually decreased over time, indicating the progressive formation of fouling. This decrease was more pronounced in LAW experiments. SW resulted in more fouling than SM due to the absence of casein micelles. Indeed, caseins hinder the transport of whey protein aggregates to the surface, and affect the association of whey proteins with calcium ions, thus resulting in aggregates less prone to fouling (Jeurnink et al., 1996; Jeurnink, 1995; Varunsatian et al., 1983). LAW showed the highest fouling formation over time. As the pH of this concentrated solution is closer to the isoelectric point of whey proteins, leading to less electrostatic repulsion, the increased fouling formation could be due to greater

probability of adsorption of whey proteins to the protein layer deposited and thus complexation of minerals for the protein layer.

Table 7.1 shows the enthalpy balance values for the three dairy products studied. The EE decreased when fouling was identified. The EE was constant (77 ± 3 %) for SM experiments, since there was no fouling. The EE decreased from 73 % to 62 % and from 75 % to 62 %, for SW and LAW experiments, respectively. This decrease was due to the increase in the heat transfer resistance between the steam and the product due to the fouling layer on the evaporator walls. However, the energy losses, $\dot{q}_p$, calculated according Eq. 4.3, remained constant and equal to a similar value (7 ± 1 %) to that found by Silveira et al. (2013) whatever the product. As $\dot{q}_p$ corresponds to the energy dissipated toward the evaporator environment, its value was not affected by fouling.

Table 7.1. Enthalpy balance of the vacuum evaporation process at different times for skim milk, sweet whey and lactic acid whey experiments. Product inlet mass flow rate at 70 kg·h^{-1} and Heating power of 25.20 ± 0.05 kW.

Process time		Skim Milk	Sweet whey	Lactic acid whey
30 min	Energy Loss (%)	7%	8%	7%
	EE (%)	75%	73%	75%
120 min	Energy Loss (%)	6%	8%	7%
	EE (%)	80%	70%	69%
210 min	Energy Loss (%)	6%	7%	8%
	EE (%)	76%	70%	62%
300 min	Energy Loss (%)	6%	8%	-
	EE (%)	74%	62%	-
390 min	Energy Loss (%)	5%	-	-
	EE (%)	79%	-	-

EE = Efficiency energy (Eq. 4.12)

The effects of fouling on the operating parameters of the vacuum evaporation process are presented in Table 7.2. The outlet mass flow rate of SM concentrate was constant throughout the process time (43.7 ± 0.6 kg·h^{-1}). As no fouling was identified for this product, the evaporation rate (26.5 ± 0.5 kg·h^{-1}) and the TS content (379. ± 11.7 g·kg^{-1}) of the outlet concentrate remained constant.

Table 7.2. Operational parameters of the vacuum evaporator process and physical-chemical properties of skim milk, sweet whey and lactic acid whey at different process times. Product inlet mass flow rate at 70 kg·h^{-1} and Heating power of 25.20 ± 0.05 kW.

Process time	Product	Skim milk	Sweet whey	Lactic acid whey
30 min	Mass flow rate (kg·h^{-1})	44.0 ± 1.5	44.3 ± 3.9	43.4 ± 3.6
	Evaporation rate (kg·h-1)	26.0	25.7	26.6
	TS (g·kg^{-1})	374.0	398.5	414.2
120 min	Mass flow rate (kg·h^{-1})	44.4 ± 1.4	44.7 ± 4.2	47.0 ± 3.8
	Evaporation rate (kg·h-1)	26.6	25.3	23.3
	TS (g·kg^{-1})	398.0	394.8	383.4
210 min	Mass flow rate (kg·h^{-1})	43.1 ± 1.4	44.5 ± 4.1	51.3 ± 4.2
	Evaporation rate (kg·h-1)	26.9	25.5	18.7
	TS (g·kg^{-1})	381.8	396.3	351.2
300 min	Mass flow rate (kg·h^{-1})	44.1 ± 1.9	45.3 ± 4.4	-
	Evaporation rate (kg·h-1)	25.9	24.7	-
	TS (g·kg^{-1})	373.2	389.7	-
390 min	Mass flow rate (kg·h^{-1})	43.0 ± 1.7	-	-
	Evaporation rate (kg·h-1)	27.0	-	-
	TS (g·kg^{-1})	368.2	-	-

TS = Total solids

The evaporation rate decreased from 26.6 kg·h^{-1} to 18.7 kg·h^{-1} for the LAW experiments. However, the evaporation rate was constant for the SW experiments (25.3 ± 0.4 kg·h^{-1}),

although U of the third tube decreased throughout the processing time. The small decrease in U during SW experiments was not sufficient to affect the evaporation rate.

As discussed above, the formation of a fouling layer on the evaporator wall decreased the heat flow from the steam for the product, resulting in a decrease in the evaporation rate. Fouling thus caused a decrease in the concentration of the outlet product, from 398.5 $g \cdot kg^{-1}$ to 389.7 $g \cdot kg^{-1}$ and from 414.2 $g \cdot kg^{-1}$ to 351.2 $g \cdot kg^{-1}$ for the SW and LAW experiments, respectively. This decrease is more important to LAW due to a higher fouling formation presented by this product.

Table 7.3 shows the mean residence time, τ, of the three dairy products studied, calculated at different process times. As the operating parameters did not change for SM experiments, its τ was the same, 298 ± 1 s, throughout the process. However, τ decreased throughout the process for SW and LAW experiments. It decreased from 298 s at t = 30 min to 264 s at 210 min (Table 7.3) for LAW experiments. An increase in the outlet concentrate flow rate, and therefore in the flow speed of the product in FFE, was observed with fouling formation, in accordance with the decrease in the mean residence time determined here. The mean residence time thus decreased with fouling formation. However, the outlet mass flow rate of SW concentrates did not alter until 210 min, but nevertheless τ decreased. This shows that τ is not only influenced by the mass flow rate, but by other factors such a product concentration, flow profile and product interactions with the wall of the evaporator, etc. (Silveira et al., 2015). These findings indicate that τ expresses the extent of fouling in a more accurate way than the mass flow rate of concentrate.

Table 7.3. Mean residence times in the vacuum evaporator equipment calculated at different process times for skim milk, sweet whey and lactic acid whey. Product inlet mass flow rate at 70 kg·h^{-1} and Heating power of 25.20 ± 0.05 kW.

	Mean residence time (s)		
Process Time	Skim Milk	Sweet Whey	Lactic acid whey
30 min	296 ± 2	294 ± 1	298 ± 2
120 min	298 ± 3	287 ± 1	294 ± 1
210 min	298 ± 2	280 ± 1	264 ± 1
300 min	297 ± 3	276 ± 1	-
390 min	299 ± 2	-	-

The composition (%) of the products before and after evaporation are shown in Table 7.4. The composition of the SM product remained constant before and after evaporation, as fouling was not evidenced for this experiment. For the SW experiments, a decrease in minerals was identified at 210 min: ash content values decreased from 6.1 % to 5.3 % between t = 120 min and t = 210 min, respectively. This may have been due to mineral precipitation contributing to the formation of mineral deposits on the wall of the evaporator tubes. A high fouling rate was identified for the LAW experiments (Fig. 7.1), although the composition of the product before and after evaporation remained constant. This phenomenon contradicts the loss of product components due to deposit formation. This may be explained by the high concentration of minerals in the LAW products (14.6 % in dry matter), especially calcium and phosphate. Even with a loss of minerals in the deposit (fouling formation), this loss (mass deposited on the wall of the evaporator tube) was much lower than the mineral content in the product, and was therefore not identified. The SW product presented a smaller quantity of minerals than LAW, and thus a small loss of mineral content caused a decrease in the mineral content in the final product, which could then be identified.

Table 7.4. Physical-chemical properties of skim milk, lactic acid whey and sweet whey before and after evaporation at different process time. Product inlet mass flow rate at 70 kg·h^{-1} and heating power of 25.20 ± 0.05 kW.

		Skim milk	Sweet whey	Lactic acid whey
		Before evaporation		
	TS (g·kg^{-1})	235.1 ± 1.2	252.2 ± 0.4	257.4 ± 0.8
	Whey protein (% TS)	4.9 ± 0.2	4.7 ± 0.3	3.5 ± 0.0
	Ash (% TS)	8.3 ± 0.1	6.0 ± 0.0	15.0 ± 0.1
	Ca (% TS)	1.5 ± 0.0	0.9 ± 0.0	3.2 ± 0.0
Process time		Concentrate		
30 min	Whey protein (% TS)	5.0 ± 0.1	4.9 ± 0.1	3.5 ± 0.0
	Ash (% TS)	8.3 ± 0.1	6.7 ± 0.1	14.5 ± 0.0
	Ca (% TS)	1.4 ± 0.0	0.9 ± 0.0	3.0 ± 0.0
120 min	Whey protein (% TS)	4.9 ± 0.1	4.7 ± 0.1	3.5 ± 0.0
	Ash (% TS)	8.3 ± 0.0	6.1 ± 0.1	14.5 ± 0.0
	Ca (% TS)	1.5 ± 0.0	0.7 ± 0.0	3.0 ± 0.0
210 min	Whey protein (% TS)	5.0 ± 0.1	4.6 ± 0.1	3.3 ± 0.1
	Ash (% TS)	8.3 ± 0.1	5.3 ± 0.1	14.5 ± 0.1
	Ca (% TS)	1.4 ± 0.0	0.7 ± 0.0	3.0 ± 0.0

7.4. Additional information

The study of the extent of fouling formation presented above was related to the third evaporator tube (T3). However, this study was also performed for the first and second evaporation tubes (T1 and T2, respectively). Fig. 7.2 shows the evolution of U as a function of time for the three concentrated solutions studied in T1 and T2. As explained above, the blanks in the values of U for SW and LAW experiments corresponded to stops during the evaporation process to clean the conductivity and temperature probes and restart the evaporator. Fig. 7.3 shows the fouling found in the conductivity probes just after stopping the process.

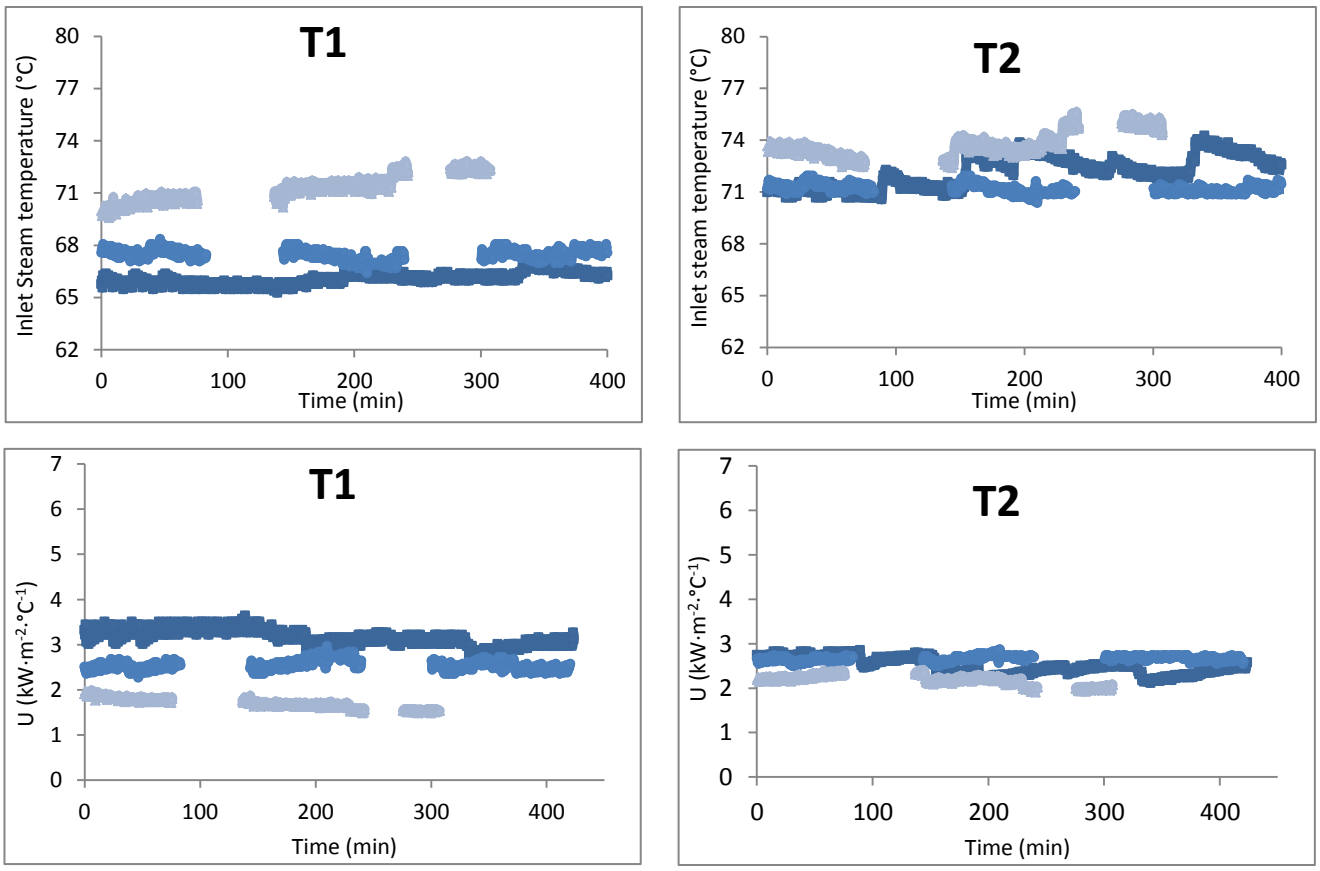

Figure 7.2. Heat transfer coefficient and inlet steam temperature of skim milk (■), sweet whey (●) and lactic acid whey (▲) as a function of time. Blank spaces between U values correspond to evaporator stops to clean probes. T1: first evaporator tube and T2: second evaporator tube. Product inlet mass flow rate at 70 kg·h^{-1} and Heating power of 25.20 ± 0.05 kW.

Figure 7.3. Conductivity probe of the third evaporator tube after the first process stop.

The U values for SM and SW measured in T1 were constant over all process times (3.2 $kW \cdot m^{-2} \cdot °C^{-1}$ and 2.5 $kW \cdot m^{-2} \cdot °C^{-1}$, respectively), indicating that no fouling formation occurred during the evaporation process. However, U values decreased over time for LAW experiments (Fig. 7.2 - A), thus indicating progressive fouling formation in T1. The U values for the three concentrated solutions studied remained constant over the process time in T2 (2.5 $kW \cdot m^{-2} \cdot °C^{-1}$, 2.7 $kW \cdot m^{-2} \cdot °C^{-1}$ and 2.2 $kW \cdot m^{-2} \cdot °C^{-1}$ for SM, SW and LAW, respectively), therefore no fouling formation was detected in these tubes during the process.

For SW experiments, fouling was identified only in T3 (Fig. 7.1), where the higher concentration and the lower flow rate of the product (end of the evaporation process) may have been the cause. For LAW experiments, fouling was identified in T1 and T3 (decrease in U over time) (Fig. 7.1 and 7.2 – B). Even with a higher concentration and lower product flow rate in T2 than in T1, fouling was not identified in this tube. This result shows that the LAW particles in the concentration range studied, which were more susceptible to the formation of fouling, attached to the wall of the evaporator tube more rapidly when submitted to a temperature difference (between heat steam and product evaporation temperature), thus producing a fouling layer on the wall of this tube. The fouling identified in T3 must be due at a higher concentration and a

lower mass flow rate of the product at this point, leading to a lower wetting rate of the tube and a higher heat transfer resistance in T3 than in the other evaporator tubes.

Table 7.5 shows the operating parameters of the vacuum evaporator process and the physical-chemical properties of the three products studied at different process times for T1 and T2. As no fouling formation was identified in T1 and T2 for SM and SW experiments, the evaporation rate in these tubes remained constant. The evaporation rate was 8.5 ± 0.3 $kg \cdot h^{-1}$ and 9.2 ± 0.3 $kg \cdot h^{-1}$ for T1 and T2, respectively.

Table 7.5. Operational parameters of the vacuum evaporator process and physical-chemical properties of skim milk, sweet whey and lactic acid whey at different process times for sections ❶ and ❷. Product inlet mass flow rate at 70 $kg \cdot h^{-1}$ and Heating power of 25.20 ± 0.05 kW.

		Skim Milk		Sweet whey		Acid whey	
Process time	Section	❶	❷	❶	❷	❶	❷
30 min	Evaporation rate ($kg \cdot h^{-1}$)	8.7	9.2	8.2	9.0	8.3	9.4
	TS ($g \cdot kg^{-1}$)	268.5	315.9	285.5	335.2	292	344
120 min	Evaporation rate ($kg \cdot h^{-1}$)	8.5	9.0	8.1	9.0	5.7	9.5
	TS ($g \cdot kg^{-1}$)	267.7	313.5	285	333.3	280.2	328.8
210 min	Evaporation rate ($kg \cdot h^{-1}$)	8.5	9.9	9.0	8.9	2.7	9.2
	TS ($g \cdot kg^{-1}$)	267.8	319.4	289.2	338.6	267.9	310.7
300 min	Evaporation rate ($kg \cdot h^{-1}$)	8.8	9.9	8.7	8.9	-	-
	TS ($g \cdot kg^{-1}$)	265.3	314.0	288	337.1	-	-
390 min	Evaporation rate ($kg \cdot h^{-1}$)	8.2	9.2	-	-	-	-
	TS ($g \cdot kg^{-1}$)	266.3	312.6	-	-	-	-

Fouling was identified in T1 and T3 for lactic acid whey experiments, therefore the evaporation rate decreased in these two tubes over the evaporation process time. At the beginning of the process (time = 30 min), and when compared to the same evaporator tube, the evaporation rate was the same regardless of the product. This result was similar to those found

and discussed in Chapter 5, where the evaporation rate between different products (in process conditions without fouling) had the same values.

For the experiments performed with lactic acid whey, the evaporation rate in T1 decreased over the process time (8.3 $kg \cdot h^{-1}$, 5.7 $kg \cdot h^{-1}$ and 2.7 $kg \cdot h^{-1}$ at 30 min, 120 min and 210 min, respectively). This decrease in the evaporation rate was due to the high fouling formation in the evaporator tube and in the preheater (installed at the equipment inlet (Fig. 4.7)), which increased the resistance of heat exchange between the hot fluid and the product. The lactic acid whey thus entered the equipment at a temperature below the evaporation temperature. As consequence part of heat exchanged by the steam in T1 was used to heat the product until its evaporation temperature (60°C) and not to evaporate it. This phenomenon, combined with the fouling formation in T1, contributed to a low evaporation rate in the first tube for lactic acid whey experiments.

The values presented above (Table 7.3) correspond to the mean residence time of section ❹ (inlet to the outlet of the evaporator equipment). Table 7.6 shows the mean residence times for SM, SW and LAW in the vacuum evaporator equipment calculated at different process times and sections ❶, ❷ and ❸. The mean residence time, measured in the same section, was constant for the SM experiments during all processing times. The mean residence time for SW experiments only changed in section ❸ and after t = 120 min. This result was similar to that found in section ❹ (Table 7.3), indicating that the formation of fouling in the SW experiment occurred only in the last evaporator tube (T3).

The mean residence time for LAW experiments decreased over the evaporation process for section ❶. Therefore in section ❶ at t = 30 min this value was the same as that of the SM and SW experiments. This result also shows that at t = 30 min, the formation of fouling in T1 was not sufficient to decrease the evaporation rate of the LAW experiments. The mean residence

time in section ❷ for LAW experiments was constant until t = 120 min (56 s), decreasing at t = 210 min (52 s), although no fouling was detected and the evaporation rate was constant in this section (9.3 kg·h^{-1}). This result was due to a lower evaporation rate in the previous evaporation tube (2.7 kg·h^{-1} – Table 7.5), thus causing an increase in product flow rate in sections ❷ and ❸ (T2 and T3). The increase in the product flow rate led to a decrease in the mean product residence time.

Table 7.6. Mean residence times in the vacuum evaporator equipment calculated at different process times and sections (Fig. 3.7) for skim milk, sweet whey and lactic acid whey. Product inlet mass flow rate at 70 kg·h^{-1} and Heating power of 25.20 ± 0.05 kW.

		Skim Milk	Sweet Whey	Acid whey
Section	Process Time	Mean residence time (s)		
❶	30 min	140 ± 1	139 ± 2	140 ± 1
	120 min	140 ± 1	140 ± 1	137 ± 2
	210 min	141 ± 1	139 ± 1	132 ± 2
	300 min	138 ± 2	138 ± 2	-
	390 min	138 ± 2	-	-
❷	30 min	57 ± 4	55 ± 1	58 ± 2
	120 min	58 ± 2	56 ± 1	55 ± 2
	210 min	59 ± 2	57 ± 1	52 ± 3
	300 min	57 ± 1	56 ± 2	-
	390 min	56 ± 2	-	-
❸	30 min	89 ± 3	93 ± 1	89 ± 1
	120 min	87 ± 3	92 ± 1	80 ± 2
	210 min	88 ± 2	84 ± 1	71 ± 1
	300 min	88 ± 3	72 ± 2	-
	390 min	88 ± 2	-	-

7.5. Conclusions

The residence time distribution approach was used to indicate fouling in a falling film evaporator during concentration of skim milk, sweet whey and lactic acid whey. Fouling was monitored by the calculation of the overall heat transfer coefficient, the energy efficiency, the evaporation rate and the mean residence time. During the concentration of sweet and lactic acid whey a decrease in the overall heat transfer coefficient, evaporation rate and energy efficiency occurred over the processing time. These phenomena were related to the formation of fouling deposits on the walls of evaporator tubes. The mean residence times of the products in the falling film evaporator were calculated. A decrease in this parameter was observed as a function of time. This phenomenon was related to the increase in the flow rate, due the fouling formation and therefore an increase of the product flow velocity, which in turn contributed to a low mean residence time. This parameter was more sensitive to identify fouling than the other operating parameters used in this study.

The composition of the three concentrated dairy products was measured before and after concentration in the equipment. No significant loss of skim milk components was identified after evaporation. A decrease in mineral content was observed in the sweet whey experiment. Despite the high fouling rate identified in the lactic acid whey experiment, the composition of this product remained constant before and after evaporation. This phenomenon was related to the higher concentration of minerals in the lactic acid whey. The loss of this component in the deposits formed was much lower than the mass of minerals present in the product, which was therefore not identified.

As these results were obtained from a single experiment, they need to be confirmed by further experiments. The work will be then submitted in the *Journal of Dairy Science*.

GENERAL CONCLUSION

In the current context of intensification of global exchange, concentration and drying techniques are crucial for the dairy industry and this warrants investment in new types of concentration and drying research. Despite the fact that falling film evaporation is a widely used technique prior to the drying process, some essential aspects of the process such as product flow regime, residence time distribution, or key factors controlling product properties, etc., are not yet fully understood, thus resulting in variability of concentrate quality and process performance. As the concentrate properties contributes to the powder properties, the understanding of the vacuum evaporation process, especially with regards to modifications of the product by the process operating parameters, needs to be improved in order to predict the final product techno-functional properties.

This thesis reviewed experimental thermodynamic and hydrodynamic studies based on the falling film evaporation of various dairy products. The study focused first on the evaporation of water, as a model solution (Newtonian behavior), then on skim milk, whole milk, sweet whey and lactic acid whey, which are involved in the elaboration of several dried dairy products, such as infant formulas and fitness products (e.g. Whey protein isolates). The first part of this PhD project aimed to instrument and characterize a pilot scale, falling film evaporator (FFE) that would, from a hydrodynamic point of view, describe the same process as the industrial equipment. The choice and position of the sensors used for the instrumentation of this pilot equipment, as well as the calculation of energy consumption and process performance, can be applied to industrial scale evaporators.

Several operating data such as temperature, pressure, flow rate, conductivity, etc. were measured and recorded for the characterization of the vacuum evaporation process. The

sensors used for these measurements were positioned at different points in the equipment, in order to achieve thermodynamic balances and to monitor product dry matter during its concentration. The thermodynamic balances of the process made it possible to identify some limitations of the original equipment, such as poor distribution of certain products at the top of the evaporator tubes, barely regulation of the water sensor valves of the heating systems and lower wettability rate of the evaporator tubes for the products with higher total solids content, which resulted in a decrease in the evaporation rate. A cone-shaped concave distributor system was designed, the heating regulation was improved and the inlet flow rate of the product was adjusted in order to overcome this limitations and to provide a sufficient wettability rate of the evaporator tubes for products with higher concentrations.

Only the operating parameter (heating power, inlet product flow rate, etc.) modified the evaporation rate. Indeed, the evaporation rate calculated for given operating parameters values was constant, regardless of the product. It is of note that the heat transfer surface of this pilot (1.03 m^2) is much lower than industrial scale evaporators considering the scale reduction applied. The results of the effectiveness of evaporation showed that suitable instrumentation (choice and siting of the sensors in the vacuum evaporation equipment) can result in good thermodynamic balance and identification of possible problems, thus improving the process performance.

The second stage of this PhD project involved a hydrodynamic characterization of the vacuum evaporation process. Residence time distribution functions were used to characterize the flow profile of skim milk at three different total inlet solids and feed mass flow rates during its concentration in the three different sections of the FFE, and for the entire FFE (from the inlet to the outlet of the equipment). Methodology for the calculation of the experimental RTD curves, as well a model and the physical interpretation of this were also developed. A combination of two perfectly mixed reactor tanks in series (reactor sets A and B) was developed to model the experimental RTD functions. Flow was characterized using experimental film Reynolds numbers

(Re_f). The results showed that the mean residence time of the product increased when the flow behavior changed from wavy-laminar to laminar flow. Increasing the concentration of skim milk and the distance covered by the product resulted in an increase in the dispersion of the particles.

The model with two reactor sets in parallel was effective to model the RTD curves, in view of the very low standard deviations obtained. From the model interpretations, a main and a minor flow, consisting in two layers of product flowing through the evaporator tubes, were proposed. The minor flow would flow in contact with the inner surface of the tube and had a longer mean residence time. The main flow, which represented most of the product particles, would flow over the first layer, and had a shorter mean residence time.

The last part of this PhD thesis consisted in the application of the thermodynamic and hydrodynamic approaches used to characterize the vacuum evaporation process. A study on the fouling during the concentration of skim milk, sweet and lactic acid whey during concentration in a FFE was performed. The results confirmed that lactic acid whey presented the greatest degree of fouling formation, followed by sweet whey. No fouling formation was identified for the skim milk experiment over the processing time of 420 min. However, this time may not have been sufficient for formation of skim milk fouling.

The formation of fouling deposits on the walls of the evaporation tubes contributed to a decrease in the overall heat transfer coefficient, due to a greater resistance to be crossed by the heat flow. Therefore, an increase in the concentrated flow rate was observed with the increase in fouling formation due to a decrease of the evaporation rate. The evolution of these operating parameters thus caused a change in mean residence time, i.e. a decrease in the heat transfer coefficient (U) leading to a decrease in the product mean residence time (τ). However and despite the decrease of mean residence time, U and product mass flow rate remained almost constant whatever the processing time and the fouling deposit. This means that τ is not only

influenced by the mass flow rate, but by other factors such as product concentration, flow profile and product interactions with the wall of the evaporator. These findings also indicate that τ variation due to fouling is more sensitive than the heat transfer coefficient and evaporation rate changes, it is another tool to fouling detection.

Besides, no significant loss of skim milk components was identified after evaporation. However, a decrease in mineral content was observed over the processing time in the sweet whey experiment. Despite the high fouling rate identified in the lactic acid whey experiment related to the higher concentration of minerals in the lactic acid whey, the composition of lactic acid whey remained constant before and after evaporation. Even with a loss of minerals in the deposit (fouling formation), this loss was minor compared to the mineral content of the product, and could not therefore be identified. The sweet whey product presented a smaller quantity of minerals than lactic acid whey, and thus a small loss of mineral content caused a decrease in the mineral content in the final product, which could then be identified. Several operating parameters, such as steam and product temperature, product flow, conductivity and mean residence time were used to indicate the fouling formation of different dairy products in a FFE.

Finally, the main innovative result of the PhD project was to highlight the impact of appropriate instrumentation combined with the understanding provided by process engineering that resulted in good characterization of the falling film evaporation process, which is an important operation in the dryer dairy industry in terms of energy consumption and final powder quality. This study emphasized the crucial role of process characterization to improve the performance of FFE and product quality. Characterization of the evaporator process thus represents a potential way to tune process performance and thus achieve the anticipated functional properties of a concentrate.

FUTURE OUTLOOK

The initial framework of this PhD project comprised a study of the vacuum evaporation process performed in a falling film evaporator. Despite being an important operation used to concentrate solutions in the food industry, there are few scientific papers concerning the concentration of dairy products in falling film evaporators. The industry has achieved expertise in this domain in an empirical way. This study presents approaches to thermodynamic and hydrodynamic characterization of the falling film vacuum evaporation process, which is an essential step for studies of the interactions between product and process. The main focus of the future outlook is therefore modifications of the product during its concentration in a falling film evaporator. Considerable effort will be required in order to integrate understanding of the vacuum evaporation process into concentrate quality control and process performance. Specific development of new products will depend on the final application of the concentrate and therefore on its physicochemical and microbiological properties (protein denaturation, flavor, color reactions, nutritional aspects, etc.).

Overall, this PhD project is an investigative study which demonstrated that good characterization of the process can provide valuable information on the optimal performance of the process and on final concentrate properties. From this starting point, various investigations can be proposed, in order both to consolidate any hypothesis developed in the PhD project and to extend understanding of modifications of product properties during vacuum evaporation and their likely influence on the performance of the process. Three key points emerged: i.e. control of product quality during the vacuum evaporation process, fouling formation and cleaning procedures.

Control of product quality during the vacuum evaporation process using residence time distribution functions

As it is possible to calculate the residence time distribution function (RTD), and therefore the exact time that a given proportion of product particles takes to pass through the evaporator, the temperature profile of the product can be calculated during concentration in the vacuum evaporation process, because the evaporation temperature in such pilot equipment can be kept constant.

The residence time distribution of a product in the vacuum evaporator equipment depends, among other things, on the operating parameters, such as the flow rate, evaporation temperature, heating power, etc. Study of the influence of the operating parameters on the RTD of different products will therefore provide elements to create models for prediction of changes in the minimum, mean and maximum product residence times. This information, combined with the temperature profile of the product, can thus be used to monitor some characteristics of the product during its concentration such as the rate of protein denaturation, destruction and / or growth of microorganisms, destruction of vitamins, Maillard reaction rate, etc. This information will make it possible to produce products with specific nutritional and techno-functional qualities, such as gelling properties and water binding capacity, and to optimize sensory properties (aroma, taste, and mouth-feel). Another application of the RTD function is in the study of fouling formation and cleaning procedures of the falling film evaporator.

Fouling formation

The extent of fouling formation of different dairy products during concentration was studied in a falling film evaporator. It was shown that fouling formation throughout the process time in the same operating conditions depends on the composition of the product. The mass of the deposit formed for different products and operating parameters should therefore be

measured and its composition determined. This requires methodology that ensures the complete removal of the deposit formed on the inner walls of the evaporator tubes.

A device for collecting the deposit formed was developed (Fig. 1). This device is inserted at the bottom of the evaporator tubes and it is then removed from the top. It thus scrapes the inner wall of the evaporation tube, allowing collection of the deposits (Fig. 1 – B). However, this device collects deposits throughout the tube, i.e. in a qualitative way. It is therefore not possible to collect the deposit from a given section of the evaporation tube (e.g. only the deposits formed at the bottom or at the top of the tube). As the product properties change during passage through the tubes, the composition of the deposits must also change. Study of the composition of the deposits formed in different sections of the evaporator tube is therefore necessary. This information will provide the responses to questions such as how does the nature of the product influence fouling formation, what is the nature of product components deposited on the wall of the tube, and what is the best cleaning procedure to remove these deposits?

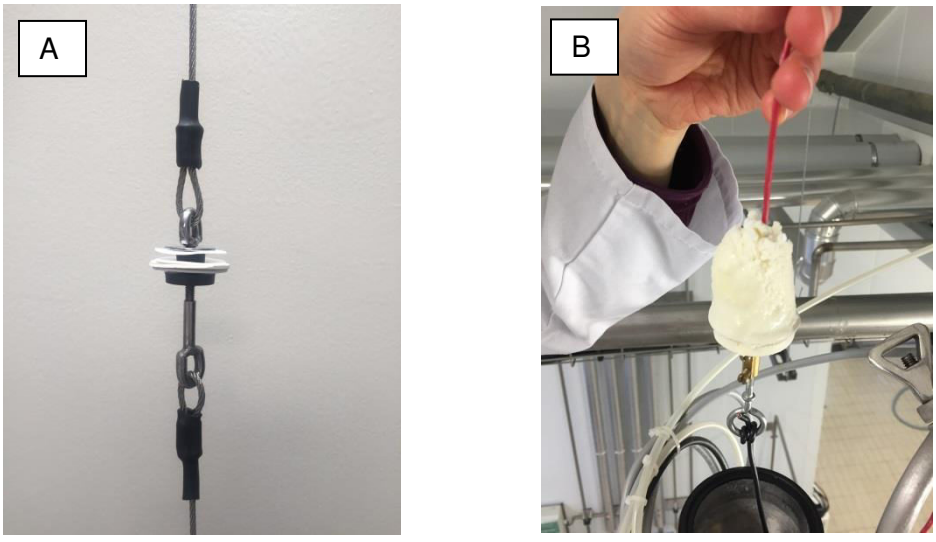

Figure 1. (A) Scraper device to collect deposits formed in the evaporation tubes and (B) Scraper device showing the deposits collected.

Vacuum evaporator cleaning procedures

Evaporator cleaning procedures in the dairy industry are not standardized. Each industry has its own way of conducting the evaporator cleaning process, i.e. process time before cleaning, circulation time, order and concentration of the cleaning agents, etc. In other words, there are as many evaporator cleaning procedures as products to be concentrated. By optimizing the cleaning procedures, a reduction in energy costs and use of cleaning agents by 50% and 25%, respectively, can be achieved (Jeurnink and Brinkman, 1994). The cleaning procedures of the falling film evaporator should be studied on the basis of measurement of product RTD in the vacuum evaporator and therefore the possibility of calculation of the time that different solutions take to pass through the equipment. The aim of such study is to optimize the cleaning and rinsing times, and the concentration of chemical cleaning agents used (nitric acid and sodium hydroxide). Moreover, a choice of a tracer or a solution property, such as conductivity, concentration, etc., should be established for calculation of the RTD functions of the cleaning solutions. This should decrease the time, and therefore the cost, of rinsing and cleaning operations, which should also contribute to decreasing the costs of the vacuum evaporation operation and improvement of the sustainability of the process. Another stage in the study of cleaning procedures is the development of different strategies for cleaning the evaporator, such as determination of the best order of use of cleaning solutions (alkaline + acid or acid +alkaline) and their concentrations. The previous study of the nature of the deposits should therefore be useful to improve cleaning procedures.

REFERENCES

Adib, T.A., 2008. Estimation et lois de variation du coefficient de transfert de chaleur surface/ liquide en ébullition pour un liquide alimentaire dans un évaporateur à flot tombant. AgroParis ech, Paris.

Adib, T.A., Heyd, B., Vasseur, J., 2009. Experimental results and modeling of boiling heat transfer coefficients in falling film evaporator usable for evaporator design. Chem. Eng. Process. Process Intensif. 48, 961–968. doi:10.1016/j.cep.2009.01.004

Adib, T., Vasseur, J., 2008. Bibliographic analysis of predicting heat transfer coefficients in boiling for applications in designing liquid food evaporators. J. Food Eng. 87, 149–161. doi:10.1016/j.jfoodeng.2007.12.013

Anurjew, E., Hansjosten, E., Maikowske, S., Schygulla, U., Brandner, J.J., 2011. Microstructure devices for water evaporation. Appl. Therm. Eng., MNF 2009 Special Issue 31, 602–609. doi:10.1016/j.applthermaleng.2010.05.009

Baldwin, A., Baucke, A., Sanderson, W., 1980. The Effect of Concentrate Viscosity on the Properties of Spray-Dried Skim Milk Powder. N. Z. J. Dairy Sci. Technol. 15, 289–297.

Baloh, A., 1979. Energy in Evaporation and Drying Operations. Zuckerindustrie 104, 943–944.

Bansal, B., Chen, X.D., 2005. Fouling of heat exchangers by dairy fluids - a review. Presented at the Proceedings of 6th International Conference on Heat Exchanger Fouling and Cleaning - Challenges and Opportunities, Hans Müller-Steinhagen, M. Reza Malayeri, and A. Paul Watkinson, Germany.

Bimbenet, J.-J., Duquenoy, A., Trystram, G., 2007. Génie des procédés alimentaires, 2 édition. ed, Technique et Ingénierie. Dunod.

Bird, R.B., Stewart, W.E., Lightfoot, E.N., 1960. Transport Phenomena. New York.

Bouman, S., Waalewijn, R., Dejong, P., Vanderlinden, H., 1993. Design of Falling-Film Evaporators in the Dairy-Industry. J. Soc. Dairy Technol. 46, 100–106.

Brans, G., Schroën, C.G.P.H., van der Sman, R.G.M., Boom, R.M., 2004. Membrane fractionation of milk: state of the art and challenges. J. Membr. Sci. 243, 263–272. doi:10.1016/j.memsci.2004.06.029

Burton, H., Franklin, J.G., Williams, D.J., Chapman, H.R., Jean, A., Harrison, W., Clegg, L.F.L., 1959. An analysis of the performance of an ultra-high-temperature milk sterilizing plant: IV.

Comparison of experimental and calculated sporicidal effects for a strain of Bacillus stearothermophilus. J. Dairy Res. 26, 221–226. doi:10.1017/S002202990000995X

Cayot, P., Lorient, D., 1998. Structures et technofonctions des protéines du lait. Arilait-Recherches, Tec et Doc Lavoisier, Paris, 1998 ISBN 2-7430-0229-8

Changani, S.D., BelmarBeiny, M.T., Fryer, P.J., 1997. Engineering and chemical factors associated with fouling and cleaning in milk processing. Exp. Therm. Fluid Sci. 14, 392–406. doi:10.1016/S0894-1777(96)00141-0

Chen, X.D., Bala, P., 1998. Investigation of the influences of surface and bulk temperatures upon fouling of milk components onto a stainless steel probe. Proc. Fouling Clean. Food Process. 25–32.

Chong, L.X.Q., Lin, S.X.Q., Chen, X.D., 2009. Concentration Dependent Viscosity in Milk Evaporation Process, In Engineering Our Future: Are We up to the Challenge?, Burswood Entertainment Complex, Barton, ACT: Engineers Australia, 1149–1158.

Chun, K.R., Seban, R.A., 1971. Heat Transfer to Evaporating Liquid Films. J. Heat Transf. 93, 391-396. doi:10.1115/1.3449836

Chun, M., Park, S., 1995. Effects of Turbulence Model and Interfacial Shear on Heat-Transfer in Turbulent Falling Liquid-Films. Int. Commun. Heat Mass Transf. 22, 1–12. doi:10.1016/0735-1933(94)00047-O

CNIEL, 2015. L'économie laitière en chiffres – édition 2015. URL http://www.calameo.com/read/002230051347964ef558f (accessed 27 august 2015).

CNIEL, 2012. Market for dried dairy products - Trade development and investments.

Croguennec, T., Jeantet, R., Brulé, G., 2008. Fondements physicochimiques de la technologie laitière. Tec & Doc Lavoisier, Paris.

Crossley, E.L., Campling, M., 1957. The Influence of Certain Manufacturing Processes on the Staphylococcus Aureus Content of Spray-Dried Milk. J. Appl. Bacteriol. 20, 65 – 70. doi:10.1111/j.1365-2672.1957.tb04518.x

Danckwerts, P.V., 1953. Continuous flow systems. Distribution of residence times. Chem. Eng. Sci., Frontiers of Chemical Engineering Science 2, 1–13. doi:10.1016/0009-2509(96)81810-0

Daufin, G., Escudier, J.P., Carrere, H., Berot, S., Fillaudeau, L., Decloux, M., 2001. Recent and emerging applications of membrane processes in the food and dairy industry. Food Bioprod. Process. 79, 89–102. doi:10.1205/096030801750286131

De Kruif, C.G., 1999. Casein micelle interactions. Int. Dairy J. 9, 183–188. doi:10.1016/S0958-6946(99)00058-8

Ducept, F., Sionneau, M., Vasseur, J., 2002. Superheated steam dryer: simulations and experiments on product drying. Chem. Eng. J. 86, 75–83. doi:10.1016/S1385-8947(01)00275-3

EMBRAPA, 2010. O mercado lacteo brasileiro no contexo mundial.

FAO, 2015. Food Outlook - Biannual report on global food markets.

Fergusson, P., 1989. Developments in the Evaporation and Drying of Dairy-Products. J. Soc. Dairy Technol. 42, 94–101.

Fox, P.F., Brodkorb, A., 2008. The casein micelle: Historical aspects, current concepts and significance. Int. Dairy J., Milestone achievements in dairy science research and their current and future industrial applications, 677–684. doi:10.1016/j.idairyj.2008.03.002

Fox, P.F., McSweeney, P.L.H., 2003. Advanced Dairy Chemistry: Volume 1: Proteins, Parts A&B: Protein v. 1, 3rd ed. 2003 edition. ed. Springer, New York.

Fryer, P.J., Robbins, P.T., Asteriadou, K., 2011. Current knowledge in hygienic design: can we minimize fouling and speed cleaning? Procedia Food Sci., 11th International Congress on Engineering and Food (ICEF11) 1, 1753–1760. doi:10.1016/j.profoo.2011.09.258

Gänzle, M.G., Haase, G., Jelen, P., 2008. Lactose: Crystallization, hydrolysis and value-added derivatives. Int. Dairy J. 18, 685–694. doi:10.1016/j.idairyj.2008.03.003

Gourdon, M., Innings, F., Jongsma, A., Vamling, L., 2015. Qualitative investigation of the flow behaviour during falling film evaporation of a dairy product. Exp. Therm. Fluid Sci. 60, 9–19. doi:10.1016/j.expthermflusci.2014.07.017

Gray, R.M., 1981. Subject: “Skim milk” Technology of skimmed milk evaporation. Int. J. Dairy Technol. 34, 53–57. doi:10.1111/j.1471-0307.1981.tb01499.x

Grossman, G., Heath, M.T., 1984. Simultaneous heat and mass transfer in absorption of gases in turbulent liquid films. Int. J. Heat Mass Transf. 27, 2365–2376. doi:10.1016/0017-9310(84)90095-4

Gutierrez, C.G.C.C., Dias, E.F.T.S., Gut, J.A.W., 2010. Residence time distribution in holding tubes using generalized convection model and numerical convolution for non-ideal tracer detection. J. Food Eng. 98, 248–256. doi:10.1016/j.jfoodeng.2010.01.004

Hartley, D.E., Murgatroyd, W., 1964. Criteria for the break-up of thin liquid layers flowing isothermally over solid surfaces. Int. J. Heat Mass Transf. 7, 1003–1015. doi:10.1016/0017-9310(64)90042-0

Hentges, D., da Silva, D.T., Dias, P.A., Santos da Conceicao, R. de C. dos, Zonta, M.N., Timm, C.D., 2010. Pathogenic microorganism survival in dulce de leche. Food Control 21, 1291–1293. doi:10.1016/j.foodcont.2010.02.014

Horne, D.S., 2003. Casein micelles as hard spheres: limitations of the model in acidified gel formation. Colloids Surf. Physicochem. Eng. Asp. 213, 255–263. doi:10.1016/S0927-7757(02)00518-6

Huppertz, T., Fox, P.F., 2006. Effect of NaCl on some physico-chemical properties of concentrated bovine milk. Int. Dairy J. 16, 1142–1148. doi:10.1016/j.idairyj.2005.09.011

IBGE, 2015. Indicadores IBGE - Estatistica da produção pecuaria.

IDF, 2014. The world dairy situation 2013.

IDF, 1993. Détermination de la teneur en azote. 4. Détermination de la teneur en azote non protéique. Lait - Int. Dairy Fed.

IDF, 1964. International Standard FIL-IDF 27. Int. Dairy Fed.

Janssen, P.W.M., 1994. Measurement of residence time distribution of processing plant using a cross correlation technique. J. Food Eng. 21, 215–223. doi:10.1016/0260-8774(94)90187-2

Jeantet, R., Ducept, F., Dolivet, A., Méjean, S., Schuck, P., 2008. Residence time distribution: a tool to improve spray-drying control. Dairy Sci. Technol. 88, 31–43. doi:10.1051/dst:2007006

Jeantet, R., Gérard, B., Guillaume, D., 2011. Génie des procédés appliqué à l'industrie laitière, 2e édition. ed. Lavoisier.

Jebson, R., Iyer, M., 1991. Performances of Falling Film Evaporators. J. Dairy Res. 58, 29–38.

Jebson, R.S., Chen, H., 1997. Performances of falling film evaporators on whole milk and a comparison with performance on skim milk. J. Dairy Res. 64, 57–67. doi:10.1017/S0022029996001963

Jeurnink, T.J.M., 1995. Fouling of heat exchangers in relation to the serum protein concentration in milk. Milchwiss. Ger.

Jeurnink, T.J.M., Brinkman, D.C., 1994. The cleaning of heat exchangers and evaporators after processing milk or whey. Int. Dairy J. 4, 347–68. doi:doi:10.1016/0958-6946(94)90031-0

Jeurnink, T., Verheul, M., Stuart, M.C., de Kruif, C.G., 1996. Deposition of heated whey proteins on a chromium oxide surface. Colloids Surf. B Biointerfaces 6, 291–307. doi:10.1016/0927-7765(95)01262-1

Jimenez, M., Delaplace, G., Nuns, N., Bellayer, S., Deresmes, D., Ronse, G., Alogaili, G., Collinet-Fressancourt, M., Traisnel, M., 2013. Toward the understanding of the interfacial dairy fouling deposition and growth mechanisms at a stainless steel surface: A multiscale approach. J. Colloid Interface Sci. 404, 192–200. doi:10.1016/j.jcis.2013.04.021

Kelly, P.M., 2006. Innovation in milk powder technology. Int. J. Dairy Technol. 59, 70–75. doi:10.1111/j.1471-0307.2006.00251.x

Kessler, H.-G., 1981. Food engineering and dairy technology. Verlag A. Kessler.

Kinsella, J.E., Whitehead, D.M., 1989. Proteins in whey: chemical, physical, and functional properties 343–437.

Kouhikamali, R., Noori Rahim Abadi, S.M.A., Hassani, M., 2014. Numerical investigation of falling film evaporation of multi-effect desalination plant. Appl. Therm. Eng. 70, 477–485. doi:10.1016/j.applthermaleng.2014.05.039

Lalande, M., Tissier, J.P., 1985. Fouling of Heat Transfer Surfaces Related to beta-Lactoglobulin Denaturation During Heat Processing of Milk. Biotechnol. Prog. 1, 131–139. doi:10.1002/btpr.5420010210

Langeveld, L.P.M., Klijn, W., Waals, C.B., 1990. Bacterial growth in evaporators for milk and whey. Voedingsmiddelentechnologie 23, 13–17.

Le Graët, Y., Brulé, G., 1993. Effects of pH and ionic strength on distribution of mineral salts in milk. Lait 73: 51–60.

Leleu, R., 1992. Evaporation. In: Techniques de l'Ingénieur, Traité Génie et Procédés Chimiques J 2320, 1–12.

Levenspiel, O., 1999. Chemical reaction engineering, 3rd ed. ed. Wiley, New York.

Levenspiel, O., Bischoff, K.B., 1963. Patterns of flow in chemical process vessels. Adv. Chem. Eng. 4: 95–198.

Li, W., Wu, X.-Y., Luo, Z., Webb, R.L., 2011. Falling water film evaporation on newly-designed enhanced tube bundles. Int. J. Heat Mass Transf. 54, 2990–2997. doi:10.1016/j.ijheatmasstransfer.2011.02.052

Lortal, S., Boudier, J.F., 2011. La valorisation de la matière première lait, évolution passée et perspectives. Innov. Agron. 1–12.

Luo, C., Ma, W., Gong, Y., 2011. Design of single vertical tube falling-film evaporation basing on experiment. J. Loss Prev. Process Ind. 24, 695–698. doi:10.1016/j.jlp.2011.06.013

Mafart, P., 1991. Génie industriel alimentaire. Lavoisier, Paris, France.

Mahaut, M., Jeantet, R., Brule, G., 2000. Initiation à la technologie fromagère. Tec & Doc Lavoisier, London ; New York.

Malcata, F., 1991. Modeling of a Series of Continuously Stirred Tank Reactors for Thermal-Processing of Liquid Foods. Int. J. Food Sci. Technol. 26, 535–546.

MDCI, 2014. Ministério do Desenvolvimento, Indústria e Comércio Exterior. URL http://www.mdic.gov.br/sitio/ (accessed 8.27.15).

Milkpoint, 2014. Balança Comercial de Lácteos: Brasil dobra exportações em 2014, mas déficit continua - Leite & Mercado - Giro Lácteo - MilkPoint URL http://www.milkpoint.com.br/cadeia-do-leite/giro-lacteo/balanca-comercial-de-lacteos-brasil-dobra-exportacoes-em-2014-mas-deficit-continua-92840n.aspx (accessed 27 august 2015).

Minton, P.E., 1986. Handbook of Evaporation Technology. Noyes Publications.

Miranda, V., Simpson, R., 2005. Modelling and simulation of an industrial multiple effect evaporator: tomato concentrate. J. Food Eng. 66, 203–210. doi:10.1016/j.jfoodeng.2004.03.007

Monnier, H., Portha, J.-F., Kane, A., Falk, L., 2012. Intensification of heat transfer during evaporation of a falling liquid film in vertical microchannels-Experimental investigations. Chem. Eng. Sci. 75, 152–166. doi:10.1016/j.ces.2012.03.008

Morison, K.R., 2015. Reduction of fouling in falling-film evaporators by design. Food Bioprod. Process. 93, 211–216. doi:10.1016/j.fbp.2014.10.009

Morison, K.R., Broome, S.R., 2014. Upward vapour flows in falling film evaporators and implications for distributor design. Chem. Eng. Sci. 114, 1–8. doi:10.1016/j.ces.2014.04.015

Morison, K.R., Worth, Q.A.G., O'dea, N.P., 2006. Minimum Wetting and Distribution Rates in Falling Film Evaporators. Food Bioprod. Process. 84, 302–310. doi:10.1205/fbp06031

Murphy, P.M., Lynch, D., Kelly, P.M., 1999. Growth of thermophilic spore forming bacilli in milk during the manufacture of low heat powders. Int. J. Dairy Technol. 52, 45–50. doi:10.1111/j.1471-0307.1999.tb02069.x

Numrich, R., 1992. Wäirmeübergang bei der Fallfilmverdampfung 331–335.

OECD-FAO, 2015. Agricultural outlook 2015-2024.

Onwulata, C.I., Isobe, S., Tomasula, P.M., Cooke, P.H., 2006. Properties of whey protein isolates extruded under acidic and alkaline conditions. J. Dairy Sci. 89, 71–81.

Ozden, H.O., Puri, V.M., 2010. Computational analysis of fouling by low energy surfaces. J. Food Eng. 99, 250–256. doi:10.1016/j.jfoodeng.2010.02.013

Panouillé, M., Durand, D., Nicolai, T., Larquet, E., Boisset, N., 2005. Aggregation and gelation of micellar casein particles. J. Colloid Interface Sci. 287, 85–93. doi:10.1016/j.jcis.2005.02.008

Paramalingam, S., Winchester, J., Marsh, C., 2000. On the Fouling of Falling Film Evaporators Due to Film Break-Up. Food Bioprod. Process. 78, 79–84. doi:10.1205/096030800532770

Park, C.D., Nosoko, T., Gima, S., Ro, S.T., 2004. Wave-augmented mass transfer in a liquid film falling inside a vertical tube. Int. J. Heat Mass Transf. 47, 2587–2598. doi:10.1016/j.ijheatmasstransfer.2003.12.017

Paterson, P.J.F., 1988. A reaction engineering approach to the analysis of fouling. Chem. Eng. Sci. - CHEM ENG SCI 43, 1714–1717. doi:10.1016/0009-2509(88)85166-2

Pehlivan, H., Ozdemir, M., 2012. Experimental and theoretical investigations of falling film evaporation. Heat Mass Transf. 48, 1071–1079. doi:10.1007/s00231-011-0962-x

Prost, J.S., González, M.T., Urbicain, M.J., 2006. Determination and correlation of heat transfer coefficients in a falling film evaporator. J. Food Eng. 73, 320–326. doi:10.1016/j.jfoodeng.2005.01.032

Rahman, M.S., 2009. Food Properties Handbook, Second Edition. CRC Press.

Runyon, C.H., Rumsey, T.R., McCarthy, K.L., 1991. Dynamic simulation of a nonlinear model of a double effect evaporator. J. Food Eng. 14, 185–201. doi:10.1016/0260-8774(91)90007-F

Schraml, J.E., Kessler, H.G., 1994. Effects of concentration on fouling at hot surfaces. Fouling and cleaning in food processing 1694, 18–25.

Schuck, P., 2002. Spray drying of dairy products: state of the art. Lait 82, 375–382. doi:10.1051/lait:2002017

Schuck, P., le Floch-Fouere, C., Jeantet, R., 2013. Changes in Functional Properties of Milk Protein Powders: Effects of Vacuum Concentration and Drying. Dry. Technol. 31, 1578–1591. doi:10.1080/07373937.2013.816316

Silveira, A.C.P., Carvalho, A.F., Perrone, Í.T., Fromont, L., Méjean, S., Tanguy, G., Jeantet, R., Schuck, P., 2013. Pilot-scale investigation of effectiveness of evaporation of skim milk compared to water. Dairy Sci. Technol. 93, 537–549. doi:10.1007/s13594-013-0138-1

Silveira, A.C.P., Tanguy, G., Perrone, Í.T., Jeantet, R., Ducept, F., de Carvalho, A.F., Schuck, P., 2015. Flow regime assessment in falling film evaporators using residence time distribution functions. J. Food Eng. 160, 65–76. doi:10.1016/j.jfoodeng.2015.03.016

Smith, J.S., Hui, Y.H., 2008. Food Processing: Principles and Applications. John Wiley & Sons.

Steffe, J.F., 1996. Rheological Methods in Food Process Engineering, Second Edition. ed. Freeman Press, East Lansing, USA.

Tamine, A.., Robinson, R.K., Michel, M., 2007. Structure of Dairy Products. ed. Oxford : Blackwell publishing, UK.

Thor, W., Loncin, M., 1978. Optimisation du rinçage final après nettoyage et désinfection. I.A.A., Industrie alimentaire agricole 95, 1095–1100.

Tonelli, S.M., Romagnoli, J.A., Porras, J.A., 1990. Computer package for transient analysis of industrial multiple-effect evaporators. J. Food Eng. 12, 267–281. doi:10.1016/0260-8774(90)90002-P

Torres, A.P., Oliveira, F.A.R., 1998. Residence time distribution studies in continuous thermal processing of liquid foods: a review. J. Food Eng. 36, 1–30. doi:10.1016/S0260-8774(98)00037-5

Tung, M.A., 1978. Rheology of Protein Dispersions. J. Texture Stud. 9, 3–31. doi:10.1111/j.1745-4603.1978.tb01292.x

USDA NASS, 2015. NASS - National Agricultural Statistics Service. URL http://www.nass.usda.gov/ (accessed 27 august 2015).

Varunsatian, S., Watanabe, K., Hayakawa, S., Nakamura, R., 1983. Effects of Ca++, Mg++ and Na+ on Heat Aggregation of Whey-Protein Concentrates. J. Food Sci. 48, 42–&. doi:10.1111/j.1365-2621.1983.tb14785.x

Velez Ruiz, J.F., Barbosa Canovas, G.V., 1997. Effects of concentration and temperature on the rheology of concentrated milk. Trans. ASAE 40, 1113–1118.

Verdurmen, R.E.M., Straatsma, H., Verschueren, M., van Haren, J.J., Smit, E., Bargeman, G., de Jong, P., 2002. Modelling spray drying processes for dairy products. Lait 82, 453–463. doi:10.1051/lait:2002023

Villermaux, J., 1993. Génie de la réaction chimique: conception et fonctionnement des réacteurs, 2. éd. rev. et augm. ed, Génie des procédés de l'École de Nancy. TEC-&-DOC-Lavoisier, Paris.

Villermaux, J., 1982. Chemical Reactors. Recherche 13, 868–879.

Visser, J., Jeurnink, T.J.M., 1997. Fouling of heat exchangers in the dairy industry. Exp. Therm. Fluid Sci. 14, 407–424. doi:10.1016/S0894-1777(96)00142-2

Walstra, P., Geurts, T.J., Noomen, A., Jellema, A., Boekel, M.A.J.., 1999. Dairy Technology: Principles of Milk Properties and Processes. CRC Press, New York.

Walstra, P., Wouters, P., Geurts, T.J., 2006. Dairy Science and Technology, Second Edition, 2e edition. ed. Taylor & Francis, USA.

Westergaard, V., 2004. Milk Powder Technology Evaporation and Spray Drying. Niro A/S, Copenhagen, Denmark.

Zhu, P., Mejean, S., Blanchard, E., Jeantet, R., Schuck, P., 2011. Prediction of dry mass glass transition temperature and the spray drying behaviour of a concentrate using a desorption method. J. Food Eng. 105, 460–467. doi:10.1016/j.jfoodeng.2011.03.003

TABLE OF FIGURES

TABLE OF TABLES

Thermodynamic and hydrodynamic characterization of the vacuum evaporation process during concentration of dairy products in a falling film evaporator

Abstract

Falling film evaporators (FFE) are widely used in the chemical, refrigeration, petroleum refining, desalination and food industries. In the dairy industry FFE is applied for the concentration of solutions prior to the drying step. Despite the economic importance of the vacuum evaporation process in the manufacture of dairy dried products, the knowledge about the process is mostly empirical. Research aiming to improve the efficiency of the process is therefore necessary. The objective of this PhD project was to characterize experimentally a FFE during the concentration of dairy products by means of thermodynamic and hydrodynamic approaches, in order to study the interactions between the products properties and the operating parameters. A pilot-scale, single-stage falling film evaporator that describes the same process as that of an industrial scale from a hydrodynamic point of view was instrumented and used to establish the mass and energy balances. The evaporation rate and the overall heat transfer coefficient were calculated from the experimental data to follow up the process. A methodology for the determination of the experimental residence time distribution (RTD) functions was developed. RTD functions provide global information about the flow of the products during concentration in a FFE. Increasing of the concentration of skim milk, mass flow rate and the distance covered by the product resulted in an increase in the dispersion of the products particles. The experimental RTD functions were modelled by a combination of two perfectly mixed reactor tanks in series. From the interpretation of this model, two different flows, a main and a minor flow, were identified. The RTD methodology developed on skim milk was applied to sweet whey and lactic acid whey and the study was extended to the formation of fouling during a 5-hour concentration. The mean residence time was more sensitive to identify fouling than the overall heat transfer coefficient and the evaporation rate. This study emphasized the crucial role of process characterization to improve the performance of FFE and product quality.

Keywords: vacuum evaporation, falling film evaporators, dairy products, residence time distribution, fouling

Caractérisation thermodynamique et hydrodynamique du procédé de concentration par évaporation sous vide de produits laitiers

Résumé

Les évaporateurs à flot tombant (EFT) sont largement utilisés dans les industries chimiques, de la réfrigération, du raffinage du pétrole, et alimentaires. Dans l'industrie laitière, les EFT sont appliqués pour la concentration de solutions avant l'étape de séchage. Malgré l'importance économique du procédé d'évaporation sous vide dans la fabrication de produits laitiers déshydratés, la connaissance du procédé est essentiellement empirique. Des recherches visant à améliorer l'efficacité du procédé sont donc nécessaires. L'objectif de ce projet de doctorat est de caractériser expérimentalement un EFT lors de la concentration de produits laitiers, par des approches thermo et hydro-dynamiques, afin d'étudier les interactions entre les propriétés des produits et les paramètres opérationnels. Un évaporateur à flot tombant, simple effet, à l'échelle pilote, qui décrit le même processus que celui à l'échelle industrielle, d'un point de vue hydrodynamique, a été instrumenté et utilisé pour établir les bilans massiques et énergétiques. La capacité évaporatoire et le coefficient global de transfert de chaleur ont été calculés à partir des données expérimentales. Une méthodologie pour la détermination expérimentale des fonctions distribution des temps de séjour (DTS) a été développée. En effet, les fonctions de DTS fournissent des informations essentielles sur l'écoulement des produits lors de la concentration dans un EFT. L'augmentation de la concentration, du débit massique et de la distance parcourue par le produit entraîne une augmentation de la dispersion des particules dans le flux. Ces fonctions ont été modélisées par une combinaison de réacteurs en cascade, parfaitement agités. D'après l'interprétation de ce modèle, deux flux, un principal et un secondaire, correspondant à deux couches superposées de produit circulant à travers des tubes d'évaporateur, a été proposé. La méthodologie développée pour le calcul des fonctions de DTS a été appliqué pour la concentration de produits laitiers (lait écrémé, lactosérum doux et acide). Par la suite, l'étude a été étendue à la formation de l'encrassement pendant la concentration par évaporation sous vide. Il a été montré que le temps de séjour moyen était plus sensible pour identifier l'encrassement que le coefficient global de transfert de chaleur et la capacité évaporatoire. Ainsi, cette étude a souligné le rôle crucial de l'importance de la caractérisation des EFT sous vide afin d'en améliorer leurs performances et la qualité des produits qui en sont issu.

Mots-clés: évaporation sous vide, évaporateur à flot tombant, produits laitiers, distribution du temps de séjour, encrassement

Caracterização termodinâmica e hidrodinâmica do processo de evaporação a vácuo durante a concentração de produtos lácteos em um evaporador de película descendente

Resumo

Os evaporadores de película descendente (EPD) são amplamente utilizados nas indústrias químicas, de refrigeração, de refino de petróleo e de alimentos. Nas indústrias de laticínios, os EPD são mais comumente utilizados para a concentração de soluções antes do processo de secagem por spray-dryer. Apesar da importância econômica do processo de evaporação a vácuo na produção de produtos lácteos desidratados, o conhecimento do processo é essencialmente empírico. Estudos visando a otimização do processo são portanto necessários. O objetivo deste projeto de doutorado é o de caracterizar experimentalmente um EPD durante a concentração de produtos lácteos, utilizando de abordagens termodinâmicas e hidrodinâmicas afim de se estudar as interações entre as propriedades dos produtos e os paramêtros operacionais. Um evaporador de película descendente, simples efeito, em escala piloto, que descreve o mesmo processo em escala industrial de um ponto de vista hidrodinâmico, foi instrumentado e utilizado para a determinação dos balanços de massa e de energia. A capacidade evaporativa e o coeficiente global de transferência de calor foram calculados a partir dos dados experimentais. Uma metodologia para a determinação experimental da função de distribuição dos tempos de residência (DTR) foi desenvolvida. As funções DTR fornecem informações essenciais sobre o escoamento dos produtos durante a concentração em EPD. O aumento da concentração, da vazão mássica e da distância percorrida pelo produto, provocam um aumento na dispersão das partículas do fluxo. Estas funções foram modelados por uma combinação de reatores em cascada, perfeitamente agitados. De acordo com a interpretação deste modelo, dois fluxos, um primário e um secundário, correspondendo a duas camadas de produto que fluem sobrepostas através dos tubos de evaporação, foram propostos. A metodologia para o cálculo das funções DTR foi aplicada a diferentes produtos lácteos (leite desnatado, soro de leite doce e ácido), e o estudo foi estendido para a formação de fouling durante a concentração por evaporação a vácuo. O tempo de residência médio real foi mais sensível para identificar a formação de fouling que o coeficiente global de transferência de calor e do que a capacidade evaporativa. Este estudo enfatizou o papel crucial da caracterização do processo de evaporação a vácuo para a otmização de EPD e da qualidade dos produtos oriundos dessa tecnologia.

Palavras-chaves : evaporação a vácuo, evaporador de película descendente, produtos lácteos, distribuição dos tempos de resiência, fouling